THE INFRARED MULTIPHOTON DISSOCIATION OF HEXAFLUOROETHANE

By

CARL EDGAR BROWN, B. Tech.

A Thesis

Submitted to the School of Graduate Studies

in Partial Fulfilment of the Requirements

for the Degree

Doctor of Philosophy

McMaster University

THE INFRARED MULTIPHOTON DISSOCIATION OF HEXAFLUOROETHANE

DOCTOR OF PHILOSOPHY (1987) McMASTER UNIVERSITY

(Chemistry) Hamilton, Ontario

TITLE: The Infrared Multiphoton Dissociation of Hexafluoroethane.

AUTHOR: CARL EDGAR BROWN, B. Tech. (RYERSON POLYTECHNICAL INSTITUTE)

SUPERVISOR: Professor D.R. Smith

NUMBER OF PAGES: xix, 134

ABSTRACT

The infrared multiphoton dissociation (IRMPD) of "neat" hexafluoroethane has been investigated for the first time. The stable products of photolysis are CF_4, C_2F_4, C_3F_8 and C_4F_{10}. Product analysis involved tunable diode laser (TDL) and fourier transform infrared spectroscopy, as well as gas chromatography where applicable. The high sensitivity and resolution of the TDL allows for the measurement of the stable products CF_4 and C_2F_4 after irradiation by a single infrared laser pulse.

A high frequency modulation TDL technique has been developed to monitor the transient infrared absorptions produced by the IRMPD of various fluorocarbons. The technique was applied to the detection of CF_2 and CF_3 radicals produced by the IRMPD of known precursors. In the case of hexafluoroethane the TDL modulation technique was used to confirm that the primary dissociation pathway involves C-C bond scission.

The role of added H_2, leading to elimination of CF_4 and increase of C_2F_4 as products, is clarified. Evidence for a second dissociation pathway producing C_2F_5 and a F atom is also presented. The understanding of the overall chemical mechanism of IRMPD of C_2F_6 and reaction of the intermediates formed has been considerably extended.

ACKNOWLEDGEMENTS

I would like to take this opportunity to express my sincere appreciation to my supervisor, Dr. D.R. Smith, for his guidance and support in this endeavor.

Also, I would like to thank Dr. J. Reid for his guidance and helpful discussions regarding the use of tunable diode lasers.

In particular I would like to thank Mr. John Orlando for his collaboration in the detection of trifluoromethyl radicals and the measurement of the CF_3 radical recombination rate constant (Chapter 5). In addition, his help and friendship have made the laboratory an enjoyable place to work.

The collaborative efforts of Mr. Paul Beckwith in the development of the transient TDL technique are greatly appreciated. I am also grateful for his help in obtaining the CF_2 transient data (in Chapters 4 and 5).

The loan of the Lumonics TEA 801A CO_2 laser by the Physical Chemistry Branch of the Chalk River Nuclear Laboratories is greatly appreciated. I would also like to thank Dr. A.J. Yarwood for the use of the Varian 5700 Gas Chromatograph, and Dr. W.J. Leigh for the use of the Porapak Q GC column.

In addition, I wish to extend my warm appreciation to my friends and colleagues in the Chemistry Department. The

support and encouragement of my family during the course of this work is especially appreciated.

Finally, I would like to thank my wife Anna for her love and encouragement throughout the course of this work, without her this venture would not have been possible.

TABLE OF CONTENTS

TABLE OF CONTENTS (Cont'd)

TABLE OF CONTENTS (Cont'd)

LIST OF FIGURES

LIST OF TABLES

LIST OF TABLES (Cont'd)

CHAPTER 1

INTRODUCTION

The field of infrared multiphoton absorption (IRMPA) and infrared multiphoton dissociation (IRMPD) of polyatomic molecules has been much studied since its beginnings in the early 1970's.[1] These studies were possible following the development of powerful pulsed transversely excited atmospheric (TEA) CO_2 lasers. In the decade and a half since IRMPA and IRMPD were first realized, an enormous amount of work has been undertaken in an attempt to gain a better understanding of these processes. Much of the work to date has been reviewed by several authors.[2-9]

The IRMPD of polyatomic molecules is a rather universal phenomenon. A review by Fuss and Kompa[8] indicates that greater than 100 polyatomic molecules, containing from 3 to 62 atoms, have undergone dissociation or isomerization following absorption of many IR photons from an intense IR laser field. IRMPD not only allows for the study of processes such as the unimolecular dissociation and isomerization of many polyatomics,[9] but it also provides a source of radicals which can be employed in further experiments.[8] The production of radicals via IRMPD is useful for high resolution spectroscopic and

kinetic studies. Early work on BCl_3[10] indicated that the IRMPD process was indeed isotopically selective. Much of the work on isotopically selective IRPMD deals with the separation of hydrogen isotopes in various halogenated hydrocarbons.[11]

In recent years, lead-salt tunable diode lasers (TDL's) have been increasingly used to monitor absorptions in the mid-infrared region of the spectrum. TDL spectroscopy is extremely sensitive and possesses much higher resolution than Fourier transform infrared (FTIR) absorption spectroscopy.[12] TDL's possess a narrow line width which allows for the measurement of Doppler-broadened transitions without instrumental broadening. (TDL linewidth is usually $<0.001\ cm^{-1}$). The high power output per unit spectral range and the ability to modulate the TDL wavelength, allow for very high detection sensitivity. TDL spectroscopy is highly specific in its ability to distinguish between different molecules including those of different isotopic makeup. Although the use of TDL's to monitor gas phase chemical reactions has been rather limited to date, the spectral properties along with the fact that TDL's allow for non-destructive measurement point to the increased use of TDL's to monitor gas phase reactions.

In this thesis, the IRMPD of hexafluoroethane is studied in an attempt to establish the IRMPD pathway. Tunable diode lasers are employed extensively in this work

to monitor the stable and transient products of the IR photochemistry.

In Chapter 2 a review of the processes involved in the infrared multiphoton absorption (IRMPA) and infrared multiphoton dissociation (IRMPD) of polyatomic molecules is presented. Several examples of typical experimental results are reviewed. The latter part of the chapter provides a brief review on the use of infrared tunable diode lasers in the measurement of IR absorptions. Chapter 2 ends with a discussion of the application of TDL absorption spectroscopy to the monitoring of chemical reactions.

Chapter 3 reviews the IR laser induced chemistry of several fluorocarbon species. The IRMPD studies of hexafluoroethane in the presence of scavengers are also reviewed in detail, as are the results of thermal dissociation experiments involving C_2F_6.

In Chapter 4 a discussion of the experimental techniques used to monitor the products of the IRMPD of "neat" hexafluoroethane is presented. Sample handling and preparation are described as well as the analytical techniques employed for quantification of the photolysis products. Emphasis is placed of the use of TDL's to monitor stable as well as transient species. The chapter ends with the discussion of a novel high frequency modulation TDL technique that has been developed in this laboratory to allow for the time-resolved detection of various transient

species including CF_2 and CF_3.

Chapter 5 deals with the IRMPD of hexafluoroethane. The yields of the major stable products resulting from the IRMPD of "neat" C_2F_6 are presented as a function of several experimental parameters including; pressure, fluence, irradiation frequency and number of laser pulses. To aid in establishing the IRMPD pathway, certain radical scavengers were added in some circumstances. The use of the high frequency modulation TDL technique as applied to the IRMPD of C_2F_6 is also presented.

Chapter 6 contains a summary of the important results and conclusions of this thesis. The high frequency modulation TDL technique described in Chapters 4 and 5 was developed, and applied to the detection of CF_2 molecules in collaboration with P.H. Beckwith and J. Reid. The steady-state production of CF_2 molecules described in Chapters 4 and 5 was done in collaboration with P.H. Beckwith and J.J. Orlando. The time-resolved detection of CF_3, formed by the IRMPD of hexafluoroacetone, presented in Chapter 5 was done in collaboration with J.J. Orlando.

CHAPTER 2

GENERAL THEORY

2.1 Infrared Multiphoton Dissociation

The following review section draws from references 2 to 9 and follows the general outline and nomenclature of Bagratashvili *et al*.[9]

As previously mentioned the IRMPD of polyatomic molecules is a rather universal phenomenon. IRMPD occurs following irradiation in the wavelength region of a strong vibrational absorption band by intense pulsed laser radiation. Polyatomic molecules absorb (10-40) photons successively to a level above the dissociation limit (D) from which unimolecular dissociation can occur. Although a great deal of experimental and theoretical work has been done on the IRMPD process, only semi-quantitative explanations are possible at this time.

The IRMPD process can be divided into three regions; coherent absorption of the first few photons in discrete vibrational levels, further absorption of many photons through a "vibrational quasi-continuum" to some level above the dissociation limit, followed by dissociation of the polyatomic in the continuum region.

2.1.1 Discrete Vibrational Levels

The initial step in the multiphoton excitation of a polyatomic is the traversing of the discrete lower vibrational levels. Experimentally there are little or no spectroscopic data available for vibrational levels with v = 2 or 3. Thus the theories describing excitation through these lower levels are qualitative or semi-quantitative in nature. The main difficulty in explaining IRMPD is the anharmonicity of the molecular vibrations. The infrared laser can be tuned to the first vibrational transition, however, due to anharmonicity the laser is quickly off resonance with respect to transitions to higher levels.

To study the excitation of polyatomic molecules through the lower discrete vibrational levels several techniques have been employed including: IR fluorescence,[13] double IR-IR resonance,[14] double IR-UV resonance[15] and Raman scattering.[16] Experiments reveal that the IRMPA process is both frequency and intensity dependent. Even with high values of irradiation intensity, the MPA spectrum is localized near its band of linear absorption. Therefore, the excitation of high vibrational levels is due to resonant transitions. This frequency dependence is of particular importance for laser isotope separation (LIS) schemes. As the laser irradiation intensity is increased one can observe a monotonous shift of the absorption maximum to the long-wave side (red-shift) along with band broadening with

respect to the linear absorption spectrum. The shifting and broadening of the absorption band with increasing intensity can be related to vibrational anharmonicity. The separation between successive vibrational levels decreases with an increase in vibrational energy, thus the absorption spectrum is shifted to the long-wave side. As the IR radiation intensity increases the contribution of higher vibrational transitions increases, therefore, the MPA spectrum gradually shifts to the "red" and broadens. In the case of OsO_4[17] the IRMPA spectrum clearly shows three absorption peaks related to three successive anharmonic shifts of the excited ν_3 mode.

The intensity required to move a molecule through the discrete energy levels depends on the properties of the individual molecule. The important properties include the degree of anharmonicity, position of the quasi-continuum and the splitting of vibrational levels. In general, small molecules (3 atoms) have large anharmonic shifts, a low density of states and the vibrational quasi-continuum is near the dissociation limit. Therefore, small molecules require very high irradiation intensities (10^7 to 10^9 W/cm^2). Great difficulty is encountered when attempting to dissociate triatomics, and diatomics have yet to be dissociated by IRMPD. Larger molecules possess smaller anharmonic shifts, have a higher density of states and a vibrational quasi-continuum close to the 1st vibrational

level. Thus the intensities required to excite these molecules to the quasi-continuum is much lower than that required for small molecules (10^3 to 10^5 W/cm^2).

In certain large molecules such as SF_6,[18] there does not appear to be any difference between MPA at the lower vibrational levels and in the vibrational quasi-continuum. It has been shown that the average number of photons absorbed by SF_6 molecules in the volume under irradiation, $\langle n \rangle$, has a continuous (slightly less than linear) dependence on irradiation fluence (Φ).[18] Initially, the SF_6 molecules are distributed over many rotational levels of the $v = 0$ state. A certain small fraction of these molecules is in an exact multistep resonance with the IR field and is quickly excited at a low intensity to the vibrational quasi-continuum. Further excitation in the quasi-continuum requires higher fluence. Other molecules that do not possess exact multistep resonances with the IR field in the discrete vibrational levels will require a larger IR field intensity to allow multiphoton excitation (MPE). Therefore, the observed continuous dependence of $\bar{n}(\Phi)$ for SF_6 results from the summation of all of these groups of molecules, each possessing a slightly different amount of detuning in the discrete vibrational levels.

In an attempt to illustrate this point, Alimpiev et al[19] cooled a sample of SF_6, and found the $n(\Phi)$

dependence to be more than linear. By cooling the SF_6, the number of occupied quantum states of the molecule was reduced, thereby reducing the number of possible pathways for successive V-R transitions. In this case 2- and 3-photon excitation processes leading directly to v = 2,3 are involved.[19] The probability of such processes is non-linearly dependent on laser power. In smaller molecules such as OsO_4[17] the dependence of $\bar{n}(\Phi)$ is stepwise due to molecules in different initial states entering the vibrational quasi-continuum at vastly different IR intensities. Very simple molecules such as D_2O reveal a saturation of the $\bar{n}(\Phi)$ dependence at $\bar{n} < 1$.[18]

An important consideration for experiments involving IRMPD is the fraction of molecules involved in the MP excitation process. At low IR field intensities (and at sufficiently low pressures so that rotational relaxation does not occur), the IR field interacts resonantly with a small fraction of the molecules at the rotational levels for which the v = 0 → v = 1 transition at the field frequency Ω is possible. Thermal population of these rotational levels determines the maximum fraction of these molecules that can be excited by a short pulse to the v = 1 level as the V-R transition is saturated, (ie, as the rotational bottleneck is reached).

To overcome the rotational bottleneck, a shorter, higher intensity pulse can be used to excite all the

molecules or the gas pressure can be increased.[20] The collisions resulting from the increased gas pressure provide pathways for rotational relaxation into rotational states from which IRMPA is possible. In certain cases, the addition of buffer gases induces a 50 fold increase in the dissociation yield.[21] Once the gas pressure has been increased sufficiently to involve all molecules in the IRMPA process, a further increase in the pressure will lead to deactivation of some absorber molecules due to V-V and V-T,R relaxation. This fraction of molecules varies significantly with gas temperature and the particular molecule under investigation.

Experimentally Alimpiev et al[22] observed the bleaching of several IR absorption bands simultaneously and reasoned that many initial rotational states were depleted by the intense IR laser pulse. Thus at fluences of 10^{-2} to 1 J/cm^2 the fraction of molecules $q(\Phi)$ involved in the MPA process is much larger than the fraction of molecules f interacting with the field in the linear limit.

The question arises as to how q varies with Φ, and at what point does q approach unity? By way of Raman scattering (RS) it has been demonstrated that under typical experimental conditions MP excitation produces two groups of molecules.[23] One of these groups contains the vibrationally "hot" molecules (q), while the other "cold" group (1-q) is composed of molecules in the lower

vibrational levels very near their original state.[23] The two groups of molecules necessitate the definition of two terms to describe the average absorbed energy, the average number of photons absorbed per molecule $\bar{n}$ and the average number of photons absorbed per "hot" molecule $\bar{n}_q$. The average number of absorbed photons per molecule n is then equal to the product of $\bar{n}_q$ and q. Experimental studies on the dependence of $\bar{n}_q$ and q on excitation field frequency (Ω) indicate that the number of molecules reaching the quasi-continuum decreases as the excitation wavelength is red-shifted. At the same time, the absorption cross-section increases in the quasi-continuum. Thus the overall resonant character of IRMPA is determined by the fraction of molecules reaching the quasi-continuum.[9]

Polyatomic molecules are able to absorb 10-40 IR photons directly from a high intensity CO_2 laser pulse even though the anharmonic nature of molecular vibrations would seem to preclude such excitation. Several theories have been proposed to explain the ease of absorption of the first few photons and the overcoming of problems related to anharmonicity. Many of these theories are discussed in the review by Fuss and Kompa.[8] Among the schemes to overcome anharmonicity are power broadening, rotational compensation and splitting of degeneracies in certain circumstances.

The vibrational energy levels of a polyatomic molecule are given by:[8]

$$E_{v_i}/hc = \Sigma_i \nu_i v_i + \Sigma_i \chi_{ii} v_i(v_i-1) + \Sigma_{i,j>i} \chi_{ij} v_i v_j \qquad (2.5)$$

where ν_i are the fundamental frequencies and χ_{ii} and χ_{ij} are the diagonal and cross-term anharmonicities respectively. It can be seen that the energy difference between v-photons and the v-th level increases quadratically with v.[8] Power broadening by the IR field is proportional to $(v + 1)^{0.5}$. Thus power broadening can only compensate for the anharmonic shift in the first couple of steps if at all. In typical IRMP excitation experiments power broadening is between 0.1 and 1 cm^{-1}.

At room temperature several rotational levels of the ground vibrational state are populated. The effect of anharmonicity may be partially overcome by this rotational energy.[8] Several rotational compensation schemes have been proposed to account for the ease of absorption of the first few photons in the discrete vibrational levels of an anharmonic oscillator. The first of these schemes[24,25] involves three consecutive vibrational steps with a change in rotational quantum number $J_o \rightarrow J_o - 1 \rightarrow J_o - 1 \rightarrow J_o$ in a spherical top such as SF_6. In this so-called "PQR" scheme, the transitions will occur at the approximate frequencies $\nu_o - 2BJ_o$, $\nu_o + 2X$, $\nu_o + 4X + 2BJ_o$. In this case all three frequencies are the same if $BJ_o = -X$. For the appropriate J_o, this condition can always be met, but at room temperature

only a few of the populated rotational levels can take part in this type of 3-photon PQR resonance. The width and spectral position of this resonance are equal to the width and position of the Q-branch of the $v = 1 \rightarrow 2$ transition. Spectroscopic investigation[24,25] of SF_6 indicates that these expected positions do not match up with the most prominent peaks observed in the MPA spectrum. The dominant peaks in the MPA spectrum correspond to the Q branches of direct 2- and 3-photon resonances. These PQR resonances are thus believed to be of little relevance.

A similar type of rotational compensation has been proposed by Platonenko.[26,27] The first three steps are 3-photon PQR resonances as above, followed by a stimulated P or Q branch emission from a populated $v = 3$ sublevel to a sublevel of $v = 2$ which is not directly populated by absorption. From this sublevel the entire MPA process can repeat itself.

In certain molecules such as SF_6, UF_6 and SiF_4 the laser excites a degenerate vibration.[8] At levels $v > 1$, the degeneracies are higher than required by symmetry and are thus split by anharmonicities. The splitting of multiplets may be greater than their mean anharmonic shift. Any number of quanta can now be absorbed strongly near resonant transitions. If the splitting is smaller, this effect in conjunction with rotational compensation can be a useful way to support MP excitation.[8]

Experimental evidence reveals that a factor of about 2 or more rotational states respond to laser radiation than expected as a result of power broadening alone. This increased number of states is most likely due to direct 2-photon transitions.[28,29] The spectrum of these molecules is shifted by anharmonicity to longer wavelength and contain rotational branches with $\Delta J = \pm 2, \pm 1, 0$ and possibly with $\Delta R \neq 0$.[30] A portion of this spectrum overlaps the 1-photon spectrum, allowing additional rotational states to be excited. Experimental evidence has been obtained in experiments on BCl_3[31] or $(CF_3)_2CO$[32] which have maximum excitation possibilities far beyond the range of the 1-photon spectrum. Further evidence appears in the dissociation probability spectrum of C_2H_5Cl[33] where distinct 2- and 3-photon resonances are observed. In addition, 2-photon transitions were reported by Fukumi[34] in an optoacoustic study involving the IRMP excitation of ethylene.

2.1.2 Excitation Within the Vibrational Quasi-continuum

Once a polyatomic molecule has reached the levels of the vibrational quasi-continuum (VQC), the description of its further excitation is much simpler than that in the lower vibrational levels. The density of states in the vibrational quasi-continuum is very high, and therefore a transition in resonance with the pump laser frequency is

nearly certain. Once in the VQC, further excitation is a successive multistep absorption of IR photons. There is no need for high IR field intensities to overcome the difference between the IR laser frequency and the vibrational transition frequency. There is substantial experimental evidence for a fluence dependence for excitation in the VQC. Absorption in the VQC is universal by nature and can be described in terms of an absorption cross-section $\sigma(\Omega, E_{vib})$ dependent on vibrational energy E_{vib} and excitation frequency Ω.[9] The excitation in the VQC has been referred to as strong vibrational heating of the molecule to $E_{vib} \sim D$, the requirement being absorption saturation of the transitions in the VQC.[35]

In order to study absorption in the vibrational quasi-continuum, the absorption in the discrete vibrational levels must be separated from that in the quasi-continuum. Experimentally this is done by using a 2-colour IR field.[36] In these experiments, the polyatomic molecules can be weakly excited from the ground vibrational state at frequency Ω_1 to the vibrational quasi-continuum. A second higher fluence IR laser at frequency Ω_2 (detuned from the resonance frequency of the unexcited molecules) is used to excite the molecules through the VQC. The energy absorbed by the molecules from each of the laser pulses (A_1 and A_2) are measured separately. The energy

absorbed with both lasers operating (A_{1+2}) is then measured. The absorption in the quasi-continuum is equal to the difference (A_{1+2}) - (A_1 + A_2). Recently Ivanco et al[37] have used this approach to measure absorption in the quasi-continuum of methanol photoacoustically. In general, experimental evidence shows that the spectrum of molecules excited in the VQC exhibits smooth, broad bands grouped around the active IR absorption frequencies; however, anharmonicity shifts the absorption maxima to the "red" as the molecular vibrational energy increases.[9]

Models for absorption spectra in the VQC have been developed which correlate well with experimental data.[38] The absorption cross-section can be described by a Lorentzian contour as follows:

$$\sigma_{qc}(\Omega, E_{vib}) = \frac{\sigma_{int}(E_{vib})(1/\pi)\delta(E_{vib})}{[\Omega - \nu_{max}(E_{vib})]^2 + \delta^2(E_{vib})} \qquad (2.10)$$

where ν_{max} is the center frequency and δ is the absorption band half width from a state with E_{vib} in the VQC. The integral absorption cross-section $\sigma_{int}(E_{vib})$ increases gradually with increased E_{vib} due to increased vibrational amplitude of the highly excited molecule.[9] The absorption half width also increases as the vibrational energy increases.

Qualitatively then, there is a two dimensional dependence $\sigma(\Omega, E_{vib})$ for MP excitation of a polyatomic. Experimentally there is a dependence of $\bar{n}(\Omega)$ resulting from the successive superposition of absorption spectra as the vibrational energy increases. Therefore a "red" shift of the $n(\Omega)$ dependence is seen as the molecular vibrational energy increases. The decreasing growth of $\bar{n}(\Phi)$ with increasing fluence is also related to the "red" shift of the absorption band. Therefore the absorption cross-section for molecules highly excited at Ω drops and higher fluence is needed for further excitation. Note that the width of these peaks is greater than the bandwidth, indicating a non-resonant character of absorption in the quasi-continuum.

Although several experimental reports have indicated a fluence dependence of the absorption by polyatomic molecules in the vibrational quasi-continuum, Mukerjee and Kwok[39] have recently reported observing an intensity dependence of absorption by C_2F_5Cl in the vibrational quasi-continuum.

2.1.3 Vibrational Energy Distribution Under MP Excitation

When a powerful CO_2 laser pulse acts on molecules distributed over many initial states, the distribution of vibrational energy becomes nonequilibrium. The intermolecular distribution of vibrational energy is

nonequilibrium because the powerful CO_2 laser pulse creates two groups of molecules; a vibrationally excited group of molecules around the vibrational quasi-continuum (hot group) and a cold group of molecules at the lower vibrational levels. The formation of these two groups can be avoided by use of a shorter (more intense) pulse to excite all molecules to the vibrational quasi-continuum. One could alternatively add a buffer gas to induce strong rotational relaxation, but not vibrational deexcitation, and thereby suppress the effect of a rotational bottleneck. Following the laser pulse hot and cold molecules collide resulting in vibrational energy exchange which leads to one group of molecules with the same total vibrational energy.

A great deal of the information on the intermolecular vibrational energy distribution has been observed in measurements of the Raman scattering spectrum[40] of molecular vibrations of molecules excited by CO_2 laser pulses. Before the CO_2 laser pulse the Raman scattering spectrum shows a peak at the region of a fundamental vibration of the molecule. Following the excitation of the molecules by a CO_2 laser pulse, the spectrum shows an additional group of hot molecules shifted towards the Stokes region. If the probe pulse is delayed one can see that vibrational exchange between the hot and cold molecules results in the formation of one group of molecules with the same total vibrational energy. With this technique the

effect of rotational relaxation induced by the addition of a buffer gas can be seen from the fact that one group of vibrationally excited hot molecules is formed.

Although the shape of the vibrational distribution of molecules in the hot group of molecules has yet to be measured, measurements of the dissociation yield indirectly indicate that the distribution is non-Boltzmann. Bagratashvili et al[38] have calculated a vibrational energy distribution that is narrower than a Boltzmann one and which possesses an exponential tail that falls more rapidly. The absorption cross-section $\sigma(\Omega, E_{vib})$ in the vibrational quasi-continuum of CF_3I[38] has a red anharmonic shift (ν_{max}). Thus if the IR laser frequency Ω is tuned to the band center of the lower transitions, the cross-section ($\sigma(\Omega, E_{vib})$) for highly excited transitions at this frequency Ω falls. This results in a narrowing of the vibrational distribution. When the tail of the laser-created vibrational distribution is compared to a Boltzmann distribution at the same average number of absorbed photons $\langle n \rangle$, one can see the difference in the two distributions. The tail of the distribution above the dissociation limit D contributes to the dissociation yield. Thus the difference between the two distributions is well illustrated by the difference in the dissociation yield β on absorbed energy. Following the laser pulse collisions result in vibrational energy exchange and hence a Boltzmann distribution in the

hot molecules. The tail in this distribution can result in dissociation following the pulse.

2.1.4 Vibrational Energy Stochastization

The vibrational motion of molecules that have been highly excited by pulsed CO_2 laser radiation is stochastic (the vibrational energy is randomized among all vibrational modes) when the vibrational excitation energy E_{vib} reaches the dissociation energy. This conclusion was indirectly drawn from several measurements of the dependence of the molecular dissociation yield on the energy absorbed by a molecule.[9] The exact position of the stochastization energy limit is not yet known. To study the intramolecular energy distribution one should employ either spontaneous IR emission or anti-Stokes Raman scattering. It has been shown[9] that the integral intensity of the spontaneous emission radiation band in the mode active in the IR spectrum and the integral intensity of the anti-Stokes Raman scattering band in the mode active in RS are proportional to the vibrational energy in the mode.

Anti-Stokes Raman scattering[41] has been employed to observe the vibrational energy stochastization in highly excited SF_6 and CF_3I and to estimate the stochastization limit of vibrational energy. Anti-Stokes Raman scattering was observed at all active vibrational modes in the Raman scattering spectrum. Thus all of these modes show

excitation, not just the mode irradiated by the CO_2 laser. The level of excitation in these modes remained constant as the probe pulse was delayed from 20 ns to 1 μs. With the long time delay τ_d, collisional vibrational exchange must have resulted in an equilibrium vibrational energy distribution over all the modes. Therefore, the vibrational motion stochastization occurs in less than 20 ns, that is during the process of MP excitation. Using this technique,[42] the energy limit of vibrational motion stochastization in SF_6 is found to be - 4000 cm^{-1}.

2.1.5 Dissociation in the Real Continuum

Once in the region of the real continuum, a highly excited molecule may be chemically transformed in a collisionless environment by several monomolecular processes including isomerization and dissociation. The discussion presented here will deal only with the dissociation process.

The dissociation yield (β) of a molecule acted upon by an intense IR laser pulse exhibits a sharp dependence on laser fluence (Φ) and a distinct resonance dependence on laser irradiation frequency (Ω). The dissociation yield ($\beta(\Phi,\Omega)$) dependence is restricted by the corresponding dependences of the MPA rate. The threshold dependence of the dissociation yield $\beta(\Phi)$ on fluence for SF_6 was first examined by Ambartzumian et al.[43] This work

indicates a distinct threshold for molecular dissociation with $\Phi \sim 2.0$ J/cm^2. A lowering of the fluence by only 8% eliminated evidence of molecular dissociation even though the sample was exposed to more laser pulses. At fluences which exceed the threshold the $\beta(\Phi,\Omega)$ dependence was proportional to Φ^3. In other experiments on SF_6,[44] the laser pulse intensity (P) was varied by changing the pulse width from 0.5 to 100 ns while maintaining the laser fluence (Φ) at a constant value. The dissociation yield was shown to be fluence (Φ) dependent rather than intensity dependent.

Ambartzumian et al[45] investigated the threshold dependences of IRMPD by comparing the dissociation yield $\beta(\Phi)$ of SF_6 for excitation of the ν_3 active mode with excitation of the weak combination band $\nu_2 + \nu_6$ band; the thresholds were virtually the same in both cases. Thus the threshold character of MPD is associated with excitation of molecules through the vibrational quasi-continuum and not on how easily a molecule moves through the lower vibrational levels below the vibrational quasi-continuum limit. Therefore, with normal experimental conditions the fluence Φ that ensures effective excitation of molecules from the vibrational quasi-continuum to the real continuum, can be realized at intensities which are high enough to permit a reasonable fraction of molecules to move from the lower discrete vibrational levels to the vibrational quasi-continuum. The vibrational energy

distribution $F(E_{vib})$ of the excited molecules exhibits a sharp exponential fall-off towards higher energies. As the fluence is increased a small fraction of molecules in the vibrational distribution falls at first within the real continuum. This fraction increases exponentially as the fluence increases.

As previously stated the absorption cross-section in the vibrational quasi-continuum is frequency dependent, therefore the fluence required for excitation from the vibrational quasi-continuum to the real continuum is also frequency dependent. When contemplating a laser isotope separation experiment, one should consider the $\beta(\Omega)$ dependencies when choosing an irradiation frequency.

2.1.6 Overexcitation of Molecules in the Continuum

The strong absorption of a CO_2 laser pulse by a group of molecules creates a nonequilibrium vibrational energy distribution. The tail of this distribution reaches the end of the real continuum of states corresponding to molecular dissociation. The molecule is able to dissociate when its vibrational energy exceeds the dissociation energy D. The rate of dissociation is dependent upon molecular size. If the vibrational excitation energy is localized in the weakest bond (d_o), the dissociation occurs quickly, within about one vibrational period.[9] If a large fraction of the energy is in other vibrational degrees of freedom,

dissociation necessitates fluctuation to accumulate the energy in bond d_o. More than one vibrational period would be required to achieve this critical fluctuation.

The statistical theory of dissociation (RRKM theory) dictates that the dissociation products usually result from breaking of the weakest bond. With the use of a molecular beam Grant et al[46] showed that the primary dissociation step in the IRMPD of SF_6 is the breaking of a S-F bond releasing a F atom. The resulting SF_5 radical then dissociates to form SF_4. Since there were no F_2 molecules detected the alternate $SF_6 \rightarrow SF_4 + F_2$ mechanism could be rejected. By measuring the kinetic energy distribution of the resulting radicals $g(E_{vib})$, the vibrational energy of the radicals can be determined and the degree of overexcitation of the dissociating SF_6 determined. With a fluence (Φ) of 4 - 10 J/cm^2 the overexcitation of SF_6 corresponds to 6 to 10 CO_2 laser photons.[46]

In certain cases there may be two possible types of molecular dissociation. The first type of dissociation involves simple bond cleavage, without bond rearrangement and the associated energy barrier. This is the case when one atom breaks away from the parent molecule, such as the Cl atom from CF_3Cl.[9] The dissociation products in this case will have excess vibrational energy (E_{vib} - D). The second type of dissociation involves bond rearrangement and

overcoming the associated energy barrier E_{ac}. The molecule must absorb extra photons to overcome this barrier and this excess vibrational energy (E_{ac} - D) is transferred to the dissociation products. Typically this type of dissociation involves the formation of a diatomic molecule, the atoms of which are not bonded to each other in the parent polyatomic molecule. CF_2Cl_2 is such a molecule, where dissociation can occur via $CF_2Cl_2 \rightarrow CF_2Cl + Cl$ and/or $CF_2Cl_2 \rightarrow CF_2 + Cl_2$. The potential energy barrier of the second pathway reduces its dissociation probability to one tenth that of the first pathway involving simple bond cleavage.[47]

One final important aspect of MP excitation of large polyatomic molecules is their significant excitation above the dissociation limit. Experiments[48] have shown the number of absorbed photons for a $(CF_3)_3CI$ molecule is between 35 - 40, or about twice the dissociation energy of the C-I bond. For a much smaller molecule CF_3I, $n \approx 20$-21, the number of photons absorbed in the real vibrational continuum $(E_{vib} - D)/h\Omega \leq 2$.[38]

In cases where polyatomic molecules can be highly overexcited above the dissociation limit by very short laser pulses, the overexcitation (E_{vib} - D) may be enough to overcome the next dissociation limit of the molecule and dissociation through several pathways is possible.

2.2 Measuring IR Absorptions with Tunable Diode Lasers

In the past decade lead-salt tunable diode lasers (TDL's) have been used extensively for high resolution infrared spectroscopy in the laboratory and in the environment. (See reference 49 and references therein.) TDL's generally possess an emission linewidth of <0.001 cm^{-1}, which allows for measurement of Doppler-broadened transitions with negligible instrumental broadening. TDL's are commercially available to cover the 300-3000 cm^{-1} range, and are typically tunable over 100 cm^{-1}. Although TDL's are continuously tunable, by varying their operating temperature (coarse) or their bias current (fine), their emission is often multimode in character. Each mode is continuously tunable over $\simeq 1$ cm^{-1}. In certain circumstances the cold head temperature and the bias current applied to the TDL can be adjusted to give single-mode operation in the desired spectral region. If single-mode operation cannot be obtained by temperature and current adjustments, the mode can be selected with a 0.5 m grating monochromator. Among the unique features of TDL's is the high output power per unit spectral range, which along with the ability to modulate the TDL wavelength in conjunction with lock-in amplifier signal processing leads to very high sensitivity for detection.[12] Fractional absorptions of 10^{-3} to 10^{-5} can be measured in gases.[50] The narrow linewidth of tunable diode lasers allows for the distinction

between different molecules, including different isotopic species of the same molecule. Although TDL's have been used to a limited extent to study gas phase chemical reactions, their spectral properties in combination with a fast response time and non-destructive nature make them ideal instruments for such studies.

The tunable diode laser can be used to measure an infrared absorption coefficient which will give an absolute calibration if linestrength and linewidth data are known.[50] Calibration plots of absorption coefficient versus concentration are not needed. The area under the absorption line is directly proportional to the number of molecules in the path of the TDL beam. The line strength S is the proportionality constant for the individual line being measured. The linestrengths of many small molecules have been measured.[51]

It is usually easier to measure the line center absorption α_o, which can be calculated from:

$$I(\nu_o) = I_o(\nu_o)\exp(-\alpha_o(\nu_o)L) \qquad (2.11)$$

where L is the absorber path length, ν_o is the absorption line center frequency, and I and I_o are the transmitted and incident TDL intensities respectively. At pressures below 1 Torr, one need only consider Doppler broadening of the linewidth. The Doppler halfwidth at half

maximum intensity (HWHM) is given by:[52]

$$\Delta\nu_D = 3.581 \times 10^{-7} \nu_o (T/M)^{0.5} \qquad (2.12)$$

where ν_o is the line center frequency, M is the molecular mass , and T is the temperature in degrees Kelvin. The linestrength S is related to α_o (at pressure < 1 Torr) by:[12]

$$\alpha_o = S/\Delta\nu_D (\ln 2/\pi)^{0.5} (P_A/760)(273/T) N_1 \qquad (2.13)$$

where, α_o = the line center absorption coefficient in cm^{-1}

S = line intensity in units of cm^2 $molecule^{-1}$ cm^{-1}

$\Delta\nu_D$ = the Doppler halfwidth at half maximum intensity

P_A = the pressure of the absorber gas in Torr

T = the temperature in degrees Kelvin

N_1 = the Loschmidt number at STP = (2.69×10^{19} molecules cm^{-3})

At pressures above 1 Torr, collisional broadening must be considered. The absorption shape changes from Gaussian at low pressure to a Voigt profile at intermediate pressures and finally to a Lorentzian at high pressure.[53]

The linestrength S is related to α_o at high pressures (> 100 Torr) given by:[12]

$$\alpha_o = S/\pi\Delta\nu_L \ (P_A/760) \ (273/T) \ N_l \qquad (2.14)$$

where $\Delta\nu_L$ is the pressure broadened linewidth (HWHM) given by:

$$\Delta\nu_L = \gamma_M P_T \qquad (2.15)$$

where γ_M is the pressure-broadening parameter for the gas mixture, P_T is the total gas pressure in Torr.

When dealing with more complex (larger) molecules the infrared TDL spectrum is very dense. The linestrengths of individual ro-vibrational lines have not been measured and calibration plots are thus necessary. A plot of $\alpha_o(\nu)$ versus absorber gas pressure (diluted to a known pressure in the particular parent gas used in the experiment) should yield a linear correlation.

When measurement of less than a few percent line center absorption is required second-harmonic (2f) detection techniques can be used. Second-harmonic detection is obtained by applying a sinusoidal modulation (0.5 to 10 kHz) from an external signal generator to the diode drive current. The modulation amplitude is chosen so as to optimize the 2f lineshape (see reference 54). A reference

signal from the function generator is fed into a lock-in amplifier and the absorption signal is detected synchronously at twice the modulation frequency.

2.3 Tunable Diode Lasers to Monitor Chemical Reactions

Although the use of TDL's for high resolution infrared spectroscopy has been widespread for the past decade,[49] the use of TDL's to monitor chemical reactions has been rather limited. TDL's have been used to monitor the reactions of nitric and nitrous acids,[55] the dissociation constant of H_2SO_4,[56] the reactions of HO_2 radicals,[57,58] the equilibrium between N_2F_4 and NF_2,[59] and analysis of the products resulting from the IRMPD of chloroform.[50]

Recently TDL's have been used to detect unstable species such as radicals[60] and molecular ions.[61] The use of TDL's to monitor transient infrared absorptions has been steadily increasing. Transient IR absorptions which were created in a gas following passage of a UV excimer laser pulse have been probed. Radicals such as CH_3,[62] SO,[63] CCO,[64] and CN[65] have been monitored by tuning the TDL probe to a characteristic absorption line. Other transient TDL experiments have involved probing gases which had been perturbed by Nd:YAG lasers,[66] Q-switched CO_2 lasers,[67,68] and excimer lasers.[69] In the past year there have been two reports dealing with TDL detection of

the transient species CF_2 following IRMPD of CF_2HCl.[70,71] Here again the TDL probe was tuned to a characteristic ro-vibrational transition of the transient species. TDL monitoring of the transient CF_2 species allowed for the measurement of reaction rate constants of CF_2 with Br_2, Cl_2 and H_2.[71]

2.4 Summary

In this thesis, the IRMPD of hexafluoroethane is studied using tunable diode lasers to monitor the stable and transient products of photolysis. Chapter 2 has provided a review of the processes involved in IRMPD, and also furnished the theory required for the quantitative analysis of stable photolysis products using tunable diode lasers.

CHAPTER 3

FLUOROCARBONS

3.1 IRMPD of Fluorocarbons

There have been a number of reports concerning the IRMPD of fluorocarbons. Fluorocarbons are ideal molecules for studies involving IRMPD; they exhibit strong IR absorption features in the region of emission of the CO_2 laser and are relatively easy to dissociate due to the high density of vibrational states.

Several reports on IRMPD deal with the unimolecular elimination of vibrationally excited $HF^{\dagger}$. One such study was that of Levy et al[72] involving the IRMPD of C_2H_5F, CH_2CHF, CH_2F_2 and CH_3CHF_2. The elimination of $HF^{\dagger}$ was monitored by IR chemiluminescence under collision-free and collisional conditions with added inert buffer gas. It was found that the degree of dissociation increased with the addition of buffer gas. The increase was more pronounced at lower fluence and was attributed to rotational relaxation of the fluorocarbon. In a similar study, Jang and Setser[73] reported on the elimination of $HF^{\dagger}$ from the IRMPD of C_2H_5F and CH_3CF_3. In this case the reaction yield of $C_2H_2F_2$ and C_2H_4 was measured by gas chromatography. The effect of added buffer gas was

studied at high and low fluence. At low fluence, long or medium length laser pulses resulted in a reduced dissociation yield when buffer gas was added. There was some enhancement with shorter pulses. At high fluence, there was enhancement or reduction of the dissociation yield with added buffer gas depending on the nature of the gas and the pulse length. The reduction of the dissociation yield was thought to be the result of collisional deactivation of highly vibrationally excited molecules by the buffer gas.

Another interesting type of IRMPD reaction involves dissociation by more than one reaction channel. One example of this type of dissociation involves the IRMPD of 1,2-dichloro-1,2-difluoroethane.[74]

$$CHClF\text{-}CHClF + mh\nu \rightarrow CClF{=}CHF + HCl^{\dagger} \qquad (3.1)$$

$$CHClF\text{-}CHClF + nh\nu \rightarrow CClF{=}CHCl + HF^{\dagger} \qquad (3.2)$$

The α,β molecular elimination of $HCl^{\dagger}$ and $HF^{\dagger}$ was monitored using infrared fluorescence. At low fluence the IR fluorescence spectrum clearly shows fluorescence due to $HCl^{\dagger}$ and faint fluorescence due to $HF^{\dagger}$. As the CO_2 laser fluence is increased the fluorescence due to $HF^{\dagger}$ grows much more rapidly than does that due to $HCl^{\dagger}$. At the highest fluence employed, the $HF^{\dagger}$ fluorescence totally dominates the fluorescence spectrum. The authors conclude

that the IRMPD of CHClF-CHClF involves the competitive molecular eliminations of $HCl^{\dagger}$ and $HF^{\dagger}$. The energetics of the two dissociation channels are not known, however the authors assume there is a difference of a few kcal mol^{-1} in the threshold energy between HCl and HF elimination. The pre-exponential factor A is assumed to be larger for the HF elimination than for HCl. The experimental results indicate that 1,2-dichloro-1,2-difluoroethane dissociates predominantly via the lower activation energy channel, HCl elimination, at low fluence. At higher fluence, the more highly excited molecules dissociate preferentially by HF elimination due to the larger A factor for this process.

In a recent publication by Kato et al[75] the IRMPD of $CF_3CF_2CHF_2$ was studied as a function of irradiation frequency and focal fluence. Br_2 was employed as a radical scavenger to reveal the primary and secondary dissociation pathways. This molecule exhibits two strong IR absorption peaks which can be used for excitation with a CO_2 laser. At low fluence the distribution of scavenged products remains the same regardless of irradiation frequency. The primary dissociation pathway proceeds mainly via the higher activation energy C-C bond ruptures rather than HF elimination. At higher fluence the product distribution exhibits large differences with respect to irradiation frequency. The authors propose that this difference is indicative of secondary photolysis of the

primarily produced radicals within the laser pulse at higher fluence, depending strongly on irradiation frequency. These results indicate that the primary dissociation pathway is independent of irradiation frequency, as expected from RRKM theory.

Another area of IR laser induced chemistry is isomerization. Yogev and Benmair[76] have reported on the IR laser induced electrocyclic isomerization of perfluorocyclobutene to the thermodynamically less stable hexafluorobutadiene in the presence of excess helium. Although the reaction rate is reduced upon the addition of helium, the reverse reaction reforming perfluorocyclobutene is completely quenched by the addition of 16 Torr of helium. This allows the quantitative conversion to the less stable isomer.

A similar reaction is the IRMP induced retro Diels-Alder dissociation of decafluorocyclohexene (DFCH) into tetrafluoroethylene and hexafluorobutadiene(HFBD).[77] The HFBD will isomerize to the more stable hexafluorocyclobutene (HFCB) unless argon is added as a buffer gas to stop the isomerization. It should be noted that the products of this IR laser induced dissociation are very different from those of thermal or ultraviolet photodecomposition. The products of thermal decomposition of DFCH are perfluorinated 1-methylcyclopentene, 1,2-dimethylcyclopentene and mesitylene.[78] Photodecompostion at 1849 A produces

perfluorinated 1-methylcyclopentene, methyl cyclopentane and other perfluorinated liquids.[79]

3.1.1 Laser Isotope Separation in Fluorocarbons

Fluorocarbons are prime candidates for laser isotope separation (LIS) schemes. This class of molecules exhibits strong absorption features in the output region of the CO_2 laser and is reasonably easy to dissociate. As pointed out in the previous chapter, the absorption of the first few photons by polyatomics in the discrete vibrational levels involves resonant transitions. Therefore, the IR laser can be tuned to a strong absorption feature of the desired isotopic species at a wavelength that is relatively transparent for the undesired isotopic species. The different spectral positions of the absorption bands of the two isotopic species is a result of the isotopic shift. For hydrogen isotopes the isotopic shift is typically hundreds of wavenumbers. The isotopic shift associated with heavier atoms is much smaller. The recent review by McAlpine and Evans[11] provides a detailed discussion of the processes involved in laser isotope separation as well as several experimental results related to laser isotope separation in intense IR laser fields.

A great many of the IR LIS schemes reported to date deal with the separation of hydrogen isotopes. There are several potential applications of the LIS of hydrogen

isotopes including: deuterium separation for heavy water production, tritium removal from light or heavy water moderators in nuclear reactors, and tritium removal from spent nuclear fuel.

Much of the research geared to the LIS of hydrogen isotopes deals with the IRMPD of fluorinated methanes and ethanes differing only in their isotopic (H/D/T) makeup. The degree of isotopic selectivity achieved in the IRMPD process is generally expressed by the enrichment factor β:

$$\beta(i/k) = ([i_p]/[k_p])([k_R]_o/[i_R]_o) \qquad (3.3)$$

where i and k represent the desired isotope and undesired isotope respectively. The brackets [ ] represent the concentrations of the reactant molecules (R) and the product fragments (P) of the indicated isotopic composition. The subscript o indicates the before photolysis concentration.

The first successful examples of D/H separation involved the IRMPD of the fluorocarbons CF_3CDCl_2[80] and CF_3D.[81-83] Among these experiments is the report of a single step D/H enrichment factor of >20000 by Herman and Marling.[83] For quite some time CF_3D was the most studied molecule with respect to hydrogen isotope separation. Several subsequent reports on the IRMPD of CF_3D and CF_3H have been published which discuss the effects of changing various experimental parameters

including irradiation frequency, fluence, intensity and pressure among others. These results are summarized in reference 11.

Recently there have been reports of successful T/H separation. Fluoroform (CF_3T) again was the molecule studied in IRMPD experiments by groups including Makide et al,[84,85] Takeuchi et al[86] and Neve de Mevergnies et al.[87] A T/H enrichment factor of ~ 3000 has recently been reported by Makide et al[88] in the IRMPD of C_2F_5T.

Although the isotopic shifts involved with carbon isotopes are very small, typically a few cm^{-1}, successful laser isotope separation is still possible. The majority of LIS experiments involving the separation of carbon isotopes employ halogenated methanes of the $CF_3(X)$ type, where X = Cl, Br or I. Among the successful separations of $^{13}C/^{12}C$ have been obtained with CF_3Cl,[89,90] CF_3Br,[89] and CF_3I.[91] CF_2Cl_2 has also been utilized for carbon isotope enrichment.[92] The selective dissociation of a much larger molecule, $CF_3{}^{13}COCF_3$, has recently been investigated by Hackett et al.[93-95]

A recent report by a Japanese group[96] deals with a cyclic LIS scheme involving the isotopically selective dissociation of C_2F_6 in the presence of the radical scavenger Br_2, followed by the selective dissociation of the $^{13}CF_3Br$ produced in the first step. By this process C_2F_6 with a ^{13}C content of >90% can be produced.

3.2 IRMPD and Pyrolysis Studies of Hexafluoroethane

There have been two previous studies involving the IRMPD of hexafluoroethane,[96,97] however both of these studies involve the use of radical scavengers. No results were reported for C_2F_6 in the absence of additives.

In the first study by Fisk,[97] various amounts of a hydrogen donor (H_2 or C_6H_{14}) were added to scavenge the IRMPD products. The low intensity absorption cross-section of the expected product CF_3H was measured and found to be about an order of magnitude less than that of C_2F_6 at the wavelength used for irradiation. Auxiliary experiments were performed on CF_3H that indicated this molecule was stable at the fluences used in the scavenging experiments, however it is not stated whether these studies were done in a "neat" CF_3H system or in the presence of C_2F_6.

Various amounts of the hydrogen donor were added to 3 Torr of C_2F_6 in a Pyrex cell and irradiated at 9R(36) for 30 pulses at a transmitted fluence of 6 J/cm^2. Concentrations of the reactants and products were measured on a Beckman IR4 spectrophotometer. Fisk found an increased consumption of C_2F_6 per pulse as the pressure of H_2 was increased from ~ 300 mTorr to 9 Torr. Conversely the per pulse consumption of C_2F_6 decreased from its low pressure maximum over the same pressure range when C_6H_{14} was the hydrogen donor. The major reaction products are

CF_3H and C_2F_4. CF_4 was observed in trace amounts, if any, even at low pressures of H_2. The ratio of CF_3H/C_2F_4 increased with pressure of the hydrogen donor up to ~ 1 Torr H_2 and ~ 3 Torr C_6H_{14} after which it decreases. This ratio was relatively insensitive to irradiation frequency. The consumption of C_2F_6 was reduced by a factor of 20 between R(34) and R(30). Variation of the fluence at 9R(36) did not affect the ratio greatly, however a 25% reduction in fluence reduced the C_2F_6 consumption by 3.5 times.

The experiments by Fisk suggest the primary IRMPD pathway is the result of C-C bond scission forming two CF_3 radicals. In the absence of a scavenger the consumption of C_2F_6 decreases by an order of magnitude. This should not be the case if primary dissociation produces CF_4 and CF_2. The donor can play two roles; first it can provide an abstraction pathway, and secondly the donor can collisionally deactivate vibrationally excited molecules.

The production of CF_3H via abstraction of a hydrogen atom by the CF_3 radicals from the hydrogen donor is self consistent. The pathway to the formation of C_2F_4 is less obvious. Fisk[97] proposes that at low donor pressure the majority of CF_3 radicals recombine to form vibrationally excited $C_2F_6^{\dagger}$ which, along with laser excited $C_2F_6^{\dagger}$ can then react with the hydrogen donor to form pentafluoroethane which then eliminates HF to form C_2F_4. Later Fisk concedes that the possibility of

secondary dissociation of the trifluoromethyl radicals to form CF_2 and F atoms may be the source of C_2F_4 via recombination. There is no mention of C_2F_5H as a reaction product in this work, nor has it been isolated in thermal studies. Fisk goes on to say that as the donor pressure is increased, more CF_3H is formed as recombination is less probable. As the donor pressure increases further deactivation of C_2F_6 by collisions with the donor molecules suppresses dissociation; therefore the CF_3H/C_2F_4 ratio decreases.

The second study involving the IRMPD of hexafluoroethane was done by Arai et al,[96] and employed Br_2 as a radical scavenger. As mentioned in the earlier part of this chapter this work was undertaken in an effort to produce high purity ^{13}C in a cyclic fashion by the IRMPD of C_2F_6 in the presence of Br_2, followed by a second stage IRMPD of the ^{13}C enriched CF_3Br.

In preliminary experiments Arai et al[96] irradiated 2 Torr C_2F_6 and 5 Torr Br_2 in a 36 cm long, 2 cm diameter Pyrex cell at 1084.64 cm^{-1} using a 7.5 cm focal length lens. The infrared absorption spectrum following irradiation showed product band absorptions due to CF_3Br and CF_2Br_2. The important mechanistic information gleaned from these experiments was that CF_3 radicals were the primary dissociation products resulting from the scission of the C-C bond of hexafluoroethane. These

radicals were then scavenged by Br_2 forming CF_3Br. CF_2Br_2 resulted from the secondary dissociation of CF_3 to CF_2 and F followed by bromination of CF_2 to yield CF_2Br_2.

3.2.1 Thermal Decomposition of Hexafluoroethane

The thermal decomposition of hexafluoroethane was first studied by Mercer and Pritchard[98] who pyrolysed C_2F_6 in a flow system with toluene as a carrier. In these studies the temperature was varied from 846-960°K and a rate constant for the decomposition of $C_2F_6 \rightarrow 2CF_3$ was found to be $k \approx 10^8 \exp(-50 \text{ kcal mol}^{-1}/RT)$ s^{-1}. The low activation energy and low frequency factor led Mercer and Pritchard to believe the reaction was heterogeneous and that pyrolysis was an unacceptable approach to measure the C-C bond dissociation energy in C_2F_6.

Several years later the thermal dissociation of C_2F_6 in the presence of H_2 at 1300-1600°K was investigated by Tschuikow-Roux.[99] The pyrolysis was undertaken in a single-pulse shock tube to assure short reaction times. The driver gas used was Helium. The reaction mixture was highly diluted in Argon in the ratio $Ar:H_2:C_2F_6 \approx 7500:17.4:1$. The reaction products were measured by gas chromatography using a 6 m silica gel (J) column. The principal reaction products identified were CF_3H and C_2F_4 with small amounts of C_3F_8 and trace amounts

of CF_2H_2. No C_2F_5H was detected.

The primary dissociation step in the pyrolysis of C_2F_6 involves the scission of the C-C bond. The trifluoromethyl radicals then abstract hydrogen to produce fluoroform. C_3F_8 is proposed to arise from the following sequence:

$$H + C_2F_6 \rightarrow C_2F_5 + HF \qquad (3.4)$$

$$CF_3 + C_2F_5 \rightarrow C_3F_8 \qquad (3.5)$$

Neither C_2F_5H (formed via hydrogen abstraction by pentafluoroethyl radicals) or C_4F_{10} were isolated. The formation of C_2F_4 was less certain. The author proposes that C_2F_4 comes from the decomposition of CF_3H into CF_2 and HF, followed by insertion of CF_2 to give the critically energized $C_2F_5H^{\dagger}$ which eliminates HF to form C_2F_4, and secondly from collisionally activated $C_2F_5H^{\dagger}$ formed via hydrogen abstraction by C_2F_5 radicals. CF_2H_2 formed via direct association of CF_2 with H_2 or by hydrogen abstraction and further reaction of the difluoromethyl radical:

$$CF_2 + H_2 \rightarrow CF_2H + H \qquad (3.6)$$

$$CF_2H + H_2 \rightarrow CF_2H_2 + H \qquad (3.7)$$

The first order rate constant for the dissociation of $C_2F_6 \rightarrow 2\ CF_3$ was found to be $k = 4.3 \times 10^{17} \exp(-94400/RT)\ s^{-1}$. The activation energy associated with the dissociation was listed as 94.4 ± 4 kcal/mole.

Politanski and Shevchuk[100] investigated the pyrolysis of fluoroform over a temperature range of 750-1000°C. The main products arising from the pyrolysis of fluoroform are hydrogen fluoride, tetrafluoroethylene, perfluoropropane, hexafluoroethane, perfluoroisobutylene and pentafluoroethane. Fluoroform was found to decompose homogenously by the first order reaction:

$$CHF_3 \rightarrow CF_2 + HF \qquad (3.8)$$

To determine whether CF_2 reacted with the parent CHF_3, experiments were conducted on pyrolysis of fluoroform with added C_2F_4 or CF_2HCl.

$$C_2F_4 \rightarrow 2CF_2 \qquad (3.9)$$

$$CF_2HCl \rightarrow CF_2 + HCl \qquad (3.10)$$

Although the thermal dissociation rate constants for reactions $k_{3.9}, k_{3.10}$ are $>> k_{3.8}$,[100] the pyrolysis rate of CHF_3 is not changed in the presence of C_2F_4 or CF_2HCl.

The authors thus concluded that the reaction scheme proposed by Tschuikow-Roux[101,102]

$$CF_2 + CHF_3 \rightarrow C_2F_5H^{\dagger} \rightarrow C_2F_4 + HF \quad (3.11)$$

$$C_2F_5H^{\dagger} + Ar \rightarrow C_2F_5H \quad (3.12)$$

does not occur. The small amount of C_2F_5H formed was a result of conversion of C_2F_4 and HF on the reactor wall. Further experiments on the pyrolysis of a C_2F_4-HF mixture under the same conditions as the fluoroform work indicate pentafluoroethane is one of the reaction products.

3.2.2 Thermodynamics

Thermodynamically the most favourable dissociation pathway of C_2F_6 leads to the production of CF_4 and CF_2. However, shock tube studies[103] suggest that this pathway possesses a large energy barrier. The next most favourable pathway is the result of C-C bond scission forming two CF_3 radicals, reaction (3.14).

		ΔH_o (kJ/mole)	
$C_2F_6 \rightarrow$	$CF_4 + CF_2$	-225.94	(3.13)
$\rightarrow$	$2\ CF_3$	-400.83	(3.14)

$\rightarrow$ $C_2F_5 + F$ +512.96 (3.15)

$\rightarrow$ $C_2F_4 + F_2$ +680.32 (3.16)

3.3 Summary

In the first part of this chapter a few examples of IRMP induced unimolecular dissociation and isomerization of fluorocarbons were presented. Fluorocarbons are ideal molecules for this type of study since they possess strong IR absorption features in the emission region of the CO_2 laser, and are relatively easy to dissociate. The resonant nature of absorption of the first few IR photons in IRMPA provides the basis for laser isotope separation of fluorocarbons differing only in their isotopic makeup. A few examples of LIS involving fluorocarbons were presented. The final section of Chapter 3 provides a review of the previous IRMPD and pyrolysis studies of hexafluoroethane.

CHAPTER 4

EXPERIMENTAL

4.1 Introduction

In Chapter 4 a description of the experimental techniques used in this thesis will be presented. Included will be discussions of gas handling techniques, sample preparation and CO_2 laser techniques. The middle section of the chapter will discuss the analytical techniques employed including; quadrupole mass spectrometry (MS), gas chromatography (GC), as well as Fourier transform infrared (FTIR) and tunable diode laser (TDL) infrared spectroscopy. Lastly a discussion of the high frequency modulation TDL technique, developed to monitor transient IR detection, will be presented.

4.2 Sample Handling

All gas samples were manipulated on a grease-free Pyrex vacuum line capable of achieving a background pressure of 10^{-6} Torr with a two stage Edwards E2M2 mechanical pump and an Edwards EO 40/55 vapour diffusion pump. The vacuum line was equipped with an Edwards PR10-C Pirani gauge (for roughing pressures) and an Edwards CP25-K Penning gauge to measure background pressures. Sample pressures were

measured with a Datametrics 600A Barocel Pressure Sensor (10.000 Torr), the calibration of which was verified using an oil manometer. and displayed on a Sonotek DRS4000K0B3 digital readout. Gas mixtures were made in cells or bulbs with cold-fingers that could be isolated with Pyrex O-ring type stopcocks from Ace Glass Incorporated.

The gases used in the two CO_2 lasers employed in this work were obtained from Canada Liquid Air Ltd., and included; He (high purity, 99.9995%), CO_2 (bone dry, 99.8%), compressed air (dry), and N_2 (high purity, 99.998%). Other gases obtained from Canada Liquid Air Ltd. include; H_2 (research purity, 99.9995%), CF_3H Freon 23 (98.0%), CF_4 Freon 14 (99.7%), O_2 (99.9%), and H_2 (zero grade) for gas chromatography. Gases obtained from Matheson Gas Products Canada Ltd. included; C_2H_4 (99.5%), C_3F_8 (99.3%), CF_3Br Freon 13B1 (99.0%), C_2F_6 Freon 116 (99.89%), COF_2 (97.0%), Ar (research purity, 99.9995%), CF_2HCl Freon 22 (99.9%), C_3F_6 (99.0%), $(CF_3)_2CO$ (99.9%) and N_2O (99%). The following fluorocarbons were obtained from SCM Specialty Chemicals, Gainesville, Florida (all purities are from 97-99%); C_4F_{10}, C_2F_5I, C_2F_4 (inhibited by d-limonene), C_2F_3Cl (inhibited by tributylamine), and CF_3I. CH_4 (99.5%) was obtained from Fisher Scientific Co. Ltd., CF_3D (98.0+ atom % D) and D_2 (99.5+ atom % D) from MSD Isotopes of Canada. n-Hexane (99.0% min) was

obtained from Caledon Laboratories Ltd.. Fluorocarbons were purified before use by bulb-to-bulb vacuum distillation using liquid nitrogen. Gas purity was checked by FTIR and TDL spectroscopy (where applicable) and periodically by quadrupole mass spectrometry.

The cells used for irradiation, stable product analysis and for Beer's Law plots were constructed of Pyrex or Monel. The cells were 2.5 cm in diameter, 10 cm long and equipped with Ace Glass Inc. O-ring sealed stopcocks. Each cell possessed a cold finger which could be isolated by a stopcock from the rest of the cell. The optical windows employed were made of NaCl or KCl (Janos Optical Corporation), the windows (slightly tilted off perpendicular to avoid laser feedback) were sealed to the cells with 5-minute epoxy (Lepage Ltd.).

4.3 Stable Product Analysis

Stable products were analyzed by quadrupole mass spectrometry (MS), and FTIR or TDL absorption spectroscopy. Qualitative results were periodically obtained with a Dycor Electronics Incorporated M200 Quadrupole Mass Spectrometer. FTIR spectra were recorded in the irradiation cells using a Nicolet 7199 FTIR spectrometer, at a resolution of 4 cm^{-1} unless otherwise stated. The tunable diode lasers employed were obtained from the Laser Analytics Division of Spectra Physics. The TDL'S were housed in a Laser Analytics, model

LS-3 cold head. The cold head was cryogenically cooled by a CTI Cryogenics helium compressor unit. The laser control module (LCM) and cryogenic temperature stabilizer (CTS) were obtained from Laser Analytics Inc..

The CO_2 laser employed was a low repetition rate (0.5 Hz) Lumonics K 922S TEA CO_2 laser, using a mixture of CO_2:N_2:He, fired with the use of a spark-gap. Approximately 70% of the laser pulse energy is contained in a narrow spike (200 ns) and the remainder in a tail of about 1 µs duration. The CO_2 laser beam was mildly focussed (at the center of the Pyrex cell) using a 25 cm focal length BaF_2 lens (Janos Optical Corp.). The laser focal fluence was calculated from the measured focal burn spot area on thermal sensitive paper and the pulse energy as measured on a Gentec, model ED-500 Joulemeter. The energy of the incident laser pulse was attenuated by a series of polyethylene sheets as necessary, to obtain the desired pulse energy and hence desired fluence.

The optical arrangement for the analysis of stable products using the TDL is shown in Figure 4.1. The cold head temperature and bias current applied to the TDL are adjusted to give single-mode operation in the desired spectral region. The TDL beam is collimated with an f/1 Ge lens, chopped by a mechanical chopper and passed through a sample cell after which it is focussed by an f/2 Ge lens onto a fast response time (400 ns) HgCdTe detector (Infrared

FIGURE 4.1

Tunable diode laser optical arrangement for the analysis of stable products.

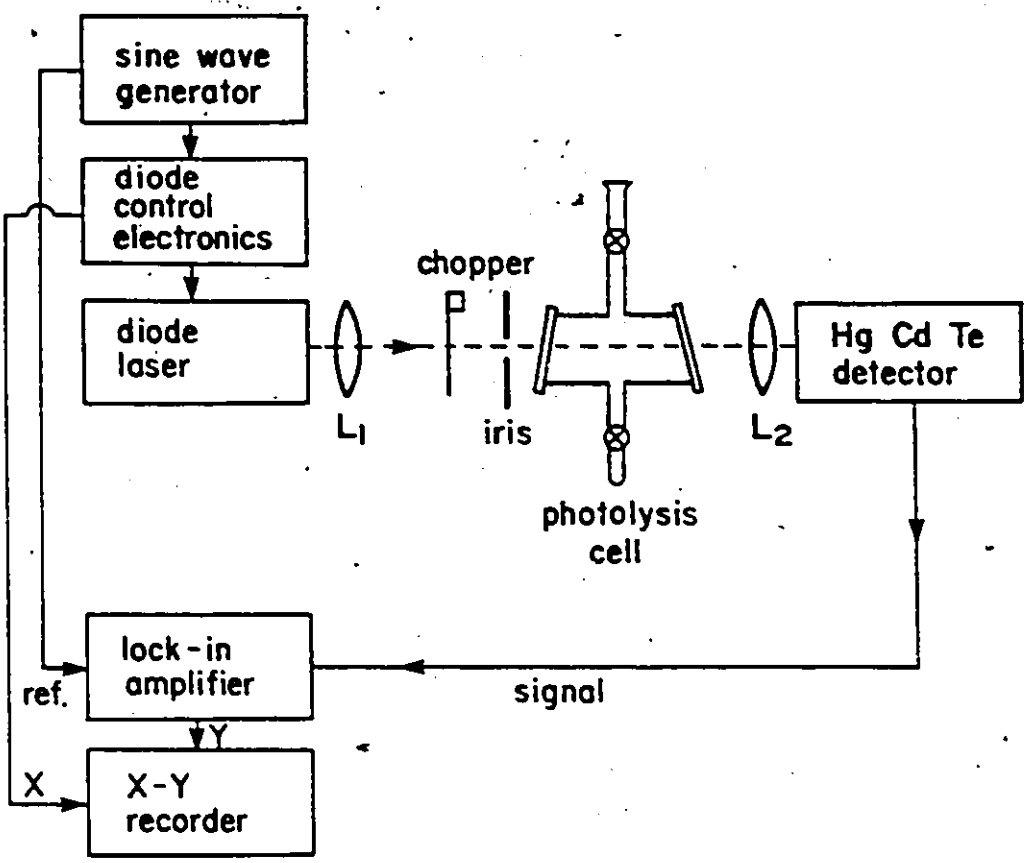
sine wave generator
diode control electronics
diode laser
chopper
L1
iris
L2
photolysis cell
Hg Cd Te detector
lock-in amplifier
ref.
signal
Y
X
X-Y recorder

Associates Inc. model HCT-100). The detector signal is fed into a lock-in amplifier (Princeton Applied Research model 126), phase-matched to the chopper to allow for phase sensitive detection. The output signal from the lock-in amplifier is fed into the Y input of a Hewlett-Packard model 7004B XY recorder. The recorder out signal from the LCM is used to ramp the X scale of the XY recorder. To record a spectrum, the TDL current is scanned across the absorption feature of interest. A 0.5 m grating monochromator (Jarrell-Ash model 82010) was used for wavenumber calibration of individual spectra to the nearest $\pm$ 0.1 cm^{-1}. A more precise frequency calibration can be obtained by employing calibrated absorption lines and a transmission etalon. As mentioned in Chapter 1 the linestrengths of individual ro-vibrational lines of larger molecules have not been measured. Therefore, from Beer's Law, $I(\nu_o) = I_o(\nu_o)\exp(-\alpha_o(\nu_o)L)$, plots of line center absorption coefficient (α_o) per cm^{-1} versus partial pressure of the absorber gas (diluted in hexafluoroethane) are made. Figure 4.2 illustrates the incident and transmitted intensities ($I_o(\nu_o)$ and $I(\nu_o)$) respectively. L is the absorber cell path length. In all cases, these plots were linear over the range of partial pressures involved in these studies. Figure 4.3 illustrates the line center absorption coefficient (α_o) versus partial pressure of C_2F_4 in

FIGURE 4.2

Tunable diode laser direct absorption spectrum of a CF_4 absorption feature at 1269.0 cm^{-1}. $I_o(\nu_o)$ and $I(\nu_o)$ are the incident and transmitted TDL intensities respectively.

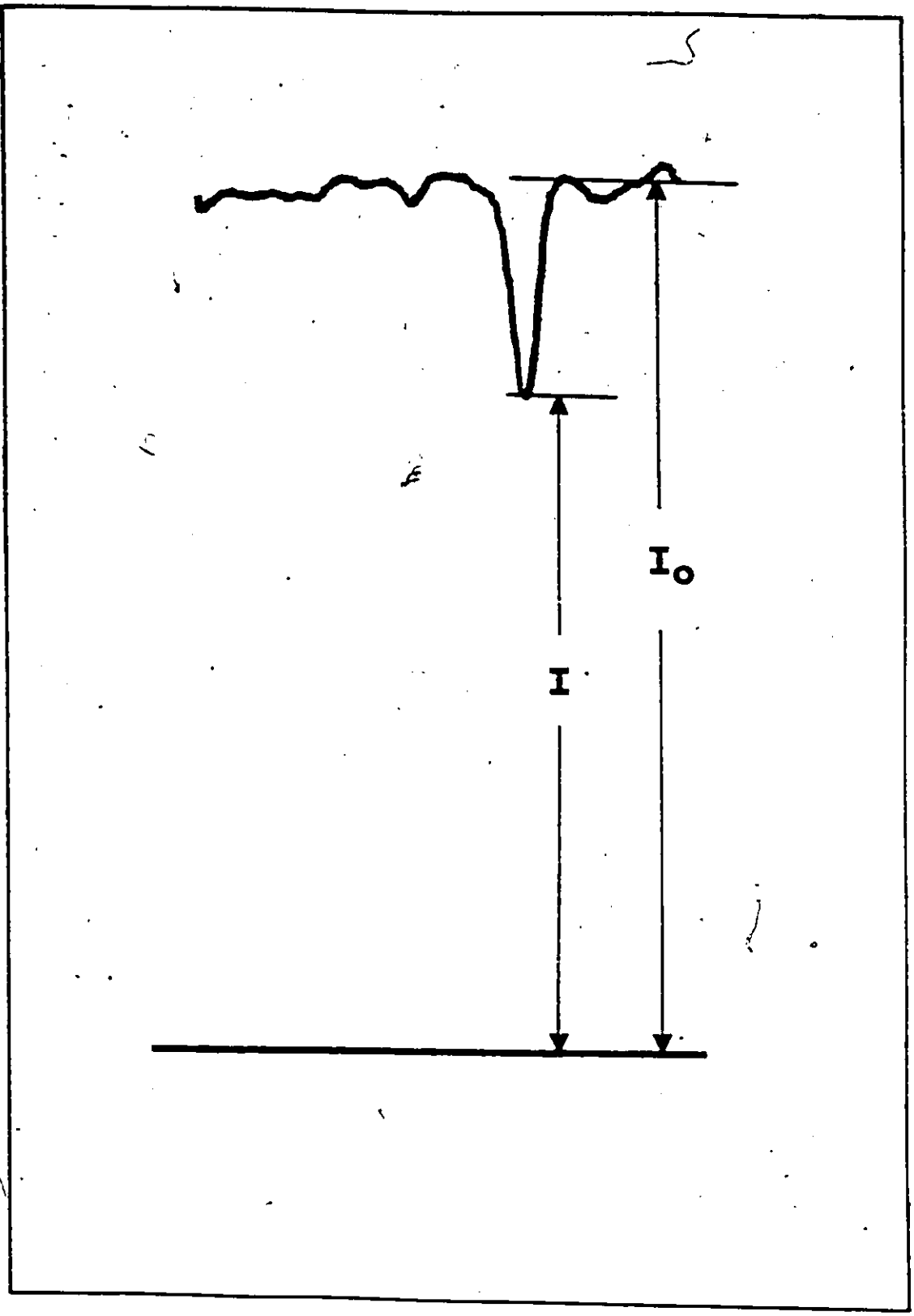
I_o
I

FIGURE 4.3

Line center absorption coefficient (α_o) versus partial pressure of C_2F_4 in hexafluoroethane (2 Torr total pressure), measured by tunable diode laser absorption spectroscopy at 1196.7 cm^{-1}.

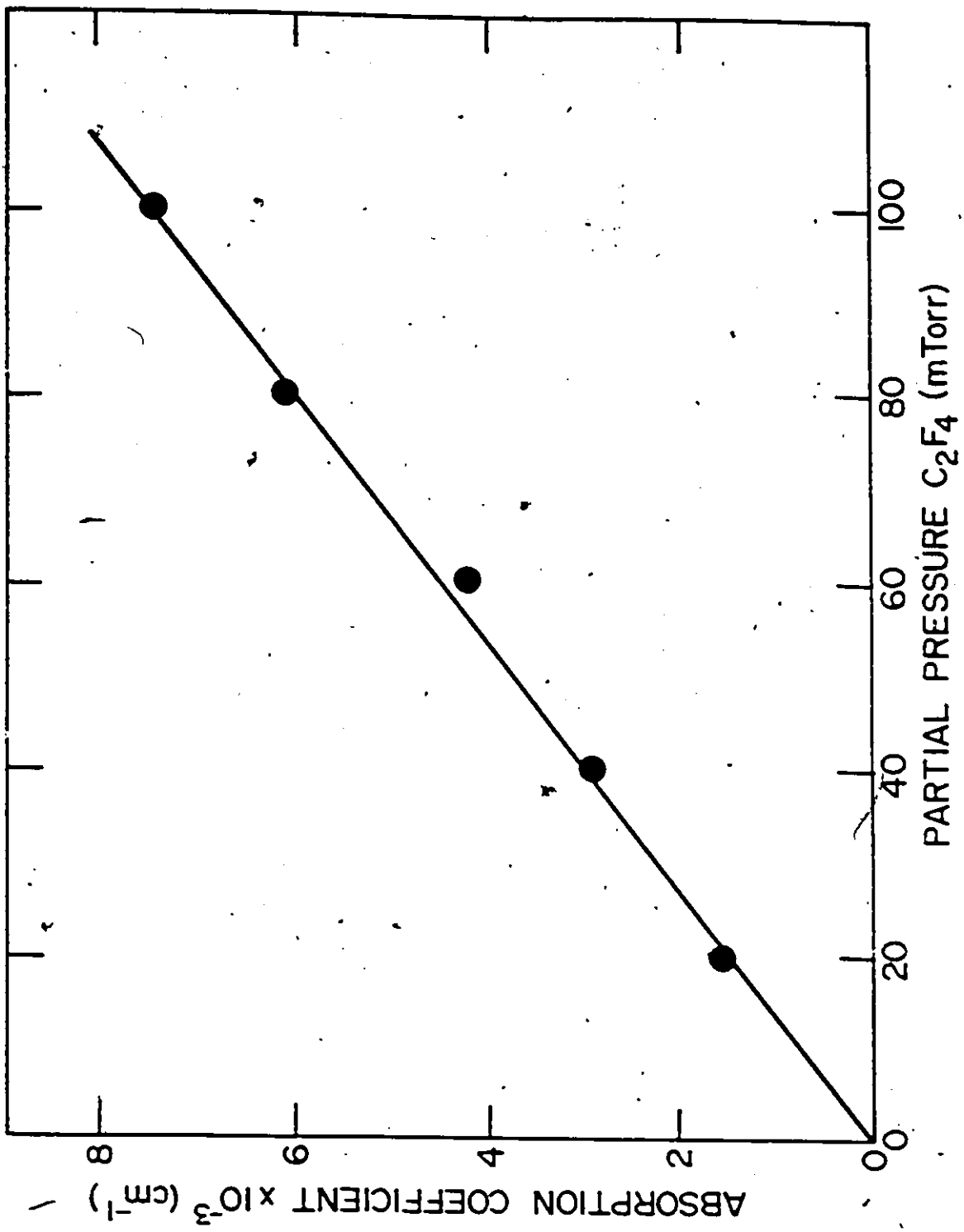
ABSORPTION COEFFICIENT x 10^{-3} (cm^{-1})
0
2
4
6
8
0
20
40
60
80
100
PARTIAL PRESSURE C_2F_4 (mTorr)

hexafluoroethane (2 Torr total pressure). Plots involving CF_4 and CF_3H are also linear over the range studied.

Second harmonic (2f) detection was used for high sensitivity work where less than a few % line center absorption was required. The TDL frequency is modulated at a few kHz by modulating the diode current. Synchronous detection at twice the modulation frequency, using the lock-in amplifier, achieves a major reduction in background noise. Quantification of the photolysis products in this case was done by comparison of the 2f signal strength to that of a standard sample containing a known and comparable amount of the fluorocarbon being measured. A full description of the second harmonic TDL detection technique is presented in reference 54. Typical 2f TDL signals of C_2F_6 before and after photolysis, as well as those of prepared standard samples are illustrated in figure 4.4.

In certain situations, stable products were measured by gas chromatography. The chromatograph employed was a Varian model 3700 equipped with a flame ionization detector (FID). Signals from the FID were sent to a Spectra Physics Autolab Minigrator for peak integration and then displayed on a Varian A-6 Chart Recorder. The column employed for GC separation was a 6 foot long Porapak Q 50/80.

To quantify the products resulting from the IRMPD of hexafluoroethane, an internal GC standard was used. A series of 1:1 mixtures of chlorotrifluoroethylene (internal

FIGURE 4.4

Second harmonic TDL absorption signals.

(A) 2 Torr C_2F_6 before photolysis.

(B) 2 Torr C_2F_6 after photolysis.

(C) Fluorocarbon standards (in C_2F_6, 2 Torr total pressure). C_2F_4 (1196.7 cm^{-1}), CF_4 (1269.0 cm^{-1}), CHF_3 (1162.6 cm^{-1}). CHF_3 is observed if H_2 is added prior to photolysis.

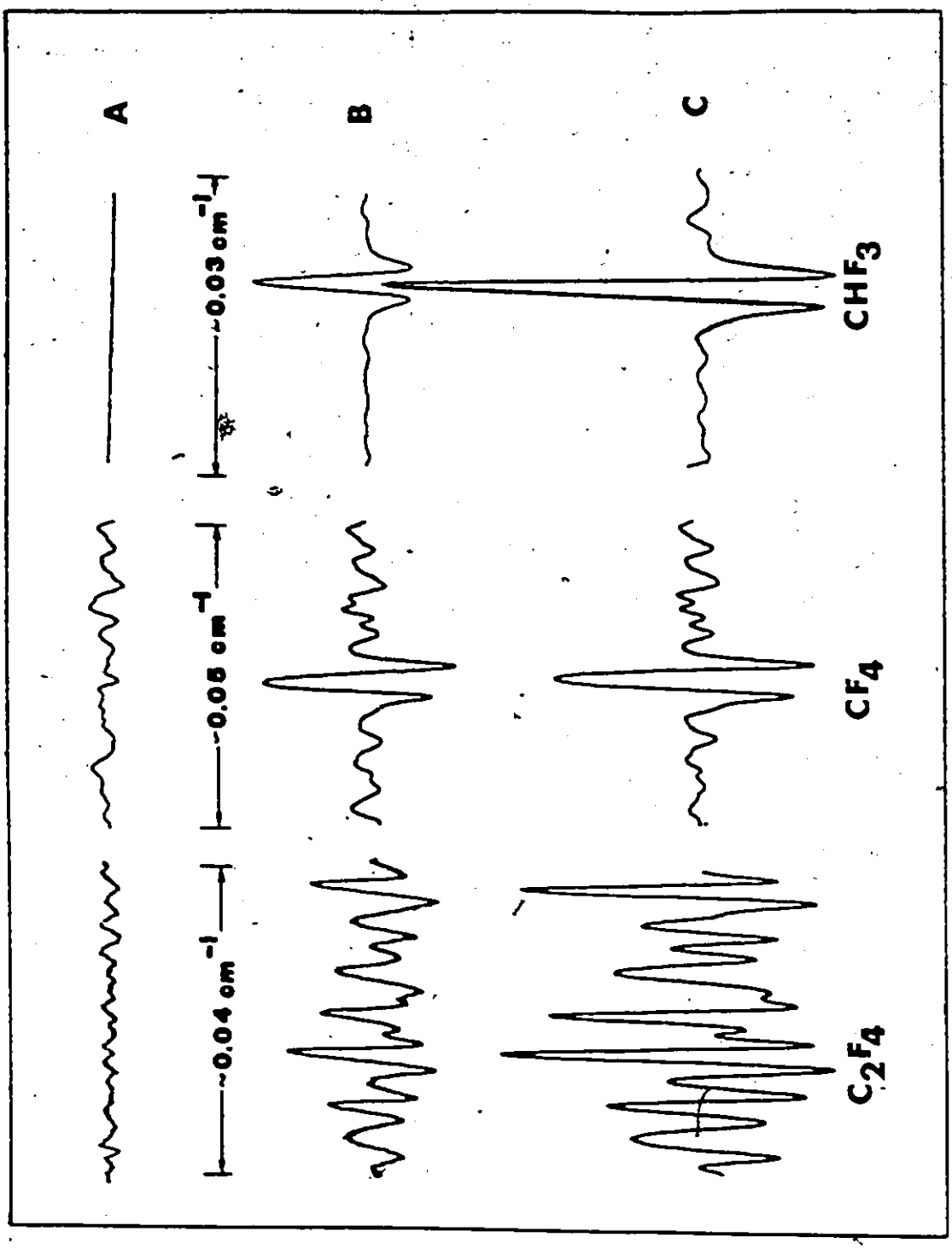
A
B
C
~0.03 cm⁻¹
~0.05 cm⁻¹
~0.04 cm⁻¹
CHF3
CF4
C2F4

standard) and C_2F_4, C_3F_8 or C_4F_{10} was prepared on the vacuum line. The mixture of internal standard and fluorocarbon was then vacuum distilled into a Pyrex sample holder equipped with an O-ring sealed Pyrex stopcock (Ace Glass Inc.) and a Tuf-Bond (Teflon/Silicone) septum from the Pierce Chemical Co., through which a sample could be withdrawn. 3.0 ml volume samples were withdrawn using a Precision Sampling Corporation Pressure-Lok 10.0 ml gas-tight syringe, and injected into the gas chromatograph.

The responses of each of the fluorocarbons relative to chlorotrifluoroethylene were recorded. These relative responses were then used to quantify the products of IRMPD of hexafluoroethane. The photolysis products were vacuum distilled into the GC sample holder and isolated. A known amount of the internal standard was then placed in the photolysis cell and then vacuum distilled into the GC sample holder containing the photolysis mixture. After warming, a 3.0 ml aliquot of the mixture was injected into the gas chromatograph. The amount of fluorocarbon present can then be determined from the following relationship:

$$F = (A_F/A_S)\ (S/R_f) \qquad (4.1)$$

where F is the fluorocarbon being measured in mTorr

A_F is the integrated area of the fluorocarbon GC peak

A_S is the integrated area of the internal standard GC peak

S is the amount of internal standard added in mTorr

R_f is the response factor of the specific fluorocarbon relative to that of the internal standard

4.4 Transient Infrared Detection

Since the detection of transient IR absorptions of species such as CF_2 and CF_3 was desired, preliminary spectroscopic measurements were made in a conventional steady state fast flow microwave discharge system (in collaboration with P.H. Beckwith and J.J. Orlando). A 2450 MHz Electro-Medical Supplies Microtron 200 Microwave Power Generator was employed to produce transient species in a fast flow system using a 300 l/min Welch Duo-Seal model 1373 vacuum pump. Preliminary experiments were carried out to characterize the CF_2 absorption spectra in a region of good single-mode operation of the TDL probe. A detailed description of the spectroscopy of CF_2 can be found in reference 104. N_2O and CH_4 reference lines were employed as frequency standards.[105] The TDL beam made four passes of the discharge cell, resulting in a 2.4 m total path length. An illustration of the IR spectra of ground state CF_2 ($\tilde{X}^1A_1$) radicals produced in the microwave discharge is presented in chapter 5. Following the production and detection of the desired transient

species in the discharge cell, a system was developed to monitor transient species following their production via IRMPD of a suitable halocarbon precursor (in collaboration with P.H. Beckwith).[106]

Figure 4.5 illustrates the experimental apparatus employed for the TDL detection of transient infrared absorptions. The waveguide cell consists of a 1 mm bore quartz capillary tube 15 cm long enclosed in a Pyrex tube 1.25 cm in diameter and 25 cm long. The Pyrex tube is fitted with 2.5 cm diameter NaCl windows (Janos Optical Corp.), tilted to avoid feedback of the laser. Precursor halocarbon gas is flowed through a flowmeter (Matheson Gas Products R7600, model 602 tube), passes through the waveguide cell with use of Cajon Ultra-Torr fittings and following photolysis and detection is pumped away with an Edwards E2M2 two-stage vacuum pump. The beam from a high repetition rate TEA CO_2 laser (Lumonics model 801A TEA CO_2 laser) is combined with the TDL probe beam at a ZnSe beamsplitter; both beams are then focussed with a 25 cm focal length BaF_2 lens (Janos Optical Corp.) into the capillary waveguide cell. After passing through the cell, the two laser beams are separated by a diffraction grating and the TDL probe beam is focussed onto a fast response time HgCdTe detector (Infrared Associates Inc., model HCT-100, 400 ns response time). The absorber gas cells shown in Figure 4.5 are placed in the path of the TDL beam to protect

FIGURE 4.5

Schematic diagram of the apparatus for detection of transient infrared absorptions. Lens L_1 collimates the output beam of the TDL, lens L_2 focuses both beams into the capillary waveguide cell. Lens L_3 focuses the TDL beam onto the HgCdTe detector. Mirror M_1 (ZnSe) transmits ~70% of the TDL radiation and reflects ~80% of the TEA CO_2 laser beam. Cells C_1 and C_2 contain absorber gases which prevent any scattered CO_2 radiation from reaching the TDL or the sensitive HgCdTe detector.

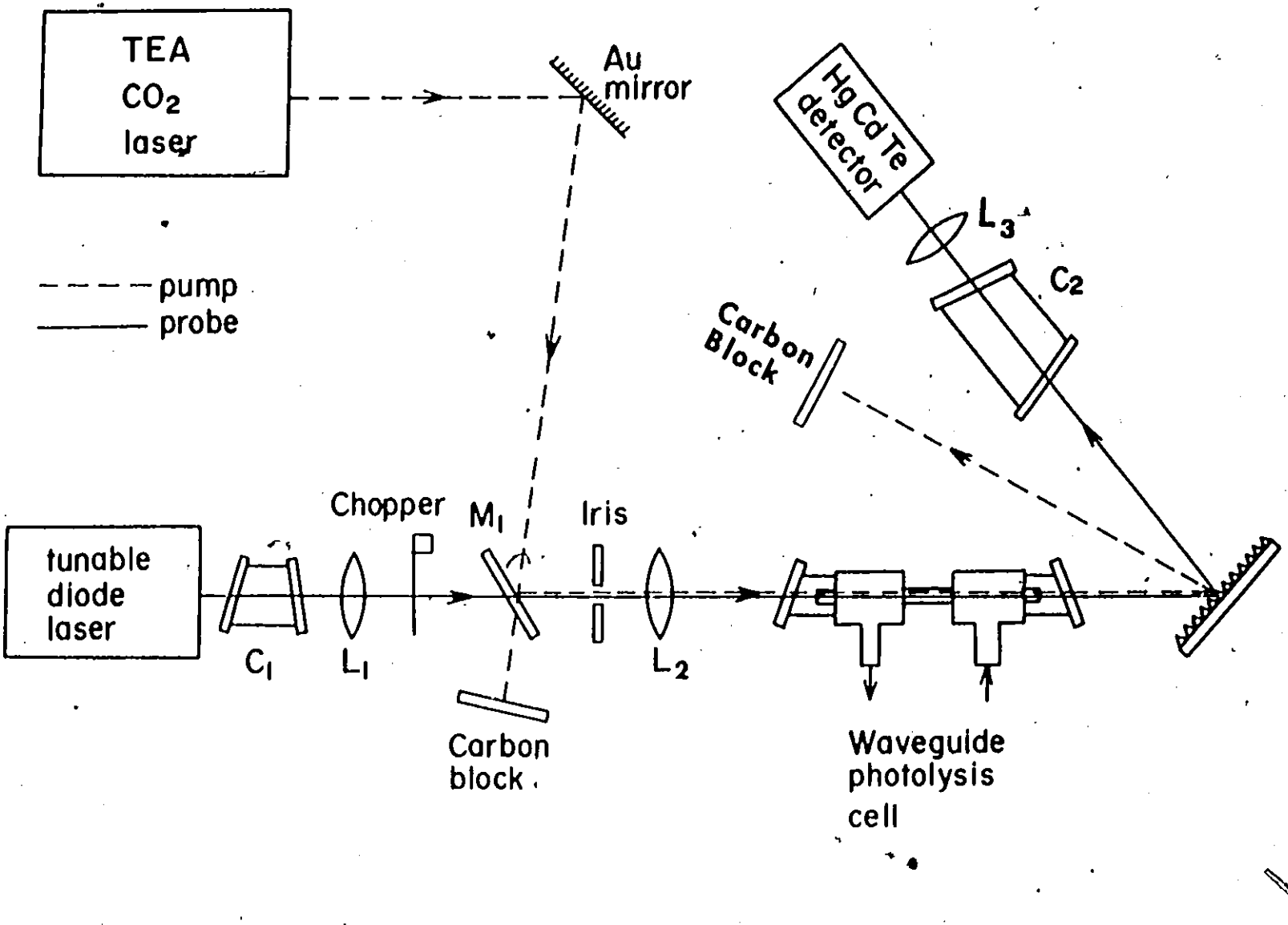
TEA
CO_2
laser
Au
mirror
Hg Cd Te
detector
L_3
C_2
pump
probe
Carbon
Block
Chopper
M_1
Iris
tunable
diode
laser
C_1
L_1
L_2
Carbon
block
Waveguide
photolysis
cell

various components of the detection system. Cell C_1 protects the TDL itself from scattered CO_2 laser radiation which could cause heating and a resultant shift in TDL output frequency. The second absorber cell C_2 is placed in front of the IR detector to protect the detector element from scattered CO_2 radiation which could damage it. These absorber cells are filled with a certain gaseous species which absorbs radiation at the output frequency of the CO_2 laser, but which is transparent at the detection frequency of the TDL probe. The gases employed as absorbers in this work and the frequency regions in which they absorb (in brackets) are; C_2H_4 (850 to 1020 cm^{-1}), $c\text{-}C_3H_6$ (990 to 1060 cm^{-1}) and $CFCl_3$ (1050 to 1095 cm^{-1}). Pulse energies of ~ 300 mJ at ~ 5 Hz repetition rate are obtained from the CO_2 laser, thus fluences up to 30 J/cm^2 can be achieved inside the capillary cell.

The main advantage of the transient TDL technique was to take advantage of the tunability of the TDL. The TDL probe wavelength was modulated at high frequency by applying a sinusoidal current (from a Hewlett Packard model 3311A Function Generator) to the TDL. This current modulation of the TDL leads to both amplitude and wavelength modulation of the TDL beam. The transient detection technique is illustrated with an idealized detector signal in Figure 4.6. Note that wavelength modulation leads to sampling the CF_2 doublet absorption feature twice per cycle in opposite

FIGURE 4.6

Schematic illustration of the transient detection of CF_2 using a wavelength modulated TDL. The TDL scans past the CF_2 doublet twice every cycle, and the detector output consists of an AM sine wave plus the absorption feature (a doublet here).

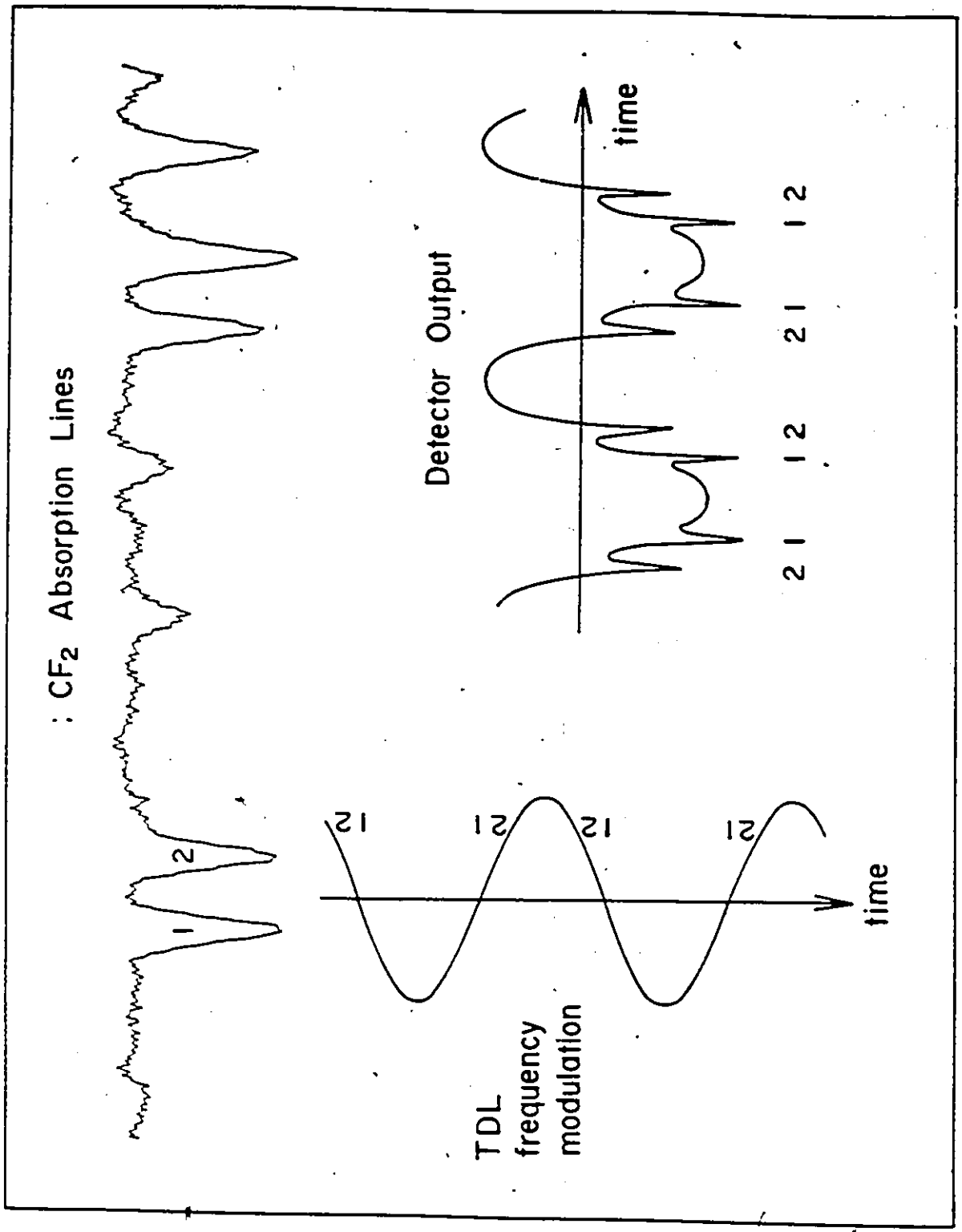
: CF_2 Absorption Lines
1
2
Detector Output
time
2 1 1 2 2 1 1 2
2 1 1 2 2 1 1 2
TDL
frequency
modulation
time

directions. The magnitude of the absorption is proportional to the concentration of CF_2 in the waveguide cell.

The TDL can presently be modulated up to 250 kHz, affording a time resolution of 2 μs. However electrical noise from the TEA CO_2 laser precludes any accurate absorption measurements for about the first 25 μs.

The signal and AM background component (CO_2 laser blocked) can both be stored on a Tektronics model 468 Digital Storage Oscilloscope. Any number of scans can be averaged to improve the signal to noise ratio. Subtraction of the AM background signal from the absorption signal on an IBM PC microcomputer removes the AM background component, as illustrated in Figure 4.7.

It has been shown that the sensitivity of the high frequency TDL modulation technique is limited by detector noise.[106] An analogue subtraction circuit was added to the experimental set up to remove most of the AM background component of the signal to allow better use of the digital storage oscilloscope's capabilities. With the addition of this analogue subtraction circuit, followed by digital subtraction, minimum detectable absorbances of ~ 3×10^{-5} were possible.[106]

Detailed descriptions of the IR spectroscopy of CF_2 and CF_3 can be found in references 104 and 107 respectively. A full description of the high frequency modulation TDL technique as it applies to the detection of

FIGURE 4.7

Experimental detection of CF_2. The CF_2 doublet (absorptions at 1242.9453 and 1242.9523 cm^{-1}) observed in the middle trace is produced by irradiating 500 mTorr of C_2F_3Cl in the capillary waveguide cell with a 9P(14) CO_2 laser pulse of ~10 J cm^{-2} fluence. Trace B is recorded with no gas in the cell, and both traces are averages of 32 successive scans performed by a digital storage oscilloscope. The TDL modulation frequency is 2.5 kHz.

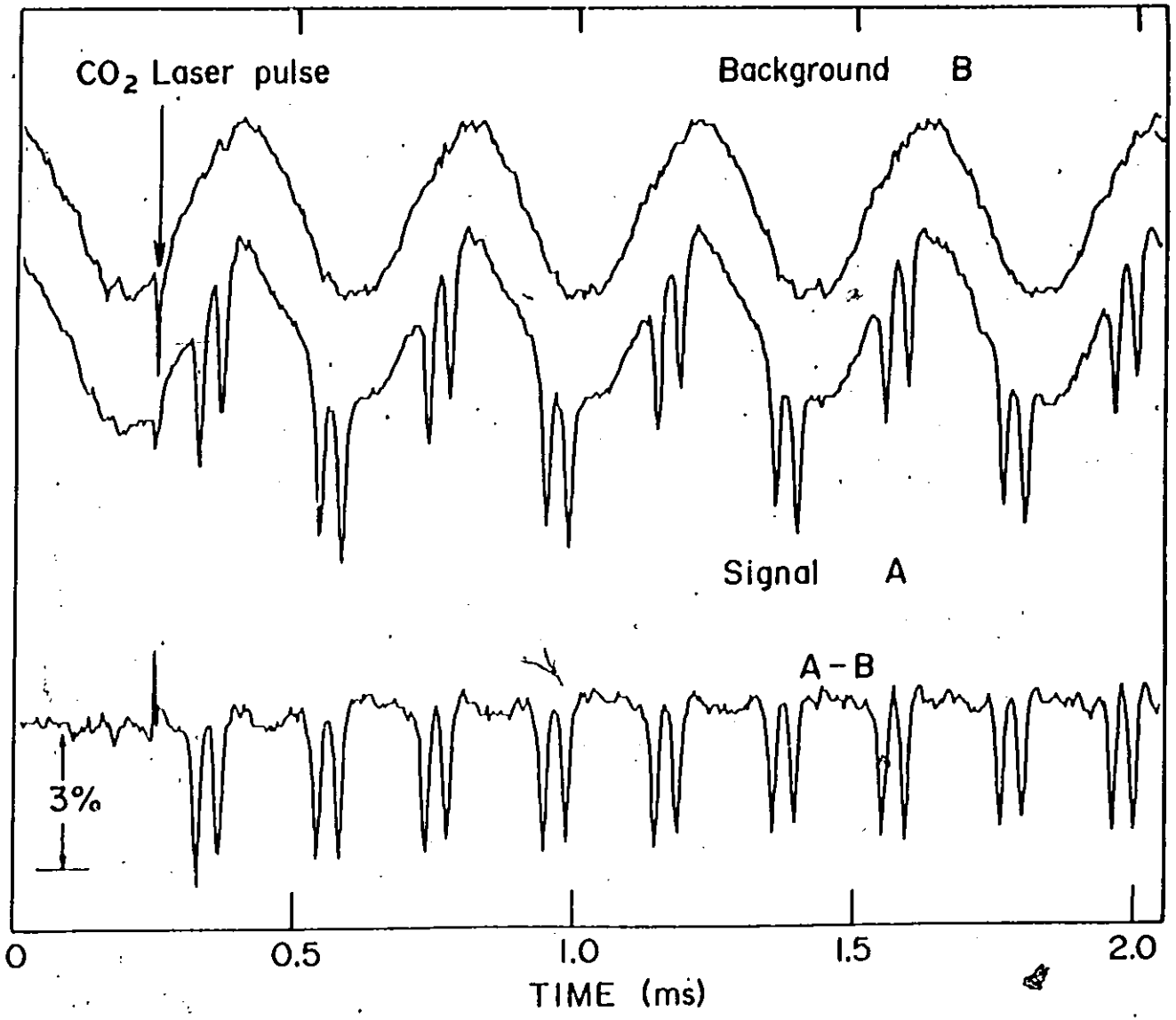
CO_2 Laser pulse
Background B
Signal A
A-B
3%
0
0.5
1.0
1.5
2.0
TIME (ms)

CF_2 and CF_3 radicals is presented in the results section of chapter 5.

Acknowledgements are due to P.H. Beckwith for his collaboration in obtaining the data for Figs. 4.6 and 4.7.

CHAPTER 5

RESULTS AND DISCUSSION

5.1 Introduction

The IRMPD of hexafluoroethane has been studied previously by two groups.[96,97] In the first of these reports, Fisk[97] irradiated hexafluoroethane in the presence of H_2 or C_6H_{14}, leading to the production of CHF_3 and C_2F_4. Several years later Arai et al[96] studied the IRMPD of hexafluoroethane with Br_2 added as a radical scavenger. The results of their experiments indicated that the major reaction products were CF_3Br and CF_2Br_2. Exploratory work in this laboratory on the IRMPD of "neat" hexafluoroethane showed that CF_4 was the major photolysis product with a lesser amount of C_2F_4. As indicated in Chapter 3, the thermodynamically most favourable dissociation pathway of C_2F_6 leads to the production of CF_4 and CF_2. However, shock tube studies suggest that this pathway possesses a large energy barrier.[103] The next most favourable pathway involves scission of the C-C bond forming two CF_3 radicals, reaction (5.2). Presumably the pre-exponential factor favours reaction (5.2) as well, since it only involves C-C bond breakage.

	ΔH_0 (kJ/mole)	
$C_2F_6 \rightarrow CF_4 + CF_2$	+225.94	(5.1)
$\rightarrow 2\ CF_3$	+400.83	(5.2)
$\rightarrow C_2F_5 + F$	+512.96	(5.3)
$\rightarrow C_2F_4 + F_2$	+680.32	(5.4)

In view of the uncertainty in the dominant reaction channel, and major discrepancy between our work and the literature, we initiated a programme to determine the overall mechanism of IRMPD of hexafluoroethane. From the outset, one of the major goals of this work was to use tunable diode lasers to measure the transient and stable products resulting from the IRMPD of hexafluoroethane.

5.2 IRMPD of "Neat" Hexafluoroethane

Efficient IRMPD of "neat" C_2F_6 was found to occur when it was subjected to relatively low fluence CO_2 laser pulses -30 cm^{-1} to the low frequency side of its ν_5 absorption band (see Figure 5.1). In our work, irradiation of "neat" hexafluoroethane samples using the 9R(30) and 9R(36) CO_2 laser lines, leads to the production of the major products CF_4, C_2F_4, C_3F_8 and C_4F_{10}.

FIGURE 5.1

FTIR spectrum of 2.1 Torr C_2F_6 in a 10 cm long, Pyrex cell, 4 cm^{-1} resolution, indicating the CO_2 laser pump lines used in irradiation.

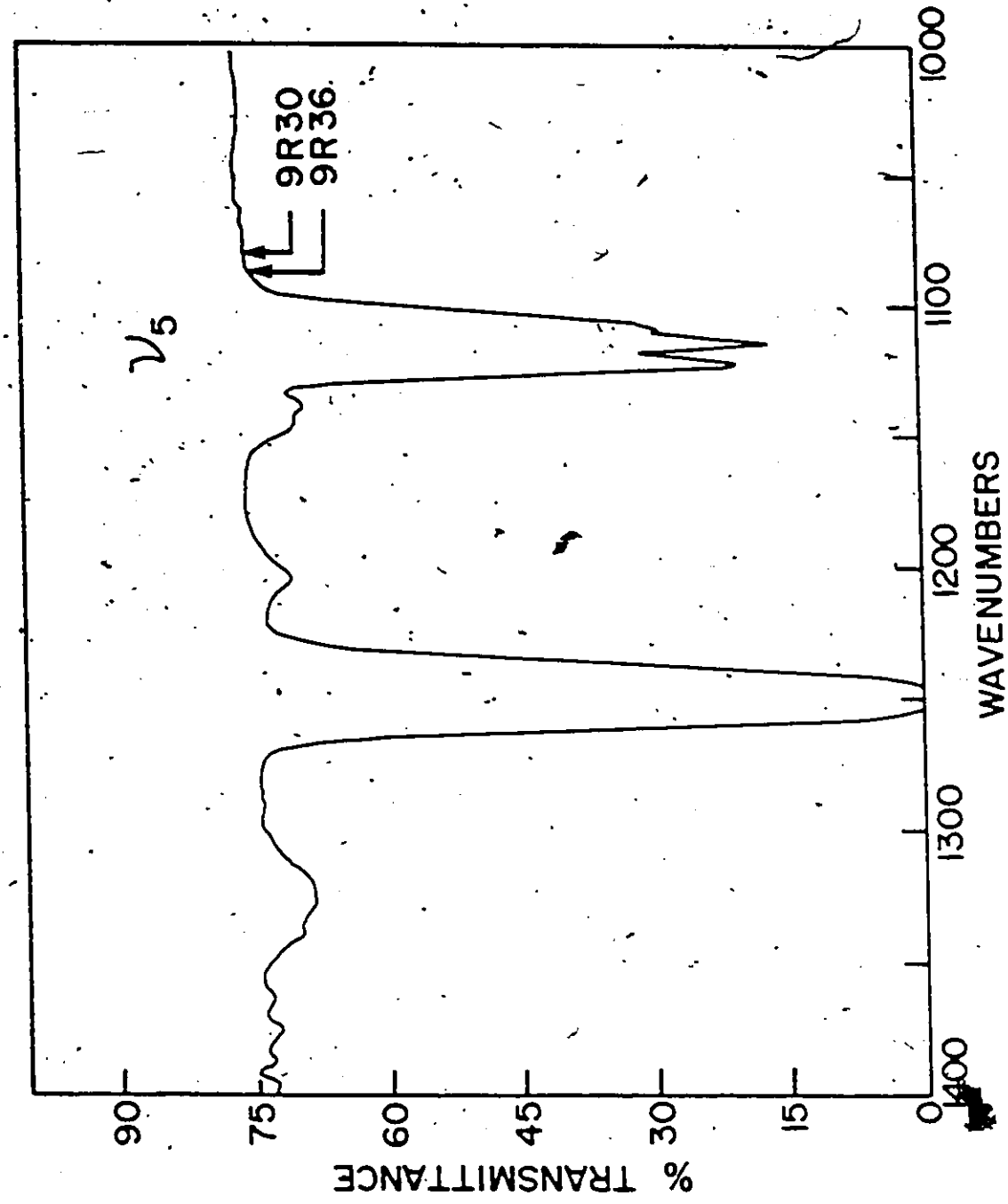
ν_5
9R30
9R36
1000
1100
1200
1300
1400
WAVENUMBERS
90
75
60
45
30
15
0
% TRANSMITTANCE

Figure 5.2 shows the FTIR spectrum of C_2F_6 after irradiation of a 2 Torr sample with 2000 CO_2 laser pulses at a fluence of 5.3 J cm^{-2} using the 9R(30) CO_2 laser line. IR absorptions due to the photolysis products CF_4, C_2F_4 and C_3F_8 are visible.

1 Torr samples of C_2F_6 were irradiated at a repetition rate of 0.5 Hz using the 9R(30) CO_2 laser line at fluences of 5.3 and 13.4 J cm^{-2}. The yields of CF_4 and C_2F_4 as a function of the number of laser pulses, (measured by TDL absorption spectroscopy), are listed in Table 5.1 and illustrated in Figures 5.3 and 5.4. CF_4 and C_2F_4 are measured using the TDL at 1269.0 cm^{-1} and 1196.7 cm^{-1} respectively. Although these plots illustrate yields after many pulses, it should be noted that TDL absorption measurements of CF_4 and C_2F_4 are possible after a single 13.4 J cm^{-2}, 9R(36) pulse using second harmonic detection (see Figure 5.5).

2 Torr samples of C_2F_6 were irradiated using the 9R(30) and 9R(36) CO_2 laser lines at fluences of 5.3 and 13.4 J cm^{-2}. With the 2 Torr samples C_3F_8 and C_4F_{10} yields are measured in addition to those of CF_4 and C_2F_4. CF_4 and C_2F_4 were first measured non-destructively by TDL absorption measurements at the frequencies listed above. C_2F_4 was also measured by gas chromatography, as were C_3F_8 and C_4F_{10}. For GC analysis, the photolyzed sample was transferred to a Pyrex

FIGURE 5.2

FTIR spectrum of 2.0 Torr C_2F_6 following irradiation with 2000 pulses using the 9R(30) CO_2 laser pump line at a fluence of 5.3 J cm^{-2}, in a 10 cm long, 2.5 cm diameter Pyrex cell.

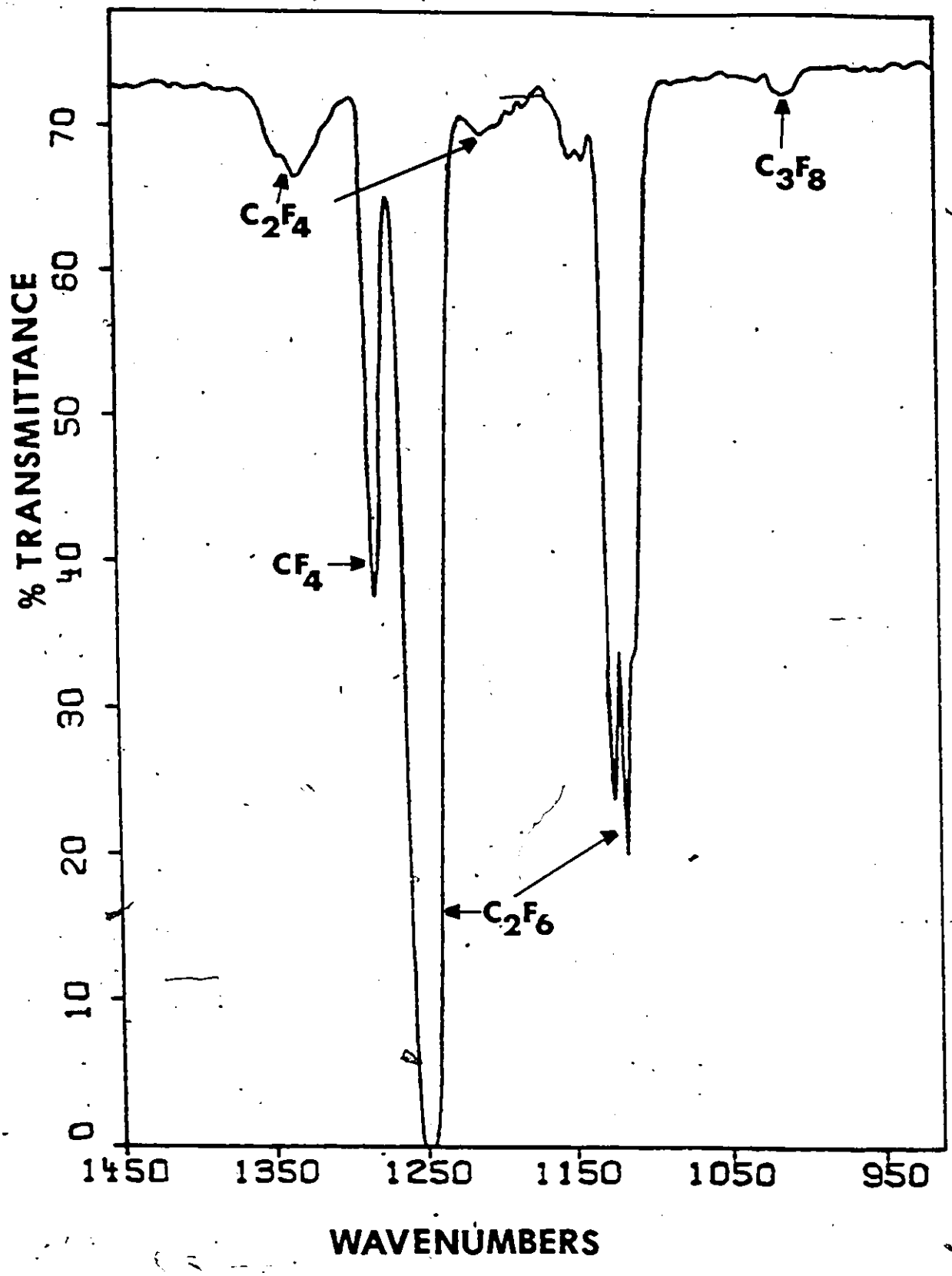
% TRANSMITTANCE
0
10
20
30
40
50
60
70
1450
1350
1250
1150
1050
950
WAVENUMBERS
C_2F_4
CF_4
C_2F_6
C_3F_8

Table 5.1

Yields of C_2F_4 and CF_4 following irradiation of 1 Torr of C_2F_6 in a 10 cm long, 2.5 cm diameter Pyrex cell with the 9R(30) CO_2 laser line, using a 25 cm focal length lens. The yields are the averages of six experiments ± one standard deviation.

Fluence ($J\ cm^{-2}$)	Number of Pulses	Yield (mTorr)	
		C_2F_4 TDL	CF_4 TDL
5.3	300	5.1±1.1	---
	600	7.9±1.9	12.6±3.2
	900	10.2±2.5	16.3±4.7
	1200	14.0±1.6	20.4±6.5
13.4	50	7.6±3.3	20.4±6.4
	100	10.3±3.5	34.7±9.9
	150	12.0±1.7	51.4±10.4
	250	17.5±4.2	80.0±11.7

FIGURE 5.3

Yield of C_2F_4 and CF_4 (mTorr) versus Number of Pulses, following irradiation of 1 Torr C_2F_6 in a 10 cm long, 2.5 cm diameter Pyrex cell, using a 25 cm focal length BaF_2 lens, at a fluence of 5.3 J cm^{-2} with the 9R(30) CO_2 laser line. O C_2F_4 TDL (1196.7 cm^{-1}), □ CF_4 TDL (1269.0 cm^{-1}).

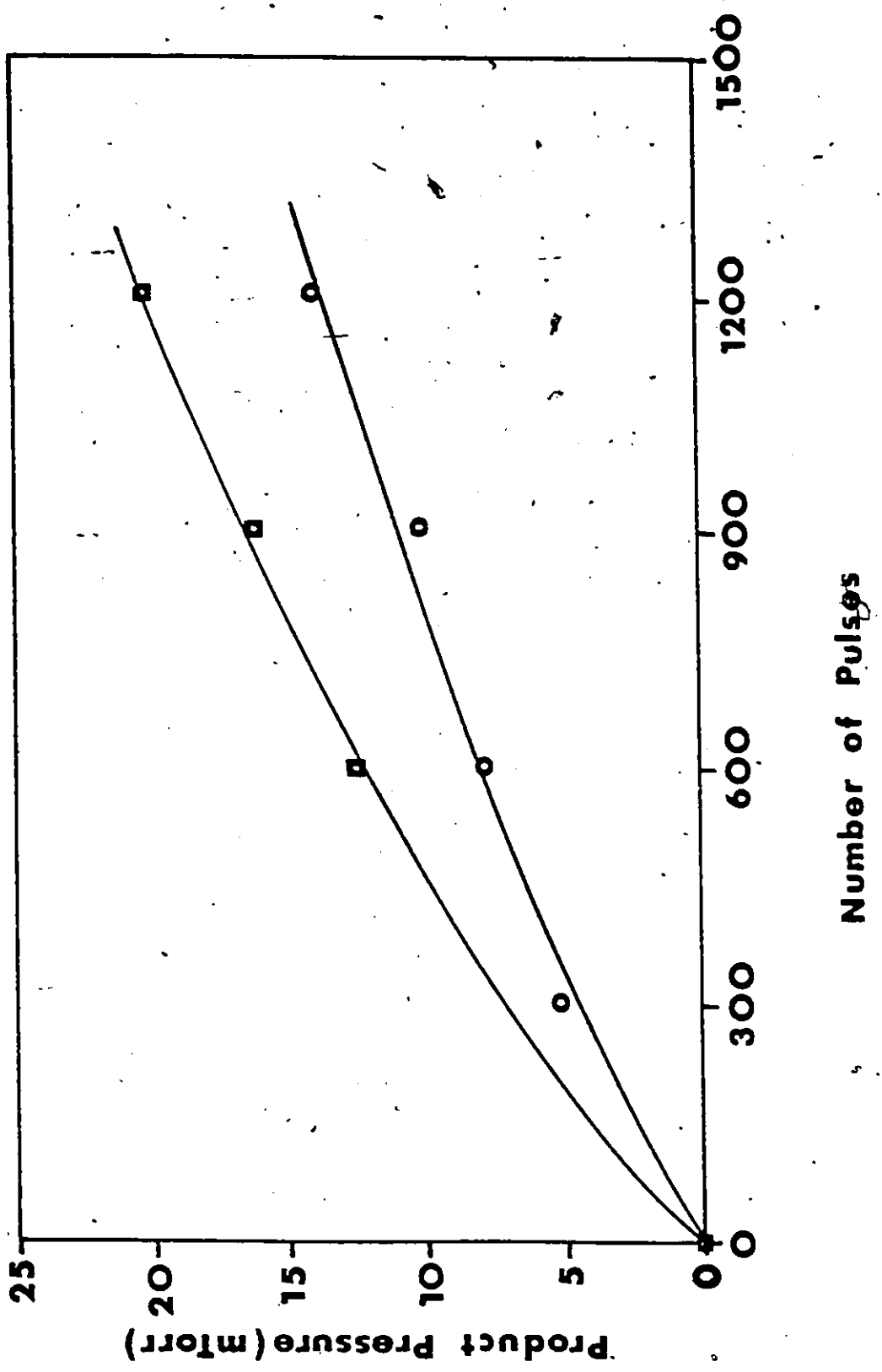
Product Pressure (mtorr)
25
20
15
10
5
0
0
300
600
900
1200
1500
Number of Pulses

FIGURE 5.4

Yield of C_2F_4 and CF_4 (mTorr) versus Number of Pulses, following irradiation of 1 Torr C_2F_6 in a 10 cm long, 2.5 cm diameter Pyrex cell, using a 25 cm focal length BaF_2 lens, at a fluence of 13.4 J cm^{-2} with the 9R(30) CO_2 laser line. O C_2F_4 TDL (1196.7 cm^{-1}), □ CF_4 TDL (1269.0 cm^{-1}).

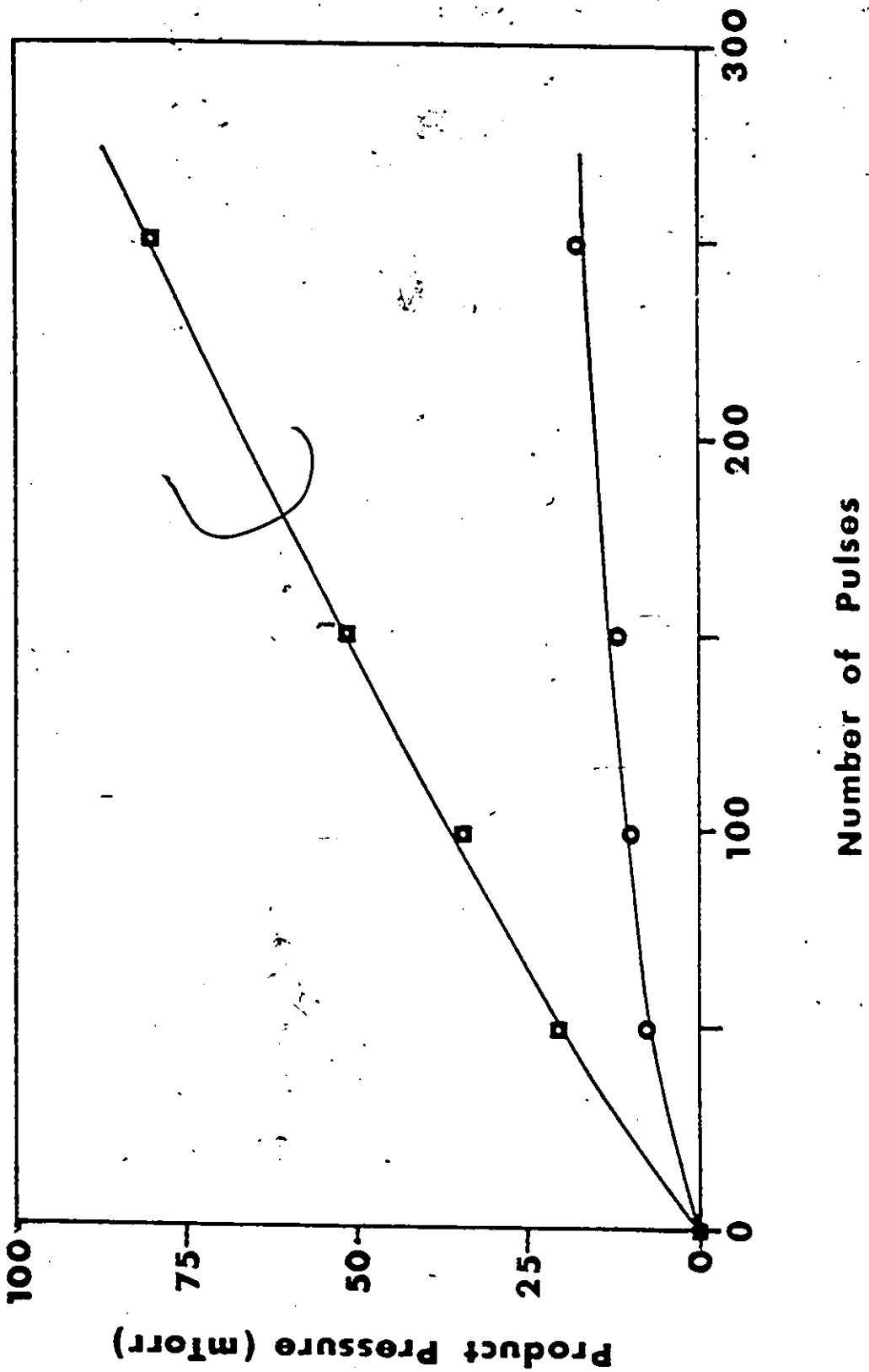
Product Pressure (mTorr)
100
75
50
25
0
0
100
200
300
Number of Pulses

FIGURE 5.5

Yield of C_2F_4 and CF_4 (mTorr) versus Number of Pulses, following irradiation of 2 Torr C_2F_6 in a 10 cm long, 2.5 cm diameter Monel cell, using a 25 cm focal length BaF_2 lens, at a fluence of 13.4 J cm^{-2} with the 9R(30) CO_2 laser line. The products were measured by second harmonic TDL absorption spectroscopy at 1196.7 and 1269.0 cm^{-1} respectively.

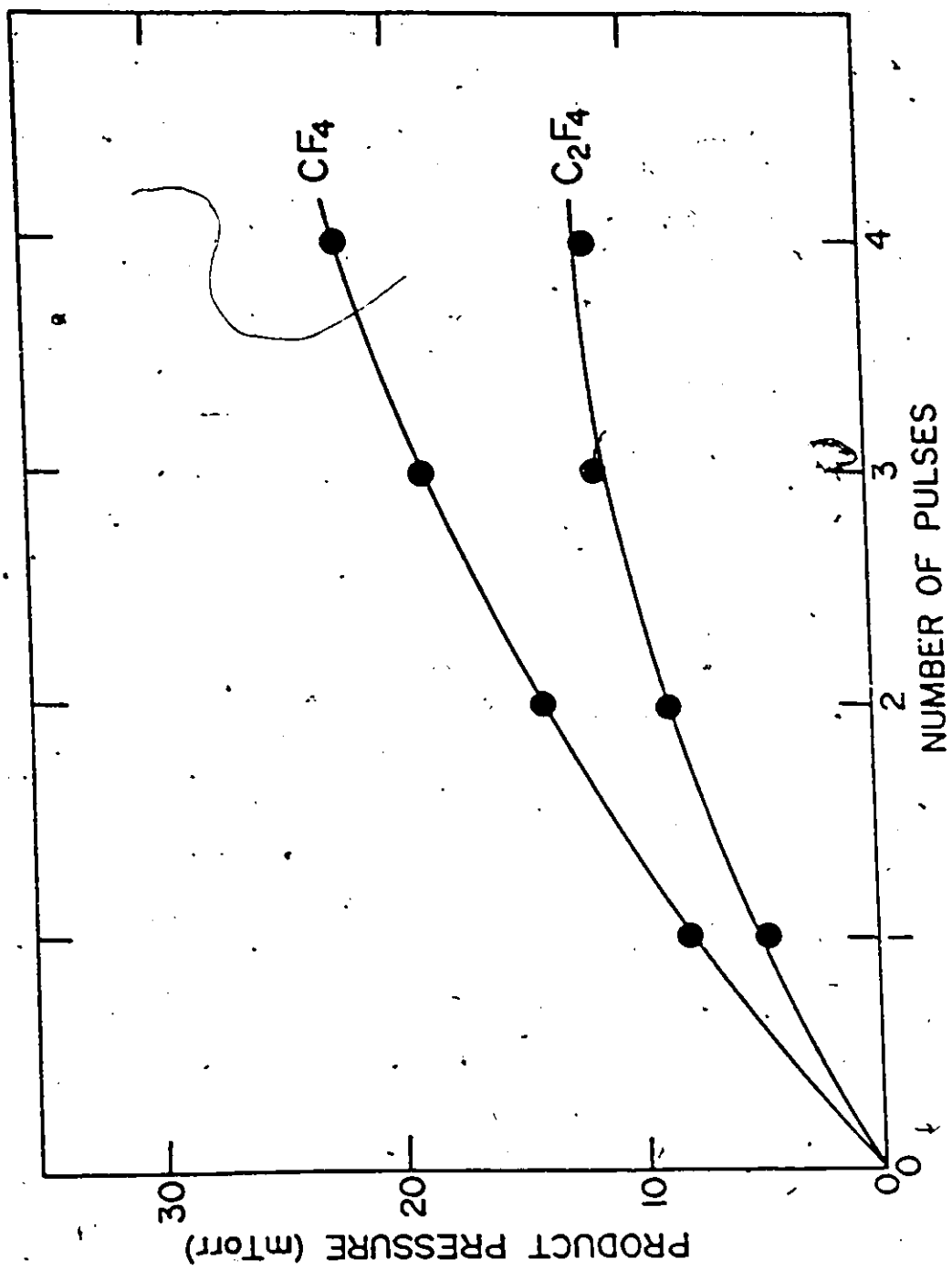
CF4
C2F4
PRODUCT PRESSURE (mTorr)
NUMBER OF PULSES
0
10
20
30
1
2
3
4

sample holder as described in chapter 4 and mixed with a known amount of internal standard (C_2F_3Cl). A 3.0 ml vapour phase aliquot of the photolyzed sample/internal standard mixture was withdrawn with a gas-tight syringe and injected onto the Porapak Q GC column. The chromatograph was maintained at 30°C for 16 minutes after which the temperature was increased at a rate of 5°C/min to a final temperature of 90°C. C_2F_6 is the first peak eluted from the GC column, followed by C_2F_4, C_3F_8, C_2F_3Cl and C_4F_{10}. The relative retention times of these compounds are illustrated in Figure 5.6. The yields of CF_4, C_2F_4, C_3F_8 and C_4F_{10} resulting from the IRMPL of 2 Torr of C_2F_6 are listed in Tables 5.2 and 5.3, and are illustrated in Figures 5.7 to 5.10. The following trends should be noted; CF_4 is the dominant product at all wavelengths and fluences studied. Conversely, the C_4F_{10} is the least abundant product in all cases. At low fluence C_3F_8 is the second most abundant product at both wavelengths. As the fluence is increased the yield of C_2F_4 increases relative to C_3F_8. Separate experiments with C_2F_4 added before irradiation indicate that C_2F_4 is also consumed in the presence of C_2F_6 under similar experimental conditions. Therefore absolute quantitative yields of C_2F_4 after several IR laser pulses are possibly not a true reflection of the overall IR photochemistry involved.

FIGURE 5.6

Gas chromatogram illustrating the relative retention times of C_2F_6, C_2F_4, C_3F_8, C_2F_3Cl and C_4F_{10}. The GC column was a 6 foot long Porapak Q 50/80, maintained at 30°C for 16 minutes after which the temperature was increased at a rate of 5°C/min to a final temperature of 90°C.

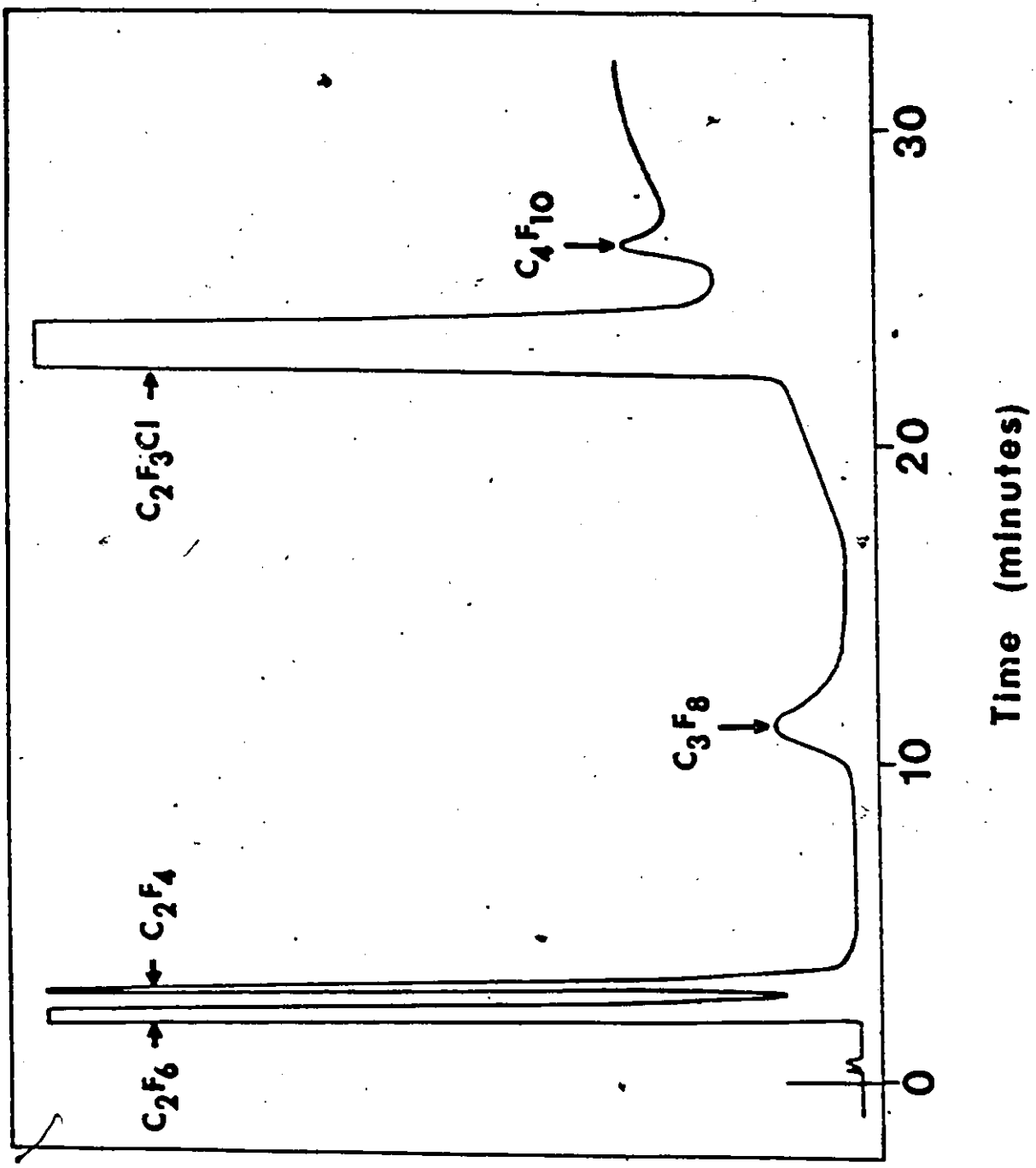
C_2F_6
C_2F_4
C_3F_8
C_2F_3Cl
C_4F_{10}
0
10
20
30
Time (minutes)

Table 5.2

Yield of products following irradiation of 2 Torr of C_2F_6 in a 10 cm long, 2.5 cm diameter Pyrex cell with the 9R(30) CO_2 laser line, using a 25 cm focal length lens. The yields are the average of six experiments ± one standard deviation.

Number of Pulses	Yield (mTorr)				
	C_2F_4		CF_4	C_3F_8	C_4F_{10}
	GC	TDL	TDL	GC	GC
a) 5.3 J cm^{-2}					
300	12.4±3.9	12.8±4.4	108.2±1.4	20.0±4.6	2.6±0.8
450	15.8±3.1	15.8±3.7	161.9±10.9	36.0±6.1	4.8±1.2
600	14.7±8.0	15.7±7.4	241.7±5.6	46.7±11.9	7.4±0.4
b) 13.4 J cm^{-2}					
50	17.8±1.4	17.9±1.3	101.4±9.3	11.9±1.3	2.1±0.5
100	25.2±2.1	25.8±2.9	175.5±6.4	27.4±2.0	4.9±1.1
200	31.1±2.6	30.9±2.6	274.7±19.4	52.3±2.9	10.6±3.8

FIGURE 5.7

Yield of products (mTorr) versus Number of Pulses, following irradiation of 2 Torr C_2F_6 in a 10 cm long, 2.5 cm diameter Pyrex cell, at a fluence of 5.3 J cm^{-2} using a 25 cm focal length BaF_2 lens, with the 9R(30) CO_2 laser line. ● C_2F_4 GC, O C_2F_4 TDL (1196.7 cm^{-1}), □ CF_4 TDL (1269.0 cm^{-1}), ▲ C_3F_8 GC, ■ C_4F_{10} GC. The symbols ● and O are always superimposed in this plot.

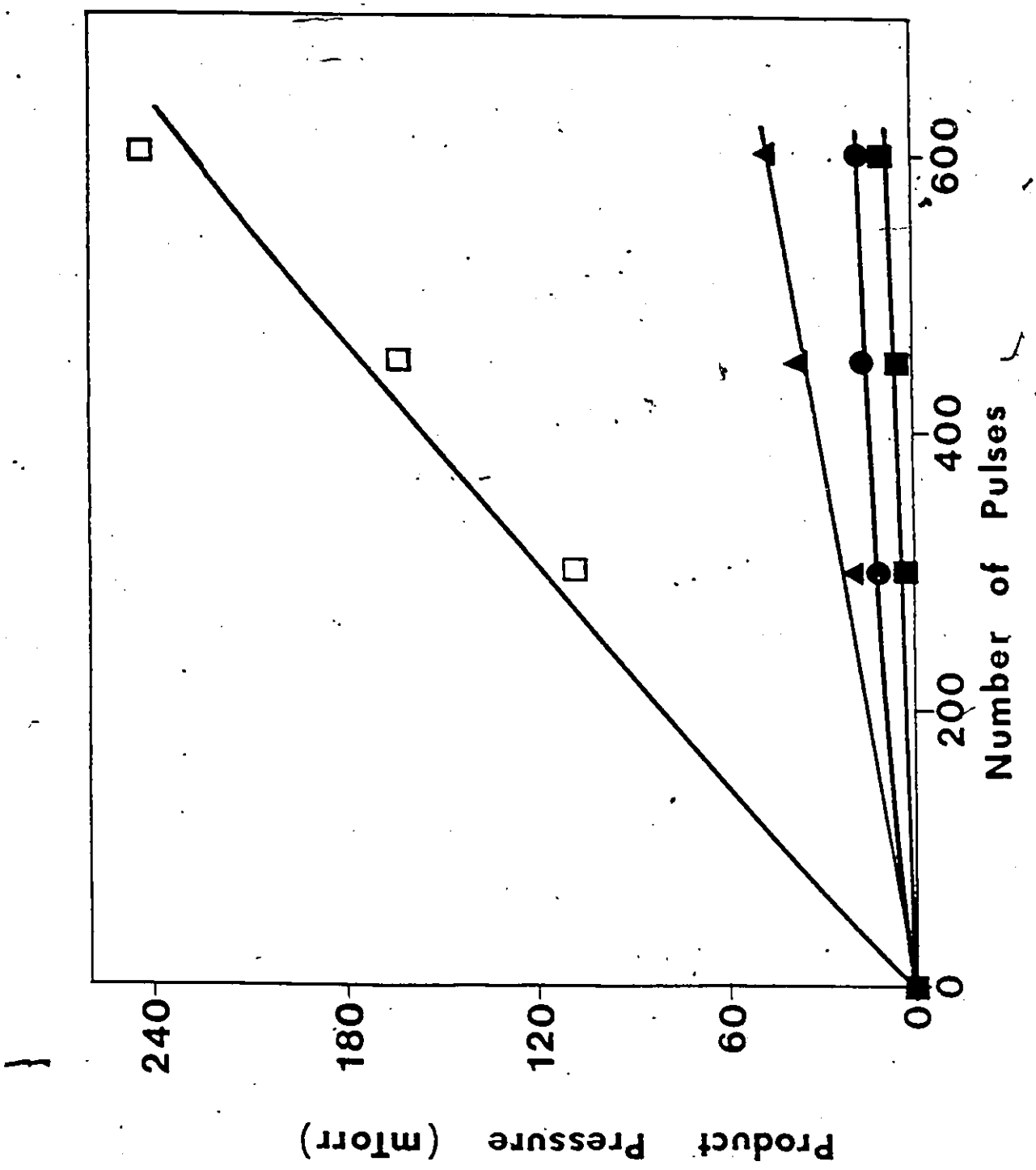
Product Pressure (mtorr)
240
180
120
60
0
0
200
400
600
Number of Pulses

FIGURE 5.8

Yield of products (mTorr) versus Number of Pulses, following irradiation of 2 Torr C_2F_6 in a 10 cm long, 2.5 cm diameter Pyrex cell, at a fluence of 13.4 J cm^{-2} using a 25 cm focal length BaF_2 lens, with the 9R(30) CO_2 laser line. ● C_2F_4 GC, O C_2F_4 TDL (1196.7 cm^{-1}), □ CF_4 TDL (1269.0 cm^{-1}), ▲ C_3F_8 GC, ■ C_4F_{10} GC. The symbols ● and O are sometimes superimposed in this plot.

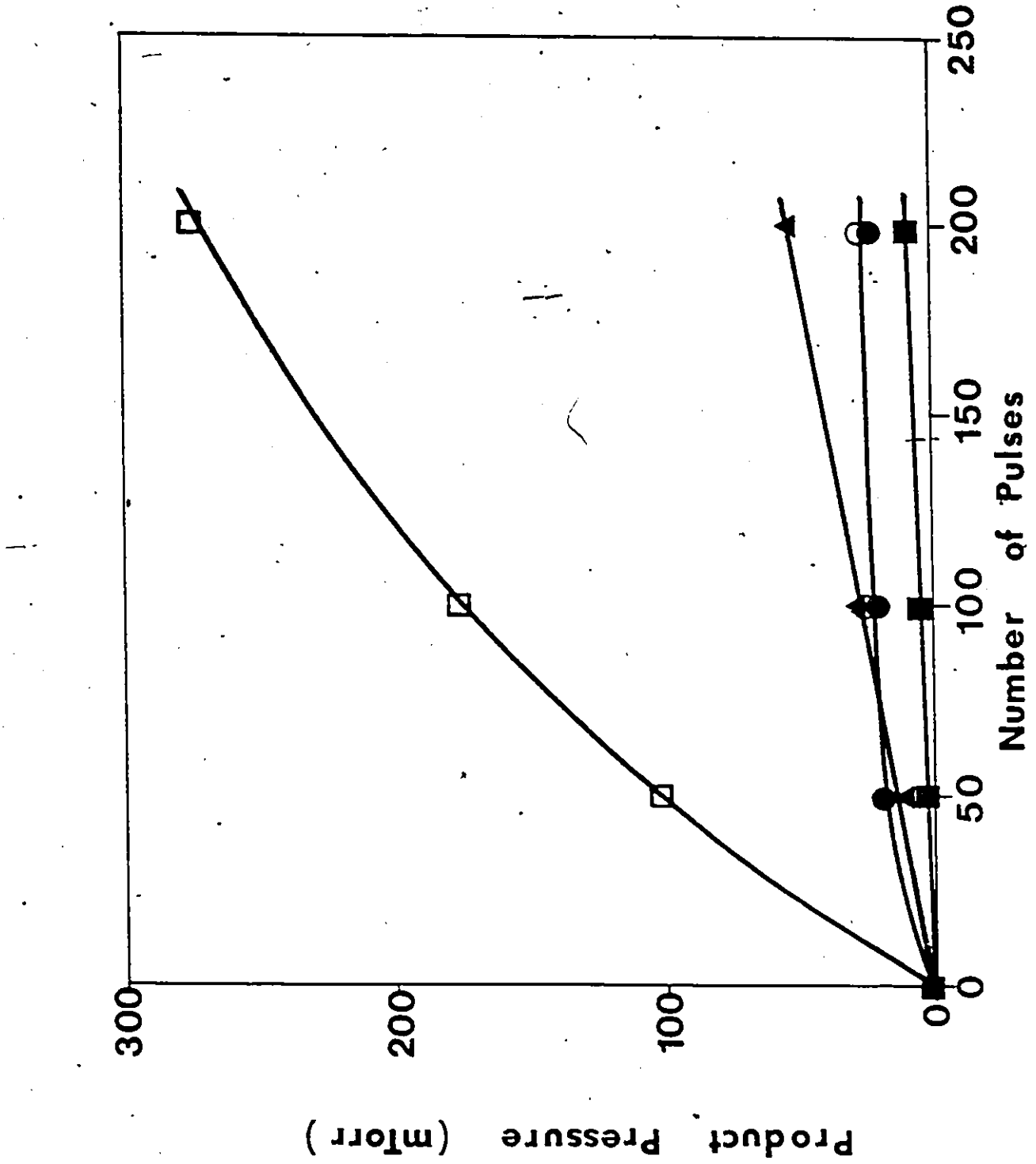
Product Pressure (mtorr)
300
200
100
0
0
50
100
150
200
250
Number of Pulses

Table 5.3

Yield of products following irradiation of 2 Torr of C_2F_6 in a 10 cm long, 2.5 cm diameter Pyrex cell with the 9R(36) CO_2 laser line, using a 25 cm focal length lens. The yields are the average of six experiments ± one standard deviation, except for the C_2F_4 TDL yields which are the average of three experiments.

Number of Pulses	Yield (mTorr)				
	C_2F_4		CF_4	C_3F_8	C_4F_{10}
	GC	TDL	TDL	GC	GC
a) 5.3 J cm^{-2}					
100	---	---	46.3±9.2	---	---
200	14.7±2.5	12.6±2.5	85.1±11.1	27.4±5.1	4.1±1.1
300	16.9±1.1	16.6±1.7	119.1±8.9	37.3±4.5	5.5±1.3
500	23.2±1.1	23.5±1.1	191.2±13.4	62.7±4.6	9.0±1.4
b) 13.4 J cm^{-2}					
35	---	---	89.8±11.4	---	---
40	26.6±5.0	30.1±6.4	93.0±7.1	16.6±2.0	3.6±2.0
70	32.1±4.5	35.3±2.9	161.0±26.5	28.3±2.7	4.9±0.6
100	36.3±5.8	38.9±8.5	204.9±38.2	39.5±4.7	6.5±1.5

FIGURE 5.9

Yield of products (mTorr) versus Number of Pulses, following irradiation of 2 Torr C_2F_6 in a 10 cm long, 2.5 cm diameter Pyrex cell, at a fluence of 5.3 J cm^{-2} using a 25 cm focal length BaF_2 lens, with the 9R(36) CO_2 laser line. ● C_2F_4 GC, O C_2F_4 TDL (1196.7 cm^{-1}), ▫ CF_4 TDL (1269.0 cm^{-1}), ▲ C_3F_8 GC, ■ C_4F_{10} GC. The symbols ● and O are sometimes superimposed in this plot.

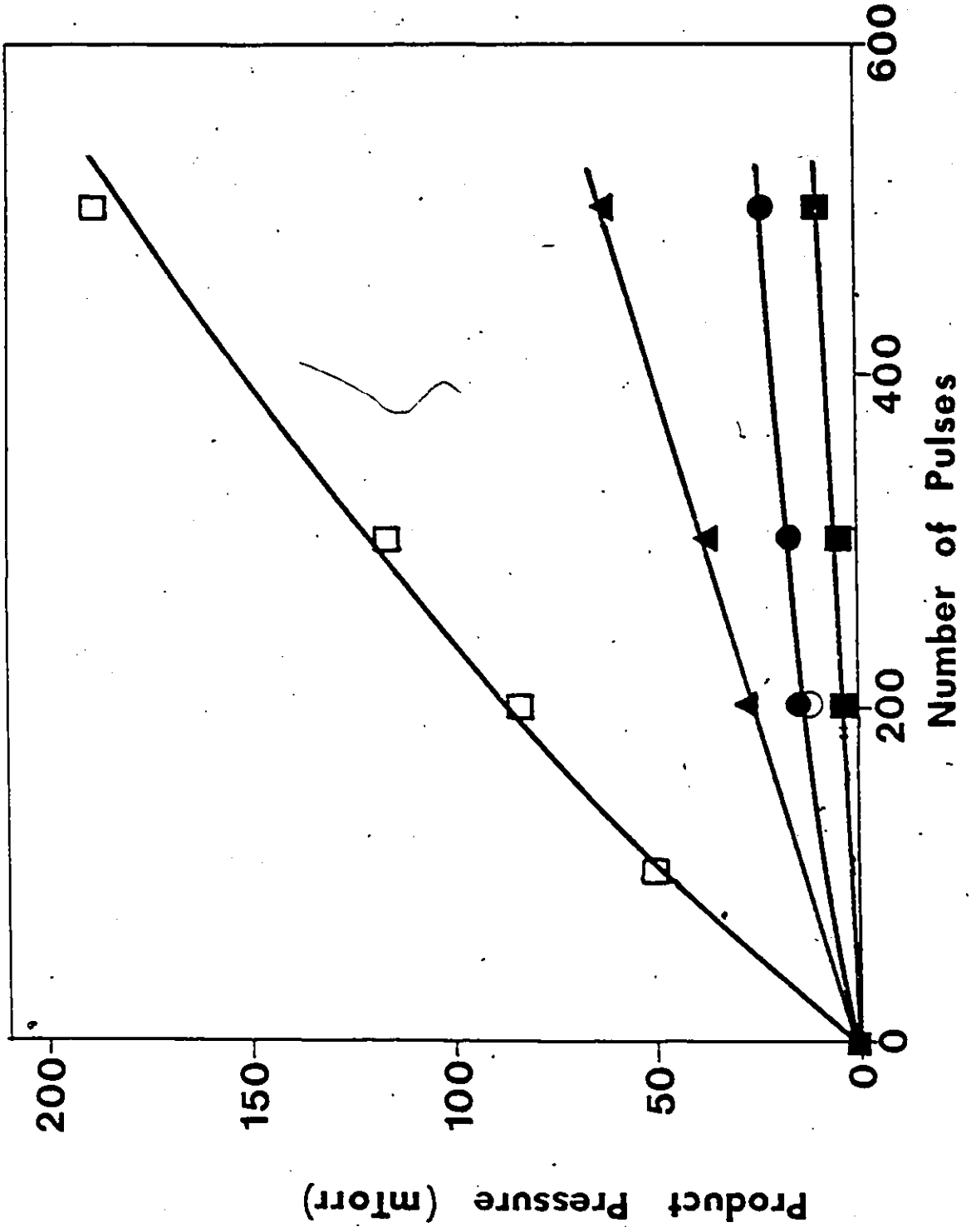
Product Pressure (mtorr)
200
150
100
50
0
0
200
400
600
Number of Pulses

FIGURE 5.10

Yield of products (mTorr) versus Number of Pulses, following irradiation of 2 Torr C_2F_6 in a 10 cm long, 2.5 cm diameter Pyrex cell, at a fluence of 13.4 J cm^{-2} using a 25 cm focal length BaF_2 lens, with the 9R(36) CO_2 laser line. ● C_2F_4 GC, O C_2F_4 TDL (1196.7 cm^{-1}), □ CF_4 TDL (1269.0 cm^{-1}), ▲ C_3F_8 GC, ■ C_4F_{10} GC. The symbols ● and O are sometimes superimposed in this plot.

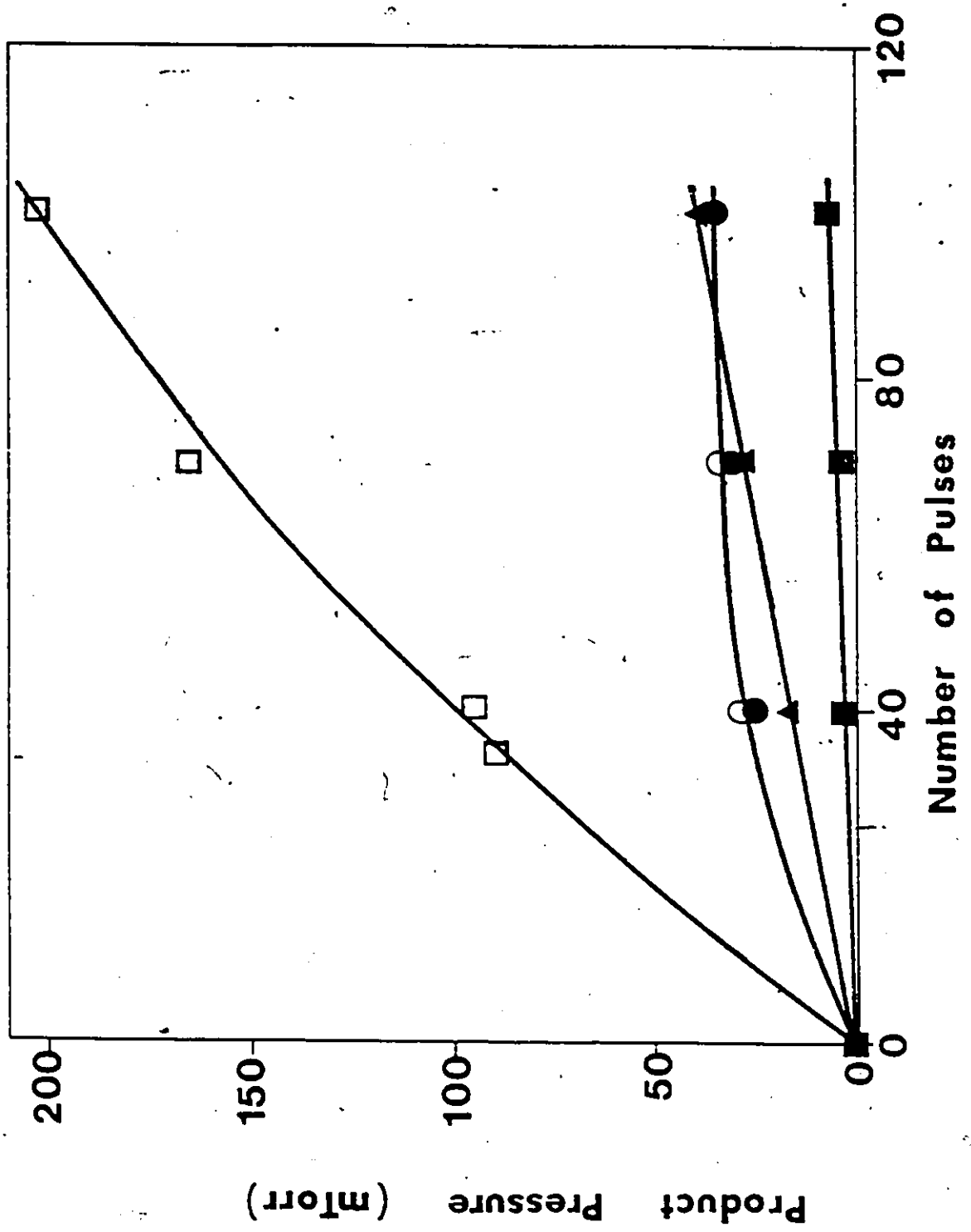
Product Pressure (mTorr)
200
150
100
50
0
0
40
80
120
Number of Pulses

Previous studies on the IRMPD of hexafluoroethane in the presence of scavengers[96,97] have suggested that the principal dissociation pathway involves the scission of the C-C bond to produce two CF_3 radicals. These trifluoromethyl radicals were either scavenged by H_2[97] or Br_2[96], forming CHF_3 or CF_3Br, or they absorbed more infrared photons and underwent secondary dissociation to difluorocarbene and a fluorine atom. Tetrafluoromethane, octafluoropropane and decafluorobutane were not mentioned in these reports.

How does one account for the presence of the observed products in the absence of scavengers? It would appear that the primary IRMPD pathway indeed involves scission of the C-C bond to form two CF_3 radicals. We propose that the secondary photolysis of trifluoromethyl radicals (as observed in several cases such as reference 108) can account for the production of CF_4 and C_2F_4 at high fluence as follows:

$$CF_3 + h\nu \rightarrow CF_2 + F \qquad (5.5)$$

$$2\ CF_2 \rightarrow C_2F_4 \qquad (5.6)$$

$$CF_3 + F \rightarrow CF_4 \qquad (5.7)$$

Formation of CF_4 and C_2F_4 via disproportionation of two CF_3 radicals has been ruled out in shock-tube studies[103] and in very-low-pressure photolysis experiments[109] and is thus not considered to be the source of these species in the present experiments.

Kato et al.[108] have studied the dissociation probability of CF_3 radicals as a function of fluence and found that this probability is greatly reduced at fluences $< 2\text{-}3$ J cm^{-2}. We believe that the C_2F_4 formed in the IRMPD of "neat" hexafluoroethane arises from the dimerization of CF_2 that results from the secondary dissociation of trifluoromethyl radicals. A lowering of the irradiation fluence should eventually eliminate secondary photolysis and thus the production of C_2F_4. We have irradiated 2 Torr samples of hexafluoroethane at 9R(36) for 4000 pulses at a fluence of about .1 J cm^{-2}. FTIR analysis revealed the presence of CF_4 and C_3F_8, while there was no evidence of C_2F_4 even via second harmonic TDL detection. Thus the secondary dissociation of trifluoromethyl radicals has been suppressed at this fluence. Without F atoms present, an additional mechanism for the production of CF_4 is required. Hence we suggest the abstraction of a F atom by vibrationally excited $CF_3^\dagger$ from the parent C_2F_6 as follows:

$$CF_3^\dagger + C_2F_6 \rightarrow CF_4 + C_2F_5 \qquad (5.8)$$

This reaction should be about 17 kJ/mol exothermic. It should be noted that in experiments done using the 9R(30) CO_2 laser pump line, the relative yield of CF_4/C_2F_4 increases as the pressure of C_2F_6 is increased from 1 to 2 Torr. The increase is more evident at low fluence (5.3 J cm^{-2}, 200 pulses) where the relative yield at 2 Torr is 5.8 times that at 1 Torr. At higher fluence (13.4 J cm^{-2}, 200 pulses) the increase in the relative yield at 2 Torr is 2.5 times that at 1 Torr. Reaction (5.8) therefore becomes more dominant as the pressure of C_2F_6 is increased, especially at low fluence where less secondary photolysis of CF_3 has occurred. Reactions similar to (5.8) have been proposed in the radiolysis of pentafluoroethyl iodide[110] and trifluoromethyl iodide.[111] C_2F_5 may then react with CF_3 to form C_3F_8, reaction (5.9), or recombine to form decafluorobutane, reaction (5.10).

$$CF_3 + C_2F_5 \rightarrow C_3F_8 \qquad (5.9)$$

$$C_2F_5 + C_2F_5 \rightarrow C_4F_{10} \qquad (5.10)$$

The secondary dissociation of pentafluoroethyl radicals has been observed previously by Hackett et al[112] in the IRMPD of pentafluoroethyl iodide. In our work, the increased yield of C_2F_4 relative to C_3F_8 as the fluence is increased at both 9R(30) and 9R(36) may be due to

the secondary photolysis of pentafluoroethyl as well as trifluoromethyl radicals.

$$C_2F_5 + h\nu \rightarrow CF_2 + CF_3 \qquad (5.11)$$

followed by

$$CF_2 + CF_2 \rightarrow C_2F_4 \qquad (5.6)$$

Reactions of CF_3[113] or CF_2[114] with C_2F_4, to form heptafluoropropyl radicals or hexafluorocyclopropane, are much too slow to be observed under the present experimental conditions.

5.3 Hydrogen Donors

The addition of 2 Torr of a hydrogen donating species such as H_2 or C_6H_{14} to 2 Torr of C_2F_6, followed by irradiation at the same wavelengths and fluences as above, leads to the elimination of the CF_4 yield. CF_4 is absent whenever the donor is present at pressures $\geq$ 0.5 Torr. The lack of CF_4 confirms that it is not a primary dissociation product (as predicted), and that reaction (5.8) is effectively eliminated when H_2 is added. Some of the trifluoromethyl radicals formed in IRMPD may be scavenged by the hydrogen donor as follows:

$$CF_3 + H_2 \rightarrow CHF_3 + H \qquad (5.12)$$

and

$$CF_3 + H \rightarrow CHF_3^{\dagger} \rightarrow CF_2 + HF \qquad (5.13a)$$

$$+ [M] \rightarrow CHF_3 \qquad (5.13b)$$

C_3F_8 and C_4F_{10} are still observable, however they cannot now be produced as previously indicated or CF_4 would also be observed (ie reaction (5.8) does not occur in the presence of a hydrogen donor). Thus we propose that C_2F_5 is formed by either reaction (5.14), as suggested by Tschuikow-Roux[99],

$$H + C_2F_6 \rightarrow C_2F_5 + HF \qquad (5.14)$$

and/or dissociation of C_2F_6 via the higher energy pathway (5.3):

$$C_2F_6 + h\nu \rightarrow C_2F_5 + F \qquad (5.3)$$

The degree of overexcitation of SF_6 molecules (dependent on pulse intensity) in IRMPD studies has been determined by Grant et al[46] to be between 6 and 10 CO_2 laser photons above the dissociation limit. C_2F_6 is of comparable

size to SF_6, thus it is plausible that C_2F_6 may be excited sufficiently to dissociate via the next highest energy channel (5.3). This would be followed by C_2F_5 combination reactions

$$CF_3 + C_2F_5 \rightarrow C_3F_8 \qquad (5.9)$$

and

$$C_2F_5 + C_2F_5 \rightarrow C_4F_{10} \qquad (5.10)$$

Fluorine atoms produced in reaction (5.3) or from secondary dissociation, reaction (5.5) will then be efficiently removed by reaction with the hydrogen donor:

$$H_2 + F \rightarrow HF + H \qquad (5.15)$$

The rate constants for reaction (5.7)[115] and (5.15)[116] are roughly equal, ($k_{5.7}$ = (1.1-1.7) x 10^{-11} cm^3 $molecule^{-1}$ s^{-1}, $k_{5.15}$=1.7 x 10^{-11} cm^3 $molecule^{-1}$ s^{-1}), however under the present experimental conditions $[H_2] \gg [CF_3]$ and reaction (5.15) should dominate.

The major products in the presence of a hydrogen donor are C_3F_8, C_4F_{10} and CHF_3, as well as greatly increased C_2F_4 yields. Their yields as a function of number of pulses with 2 Torr of H_2 added to 2 Torr

C_2F_6 are listed in table 5.4, and are shown in Figures 5.11 and 5.12.

The question arises as to why the C_2F_4 yield is greatly enhanced in the presence of hydrogen donors. Certainly the secondary dissociation of trifluoromethyl radicals should still occur to some extent, however other sources must contribute to the large increase in yield. To this end we investigated the possibility that the CHF_3 formed in reactions (5.12) and (5.13) itself undergoes IRMPD. Samples were prepared containing 20 mTorr of CHF_3 in C_2F_6 at 2 Torr total pressure and then subjected to 100 pulses 9R(36), 5.3 J cm^{-2}. After photolysis TDL measurements showed that 17.2 mTorr of the CHF_3 remained. Thus 14 % of the fluoroform was consumed, indicating that it undergoes IRMPD in the presence of hexafluoroethane under the conditions used in the scavenging experiments. Control experiments containing the same known amount of CHF_3 in N_2 show no consumption of CHF_3. It appears that collisional energy transfer between vibrationally excited $C_2F_6^{\dagger}$ and CHF_3 is required to place CHF_3 in the vibrational quasicontinuum from which it may absorb further photons and dissociate.

$$C_2F_6^{\dagger} + CHF_3 \rightarrow C_2F_6 + CHF_3^{\dagger} \qquad (5.16)$$

$$CHF_3^{\dagger} + h\nu \rightarrow CF_2 + HF \qquad (5.17)$$

Table 5.4

Yield of products following irradiation of 2 Torr C_2F_6 + 2 Torr H_2 in a 10 cm long, 2.5 cm diameter Pyrex cell with the 9R(36) CO_2 laser line, using a 25 cm length focal length lens. The yields are the average of three experiments ± one standard deviation.

Number of Pulses	Yield (mTorr)			
	C_2F_4 GC	CHF_3 TDL	C_3F_8 GC	C_4F_{10} GC
a) 5.3 J cm^{-2}				
200	85.3±12.7	5.8±0.5	12.8±1.1	2.1±0.2
300	134.3±15.2	8.2±1.3	19.5±2.8	3.8±0.8
500	204.3±5.7	11.3±0.4	33.1±1.0	6.1±0.3
b) 13.4 J cm^{-2}				
40	113.7±13.1	13.8±0.7	6.8±1.6	1.3±0.1
70	154.9±13.4	19.0±1.8	15.2±1.2	2.6±0.5
100	195.1±27.6	23.6±5.0	20.4±2.5	3.6±0.5

FIGURE 5.11

Yield of products (mTorr) versus Number of Pulses, following irradiation of 2 Torr C_2F_6 + 2 Torr H_2, in a 10 cm long, 2.5 cm diameter Pyrex cell. Irradiations were performed at a fluence of 5.3 J cm^{-2}, using a 25 cm focal length BaF_2 lens with the 9R(36) CO_2 laser line. ● C_2F_4 GC, ▫ CHF_3 TDL (1162.6 cm^{-1}), ▲ C_3F_8 GC, ■ C_4F_{10} GC.

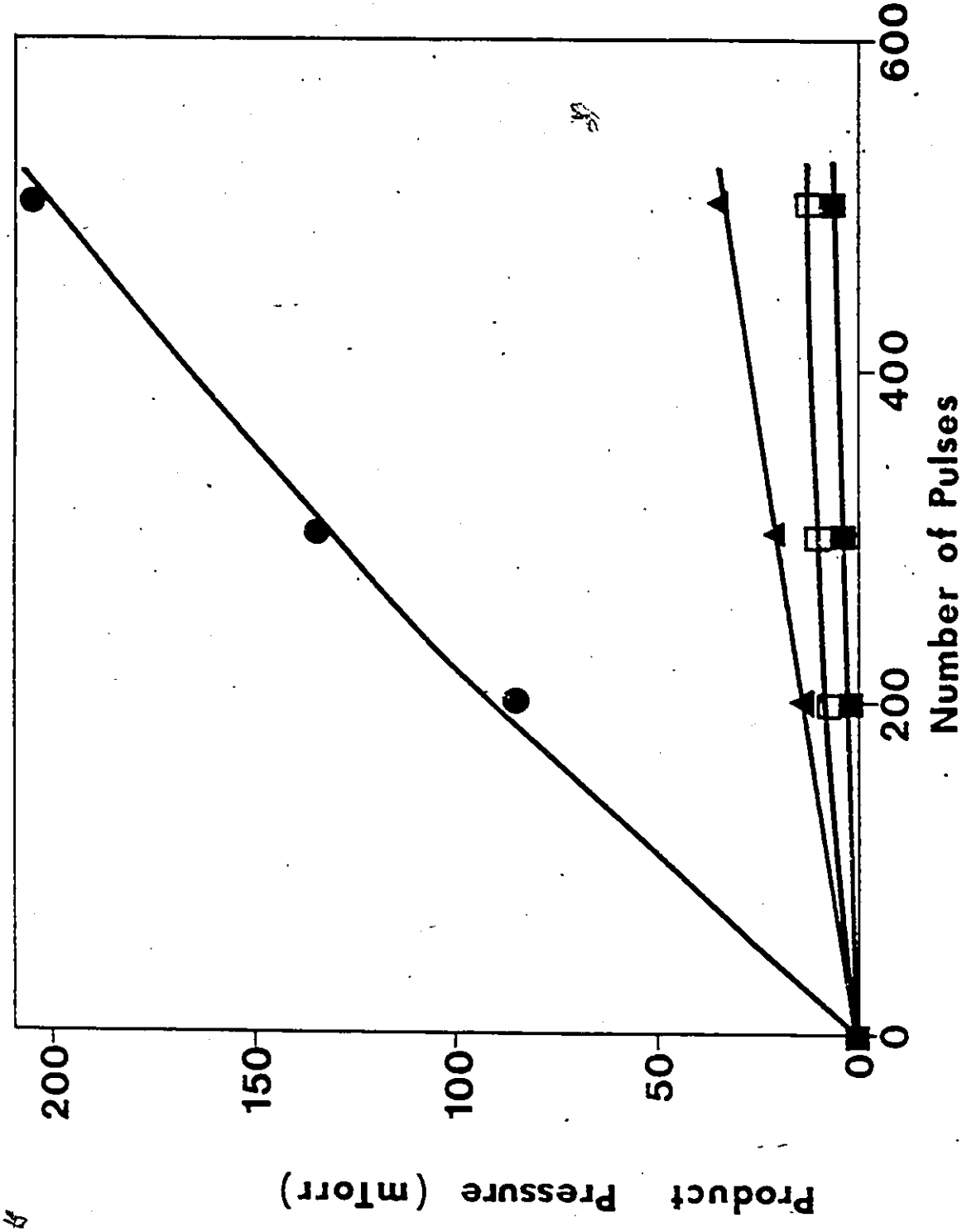
Product Pressure (mTorr)
200
150
100
50
0
0
200
400
600
Number of Pulses

FIGURE 5.12

Yield of products (mTorr) versus Number of Pulses, following irradiation of 2 Torr C_2F_6 + 2 Torr H_2, in a 10 cm long, 2.5 cm diameter Pyrex cell. Irradiations were performed at a fluence of 13.4 J cm^{-2}, using a 25 cm focal length BaF_2 lens with the 9R(36) CO_2 laser line. ● C_2F_4 GC, ▫ CHF_3 TDL (1162.6 cm^{-1}), ▲ C_3F_8 GC, ■ C_4F_{10} GC.

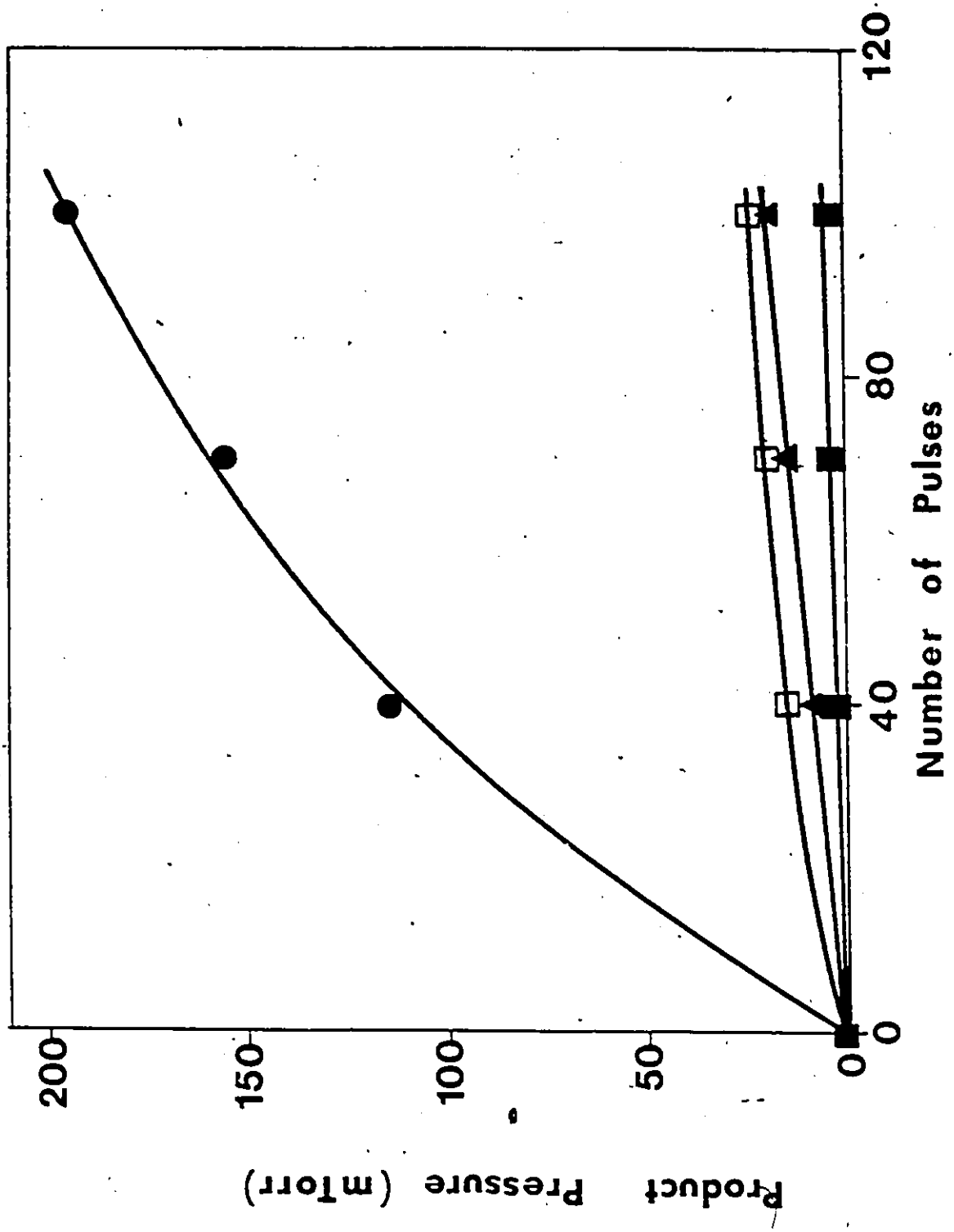
Product Pressure (mTorr)
200
150
100
50
0
0
40
80
120
Number of Pulses

The difluorocarbene thus produced would then dimerize to form C_2F_4. In view of the extremely large yield of C_2F_4, it is doubtful that the mechanisms proposed thus far can account for the total C_2F_4 yield. The difference could arise from a reaction between vibrationally excited $C_2F_6^{\dagger}$ and H_2 forming $C_2F_5H^{\dagger}$ which then eliminates HF to form C_2F_4, as proposed by Fisk[97]. Alternatively, a more energetically favoured route would be via elimination of HF from excited $CHF_3^{\dagger}$, formed by combination of H and CF_3, reaction (5.13a), followed by CF_2 combination, reaction (5.6).

$$C_2F_6^{\dagger} + H_2 \rightarrow C_2F_5H^{\dagger} + HF \qquad (5.18)$$

$$C_2F_5H^{\dagger} \rightarrow C_2F_4 + HF \qquad (5.19)$$

5.4 Transient Detection

In the beginning of this chapter, it was indicated that one of the goals of this thesis was to use tunable diode lasers to monitor the transient species produced in the IRMPD of hexafluoroethane. To that end, a technique for monitoring transient IR absorptions was developed (in collaboration with P.H. Beckwith).[106] The technique was developed and refined using known sources of the desired transient species, and later employed to monitor these same species in the IRMPD of hexafluoroethane.

CF_2 and CF_3 radicals are the most likely transient species to be produced in the IRMPD of C_2F_6. Since CF_2 is a relatively long-lived transient species, it was therefore deemed to be the first species to be investigated. The spectroscopy of the ν_1 band of CF_2 ($\tilde{X}^1A_1$) has been described in detail by Davies and co-workers.[104] Preliminary spectroscopic measurements of CF_2 were made in a conventional microwave discharge (in collaboration with P.H. Beckwith and J.J. Orlando). These first continuous wave experiments were carried out to characterize the CF_2 absorption spectra in a region of good single-mode operation of the TDL probe. Specifically, the $^rQ_3$ branch of the ν_1 band of CF_2 ($\tilde{X}^1A_1$) at 1243 cm^{-1} was chosen. A 0.5 m grating monochromator was employed to select the desired output frequency of the TDL probe. N_2O and CH_4 reference lines were then employed as frequency standards.[105] CF_2 molecules were produced in the 2450 MHz microwave discharge flow system described in Chapter 4. Chlorotrifluoroethylene was used as the precursor gas in these experiments. The optimum gas mixture in the microwave discharge was C_2F_3Cl/Ar in a 4:1 ratio at a total pressure of 280 mTorr. The strongest CF_2 absorption lines observed with the discharge had line center absorptions of ~ 10% (four passes, 2.4 m total path length). Figure 5.13 illustrates the IR spectra of CF_2 produced in this work and the results of Davies et al.[104]

FIGURE 5.13

TDL spectrum of CF_2 in the 1243 cm^{-1} region. The upper section shows the absorption lines of CF_2, $\tilde{X}^1A_1$, created in a microwave discharge by Davies et al.[104] and in the present work. Also shown are line identifications given by Davies et al. The lower trace shows an expanded view of the spectrum. The optimum gas mixture in the 2450 MHz microwave discharge was C_2F_3Cl/Ar in a 4:1 ratio at a total pressure of 280 mTorr, and the strongest CF_2 absorption lines observed in the present work have line center absorptions of ~10% (four passes, 2.4 m total path length).

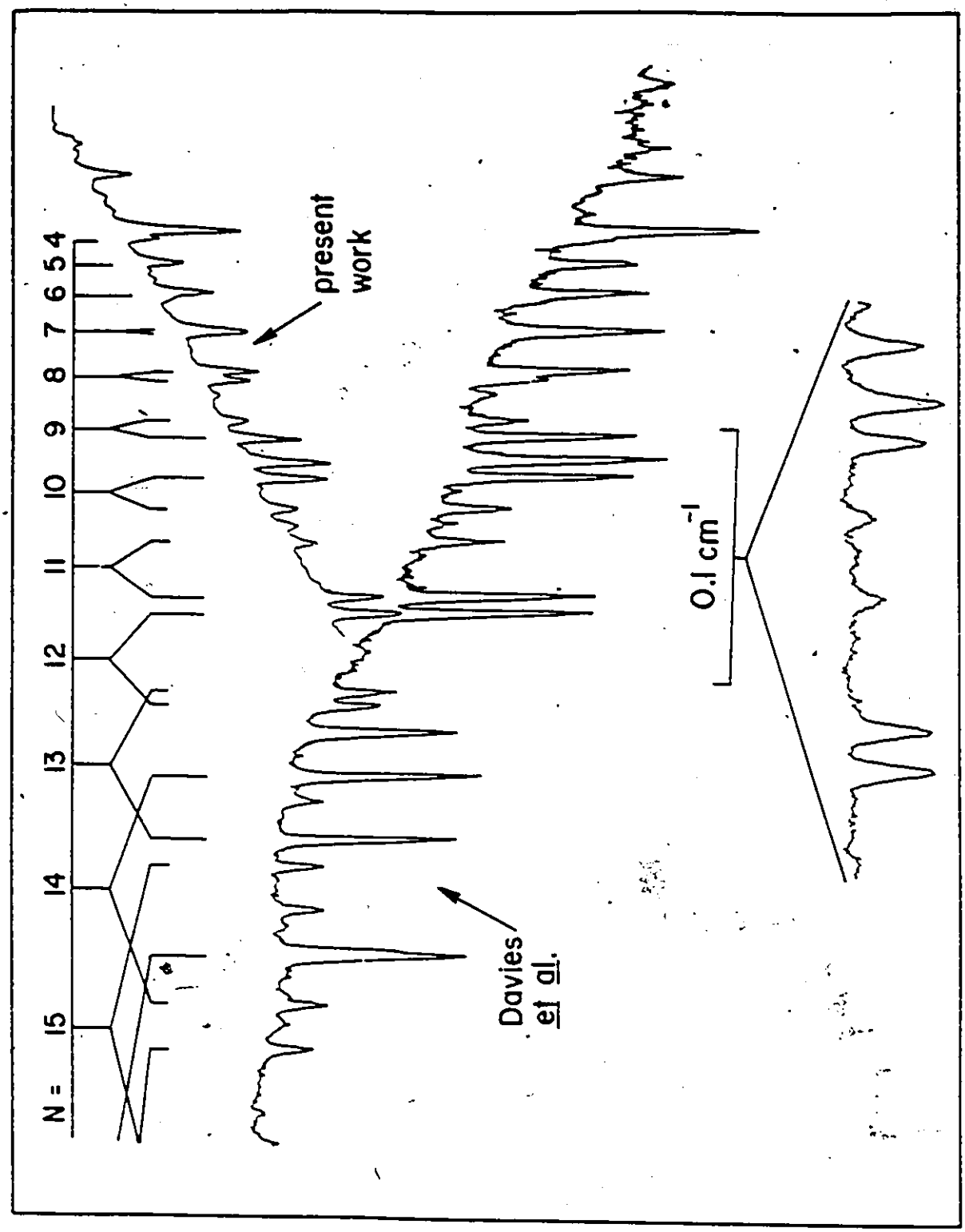
N = 15 14 13 12 11 10 9 8 7 6 5 4
present work
Davies et al.
0.1 cm⁻¹

Following the successful production and detection of CF_2 on a steady-state basis, efforts were shifted to the monitoring of transient CF_2 species produced by the IRMPD of various halocarbons (in collaboration with P.H. Beckwith).[106] Initially it was intended that the TDL probe would be tuned to the center of a strong CF_2 absorption line and absorption of the TDL beam would be monitored immediately after passage of the TEA CO_2 laser pulse. These early experiments were conducted with a conventional Pyrex photolysis cell (2.5 cm diameter, 10 cm long) and the TDL was tuned to the center of a strong CF_2 absorption line. Problems arose however with the passage of the intense TEA CO_2 laser pulse through the gas in the cell causing thermal shocks, transient refractive index changes and deflection of the TDL probe beam away from the detector. It was not possible to differentiate between probe beam deflection and true absorption. At this time a switch was made to a capillary waveguide cell which provided better confinement of the TDL probe beam and also ensured a high pump beam fluence over a long interaction length.

A description of the high frequency TDL modulation technique used for the detection of transient species was presented in Chapter 4 and illustrated in Figure 4.5. The bias current and temperature used for detection of CF_2 on a cw basis are employed for transient detection of CF_2. Previous IRMPD studies have shown that perfluoropropene[117]

and chlorotrifluoroethylene[118] are ideal sources of CF_2. In our work, IRMPD of C_3F_6 was carried out using the 9P(36) CO_2 laser transition, while the 9P(14) transition was used for the IRMPD of C_2F_3Cl. As mentioned in Chapter 4, the main advantage of the high frequency TDL modulation technique was to take advantage of the tunability of the TDL. By tuning the TDL across an absorption feature, an unambiguous identification of the transient species can be made. The CF_2 doublet absorption feature illustrated in Figure 5.13 is the same doublet that is detected using the transient TDL technique and illustrated in Figure 5.14. The modulation frequency applied to the TDL can be varied to allow one to observe the formation of CF_2 after the laser pulse and then its decay if the modulation frequency is reduced as illustrated in Figure 5.14. Note that the digital subtraction in the lower section of Figure 5.14 removes the precursor absorptions allowing observation of the transient species alone.

Once the high frequency TDL modulation technique had been developed and employed to monitor transient IR CF_2 absorptions, the technique was to be applied to a much shorter-lived species, the trifluoromethyl radical. Spectroscopy of the ν_3 band of CF_3 has been undertaken by Yamada and Hirota.[107] Several hundred ν_3 band CF_3 absorption lines have been observed and their frequencies assigned ($\pm$ 0.0005 cm^{-1}) under steady state

FIGURE 5.14

Absorption of CF_2 monitored as a function of time. The upper section illustrates the growth of CF_2 following CO_2 laser irradiation of 1.5 Torr C_2F_3Cl, averaged over 256 scans. The lower section shows the CF_2 decay; each trace is the average of 50 scans. Trace B was recorded with gas in the cell and with the CO_2 beam blocked to allow for subtraction of the steady-state C_2F_3Cl absorptions. TDL modulation frequencies in the upper and lower sections were 14 kHz and 470 Hz respectively.

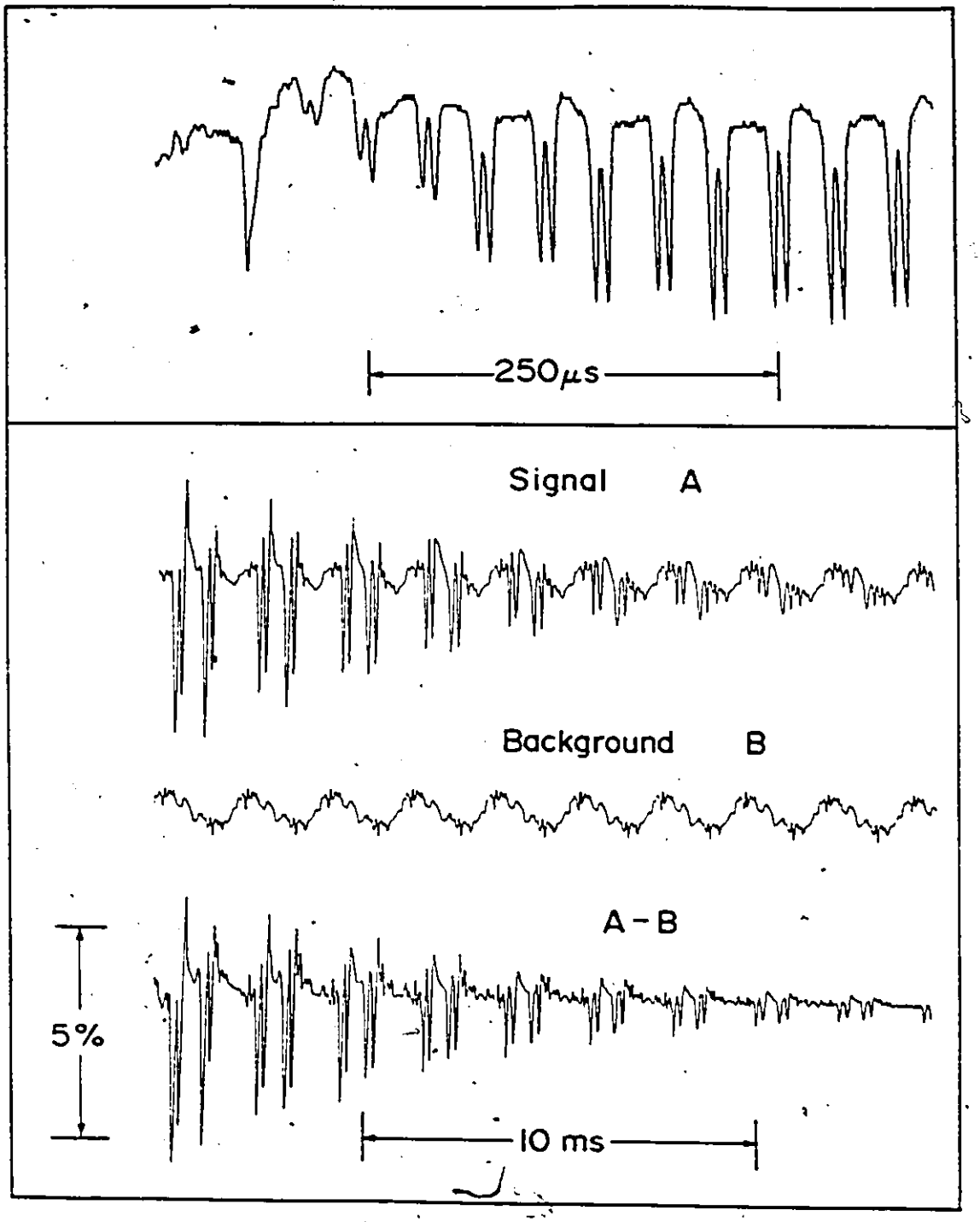
250μs
Signal A
Background B
A-B
5%
10 ms

conditions in a Zeeman modulated 60 Hz discharge system.[107] Attempts were made in this laboratory to produce CF_3 in a fast-flowing 2450 MHz microwave discharge of a mixture of CF_3I or C_2F_6 diluted in Ar. However the only absorption lines observed in the 1264 cm^{-1} region were due to CF_4. The inability to observe CF_3 radicals was probably due to the pump speed being too low (300 l/min).

The inability to observe steady-state CF_3 absorptions was not a serious problem. The line frequency assignments of Yamada and Hirota, in conjunction with the use of 0.5 m grating monochromator (Jarrell-Ash model 82010) and well calibrated N_2O and CH_4[105] lines allowed for the identification of expected CF_3 line positions to better than ± 0.001 cm^{-1}.

In the transient TDL detection of CF_3 radicals, the TDL was modulated at 40 kHz (in collaboration with J.J. Orlando).[119] The IRMPD of CF_3I[120] and CF_3Br[121] has previously been shown to produce CF_3 radicals. More recently Orlando and Smith[122] have established that the primary IRMPD pathway of hexafluoroacetone involves the production of two CF_3 radicals along with a molecule of CO. These three precursor gases were employed in this work. 74 ν_3 band CF_3 absorption lines have been observed in the 1263 - 1265 cm^{-1} region following the IRMPD of several hundred mTorr of CF_3I, CF_3Br or $(CF_3)_2CO$. Fifty of the lines coincided to better than

$\pm$ 0.001 cm^{-1} with the positions predicted by Yamada and Hirota, confirming that CF_3 radicals are indeed created. The remainder of the lines were not reported by Yamada and Hirota, however they occur in a wavelength region where their TDL appears to mode hop. Figure 5.15 illustrates the time-resolved behaviour of a transient infrared absorption signal of the $^rR_{16}(20)$ CF_3 line at 1264.739 cm^{-1} resulting from IRMPD of 360 mTorr of CF_3I at a fluence of $\sim$ 30 J/cm^2 using the 9P(18) CO_2 laser line. The data illustrated in Figure 5.15 are the average of 32 sets of observations.

The infrared linestrength (S) of the $^rR_{16}(20)$ CF_3 absorption line has been quantified by comparison of the time-resolved yields of CF_3 with CO and C_2F_6 resulting from the IRMPD of $(CF_3)_2CO$.[122] Using this linestrength, the average concentration of CF_3 radicals in the 15 cm long waveguide cell 50 μs after the CO_2 laser pulse in Figure 5.15 is $(1.8 \pm 0.4) \times 10^{15}$ molecules cm^{-3}.

The TDL modulation technique allows for the study of the decay kinetics of CF_3 produced in the IRMPD of $(CF_3)_2CO$ (in collaboration with J.J. Orlando).[119] The only decay of CF_3 is by recombination, equation (-5.2):

$$CF_3 + CF_3 \rightarrow C_2F_6 \qquad (-5.2)$$

Indeed the decay of CF_3 fits a second order plot. The

FIGURE 5.15

The time-resolved behaviour of a transient IR absorption signal of the $^{r}R_{16}(20)$ CF_3 line at 1264.739 cm^{-1} resulting from the IRMPD of 360 mTorr of CF_3I at a fluence of ~30 J cm^{-2} using the 9P(18) CO_2 laser line. The data are the average of 32 sets of observations. The TDL modulation frequency is 40 kHz.

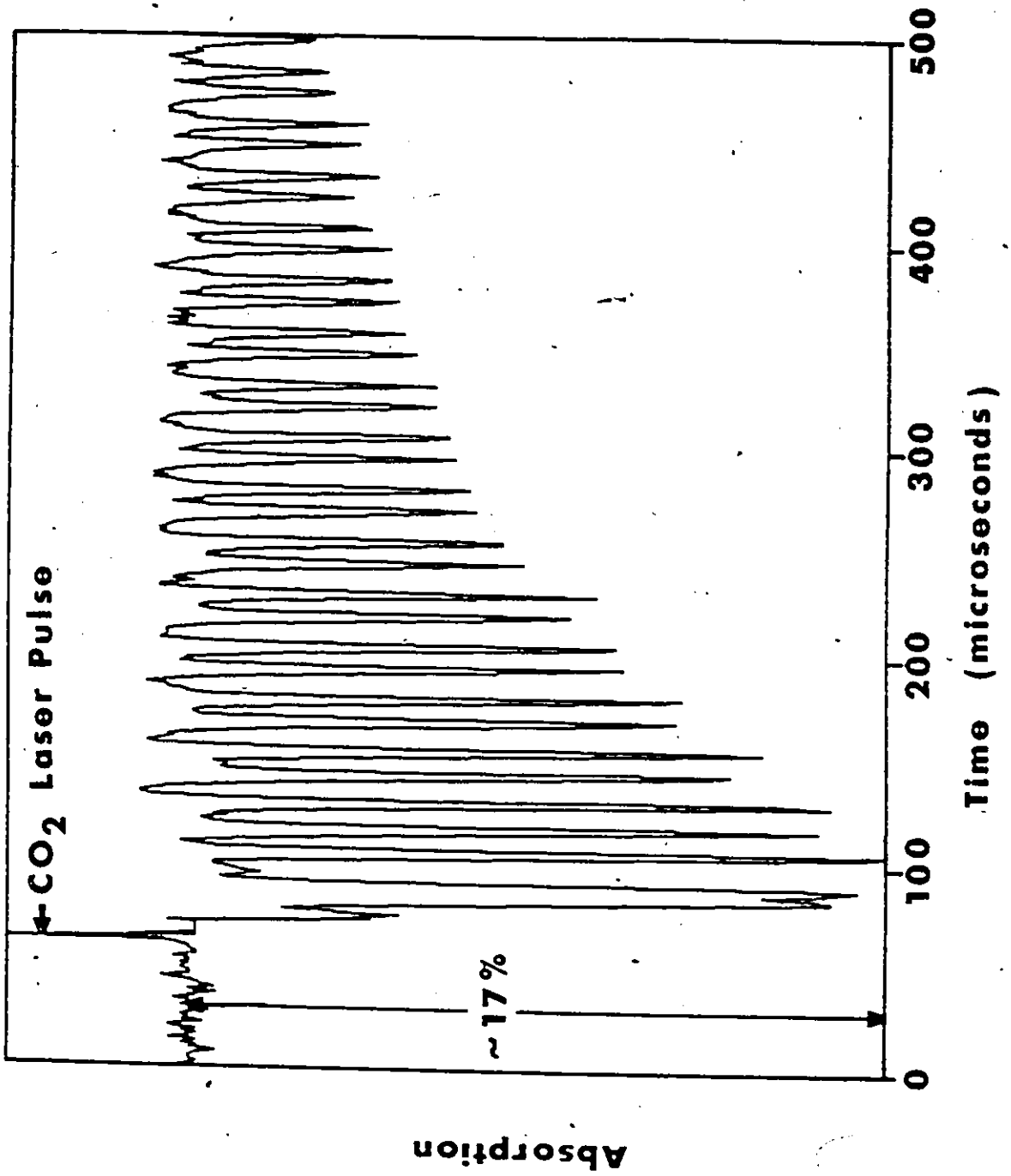
CO_2 Laser Pulse
~17%
0
100
200
300
400
500
Time (microseconds)
Absorption

initial (peak) yields of CF_3 were varied by a factor of five by changing the CO_2 laser fluence or the pressure of $(CF_3)_2CO$. The product of peak yield times the initial half-life was found to be constant to within ±10%, in fifteen separate experiments. This indicates that the decay of CF_3 is indeed second order, and that wall reactions are slow enough to be neglected. The second order plot resulting from photolysis of 600 mTorr of hexafluoroacetone is shown in Figure 5.16. A second order recombination rate constant of $(2.2 \pm 0.5) \times 10^{-12}$ cm^3 $molecule^{-1}$ s^{-1} is obtained from this plot. This value is in good agreement with the most recent value in the literature[123] of $(3.0 \pm 0.4) \times 10^{-12}$ cm^3 $molecule^{-1}$ s^{-1} in CF_3I at ~10 mTorr and room temperature. From RRKM calculations in reference 123, we expect that our results for $k_{-5.2}$ are close to the high pressure limit. To within ±25%, we observe no effect of adding 1 Torr of Ar.

5.4.1 Transient Species Produced by IRMPD of C_2F_6

Hexafluoroethane absorbs IR radiation rather strongly in the 1264 cm^{-1} region in which transient CF_3 absorptions are monitored. Although there are only a few discernable C_2F_6 absorption lines in this region, the broad continuous absorption severely reduces the amount of TDL power that reaches the HgCdTe detector. Indeed C_2F_6 pressures of greater than ~ 800 mTorr, attenuate

FIGURE 5.16

The reciprocal absorption coefficient of the $^{r}R_{16}(20)$ CF_3 line at 1264.739 cm^{-1} as a function of time following the CO_2 laser pulse. The CF_3 radicals were produced by the IRMPD of 600 mTorr of hexafluoroacetone, using the 10R(14) CO_2 laser line at a fluence of ~28 J cm^{-2}. The data are the average of 32 sets of observations. The TDL modulation frequency is 40 kHz.

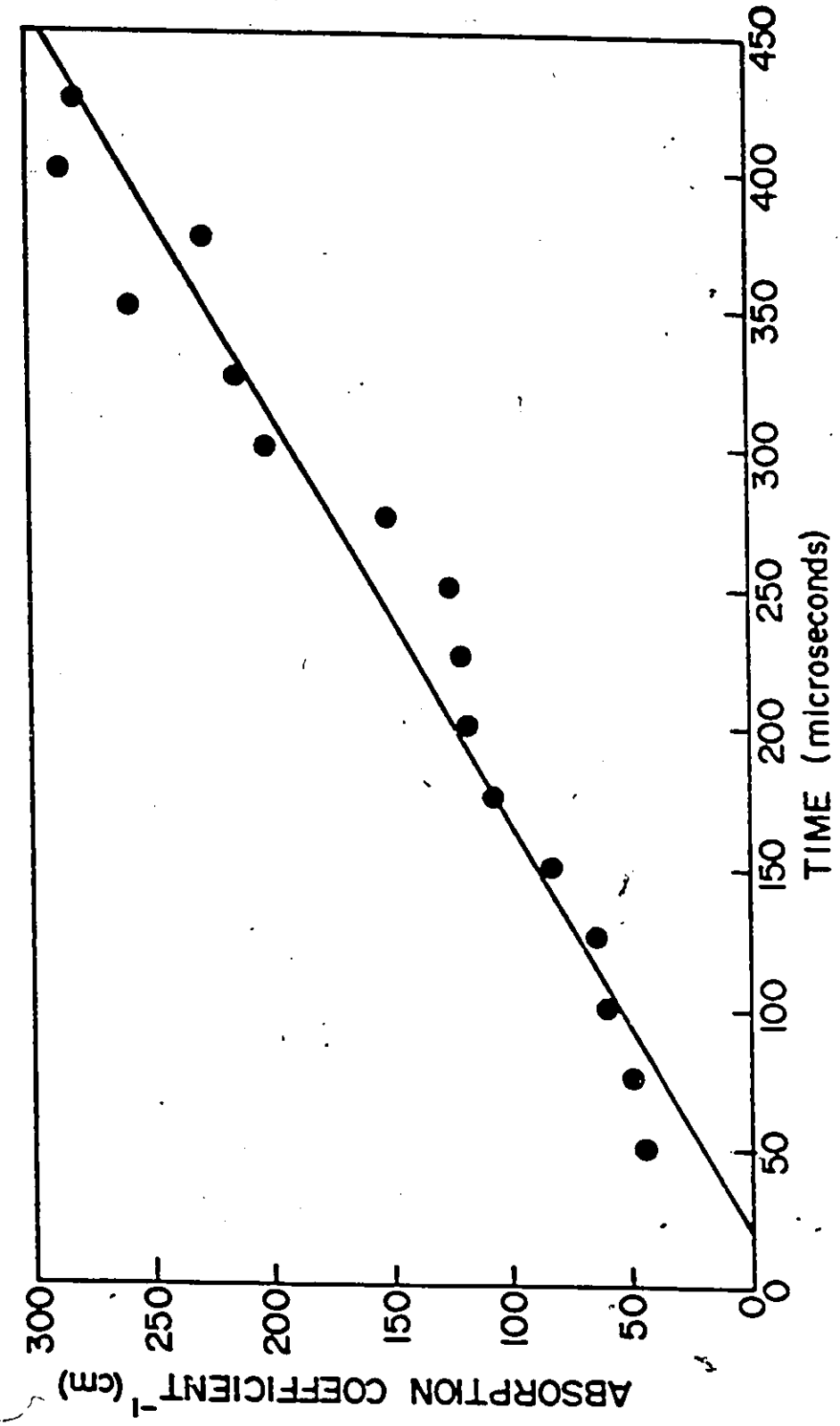
ABSORPTION COEFFICIENT $^{-1}$ (cm)
300
250
200
150
100
50
0
0
50
100
150
200
250
300
350
400
450
TIME (microseconds)

the TDL output totally. Therefore in an attempt to observe CF_3 radicals resulting from the IRMPD of C_2F_6, a pressure of 600 mTorr was employed. The production of CF_3 radicals was monitored immediately following the IRMPD of C_2F_6 via the high frequency TDL modulation technique. Unfortunately there is spectral interference in the region of the CF_3 $^rR_{16}(20)$ line calibrated by Orlando and Smith[122], thus a different absorption line was employed for quantification of the CF_3 yield. The absorption line used for quantification of the trifluoromethyl radicals in this work was not identified by Yamada and Hirota[107], however this line is also present immediately following the IRMPD of CF_3I, CF_3Br and $(CF_3)_2CO$. To obtain a relative linestrength for the chosen analysis line at ~1264.699 cm^{-1}, the intensity of this line was compared to the measured intensity of the $^rR_{16}(20)$ CF_3 line at 1264.739 cm^{-1}. To accomplish this 600 mTorr of hexafluoroacetone was irradiated at a fluence of ~ 23 J cm^{-2} using the 10R(14) CO_2 laser pump line. 3 sets of 32 laser pulses were averaged for each of the lines, under identical experimental conditions. The ratio of the line intensities (1264.699/1264.739) was found to be 1.47±0.04. The calibrated linestrength for the chosen CF_3 analysis line at 1264.699 cm^{-1} is therefore (2.0±0.5) x 10^{-20} cm $molecule^{-1}$. The CF_3 absorption line at 1264.699 cm^{-1} in the C_2F_6 system exhibits the same temporal growth and

decay behaviour as the $^{r}R_{16}(20)$ line produced in the IRMPD of hexafluoroactone.[122] In the hexafluoroacetone experiments a measurement of the gas temperature following the absorption of a CO_2 laser pulse was undertaken. A trace of N_2O was added to the photolysis cell, and the time-resolved absorption of N_2O on a temperature-sensitive transition (P(45) at 1243.795 cm^{-1}) was performed. After absorption of a CO_2 laser pulse by the hexafluoroacetone and N_2O mixture, no measurable increase in N_2O absorption (to within 10%) was noted over 20 ms. Thus there was no significant temperature increase. (A 10% increase in N_2O absorption on P(45) would correspond to a temperature change of less than 10 K). Furthermore from the calculated linestrength, a plot of the reciprocal CF_3 concentration versus time, in C_2F_6 gives a second order recombination rate of $(1.7\pm0.4) \times 10^{-12}$ cm^3 $molecule^{-1}$ s^{-1}, which is within the experimental error of the rate as determined by us.[119] We are therefore confident that we are indeed measuring the concentration of thermalized CF_3 radicals. From this linestrength, the peak yield of CF_3 produced per laser pulse by the IRMPD of 600 mTorr of hexafluoroethane (using the 9R(30) CO_2 laser pump line) as a function of fluence has been measured. As one can see from Figure 5.17 a significant amount of CF_3 is produced by each CO_2 laser pulse (> 3% dissociation per pulse at 19.8 J cm^{-2}). The lower limit in Figure 5.17 was caused by low TDL power,

FIGURE 5.17

Peak yield of CF_3 versus CO_2 laser fluence, 50 μs after single pulse irradiation of 600 mTorr C_2F_6, in a 15 cm long, 1 mm diameter quartz waveguide cell, using the 9R(30) CO_2 laser line. The illustrated points are the average of 3 sets of 32 CO_2 laser pulses.

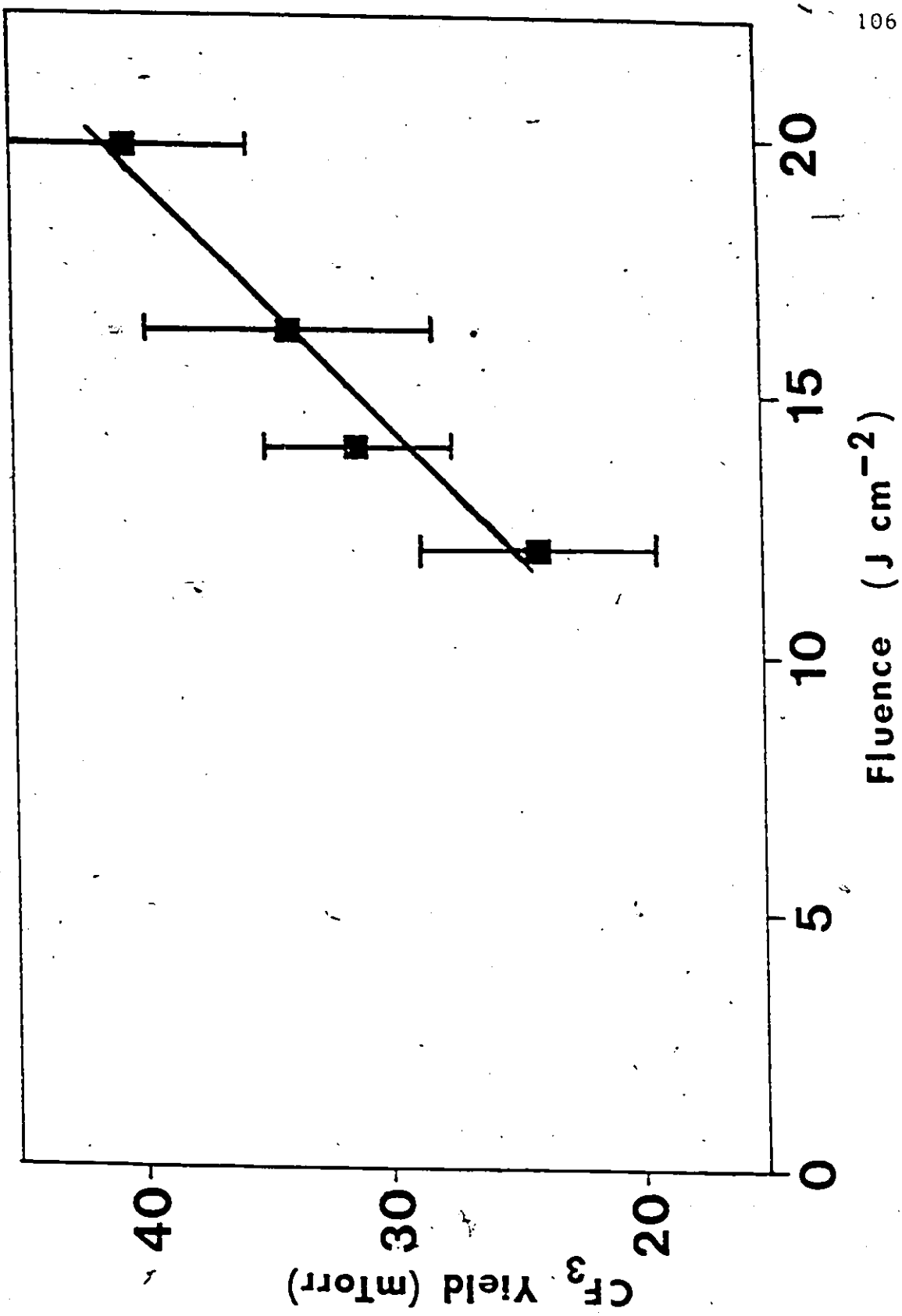
CF_3 Yield (mTorr)
40
30
20
0
5
10
15
20
Fluence (J cm^{-2})

and is not intended to indicate a threshold for the production of CF_3. Figure 5.18 illustrates the temporal behaviour of the CF_3 absorption line at 1264.699 cm^{-1} resulting from the IRMPD of 600 mTorr of C_2F_6 at a fluence of ~20 J cm^{-2} using the 9R(30) CO_2 laser line.

As is the case in the detection of trifluoromethyl radicals, C_2F_6 absorbs a portion of the TDL output in the wavelength region of interest for monitoring CF_2 molecules. CF_2 could be not be detected following the IRMPD of 1 Torr of C_2F_6, over a range of fluences from ~ 16 to 34 J cm^{-2} using the 9R(30) and 9R(32) CO_2 laser pump lines. The infrared linestrength (S) of the $^rQ_3(9)$ CF_2 absorption line at 1243.0185 cm^{-1} has been measured as $(9 \pm 2) \times 10^{-21}$ cm molecule^{-1}.[124] Based on this linestrength measurement, the noise level of the TDL absorption scans associated with the search for CF_2 molecules in the IRMPD of C_2F_6 corresponds to ~4 mTorr of CF_2. It can therefore be concluded that less than 6 mTorr of CF_2 is produced under these experimental conditions.

5.5 Summary

The IRMPD of "neat" hexafluoroethane has been investigated using the 9R(30) and 9R(36) CO_2 laser lines. Efficient IRMPD of hexafluoroethane occurs at the indicated laser frequencies even though these lines are red-shifted

FIGURE 5.18

The time-resolved behaviour of a transient IR absorption signal of the CF_3 line at 1264.699 cm^{-1} resulting from the IRMPD of 600 mTorr of C_2F_6 at a fluence of ~20 J cm^{-2} using the 9R(30) CO_2 laser line.

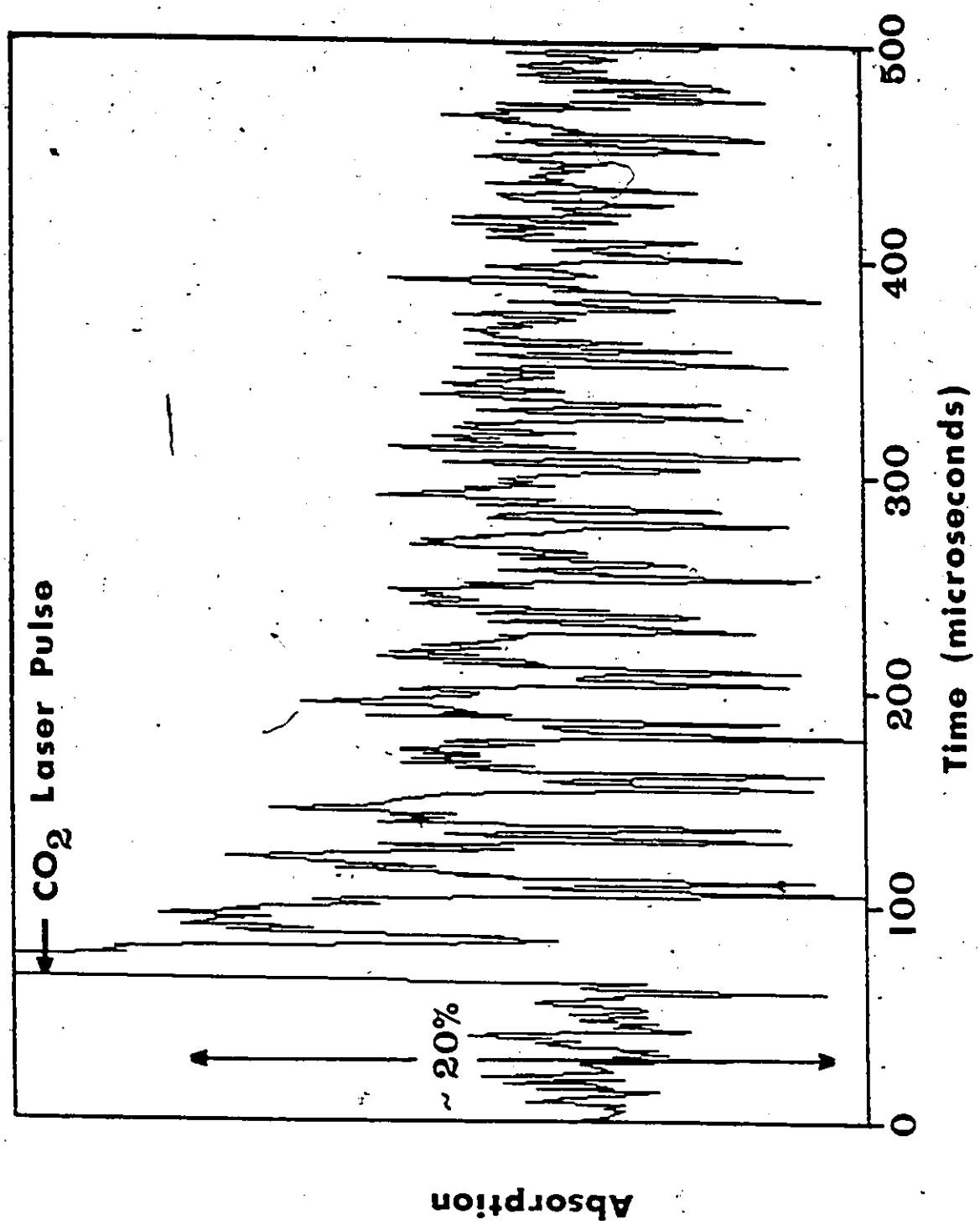
Absorption
CO_2 Laser Pulse
~ 20%
0
100
200
300
400
500
Time (microseconds)

about 30 cm^{-1} from the maximum of the ν_5 absorption band. Results indicate that the 9R(36) line is more efficient in inducing IRMPD in hexafluoroethane than is the 9R(30) line. The products of the IRMPD of "neat" hexafluoroethane detected in this work are CF_4, C_2F_4, C_3F_8 and C_4F_{10}. CF_4, C_3F_8 and C_4F_{10} were not reported in previous studies where hexafluoroethane was photolyzed in the presence of radical scavengers.[96,97] In this work C_2F_4, CHF_3, C_3F_8 and C_4F_{10} were detected when H_2 was added as a radical scavenger, however the yield of CF_4 was eliminated.

A novel technique for monitoring transient infrared absorptions have been described in this chapter. The TDL is wavelength modulated across the absorption line of interest at frequencies up to 250 kHz. This allows a time resolution of about 2 μs, however noise associated with the CO_2 laser pulse precludes any accurate absorption measurements for about the first 25 μs. Minimum detectable absorbances of ~3 x 10^{-5} are possible using this technique. The sensitivity of the technique has been shown to be limited solely by detector noise.

The modulation technique has been applied to the detection of CF_2, and CF_3 absorptions produced by the IRMPD of various fluorocarbons with a TEA CO_2 laser.

The time-resolved detection of CF_3 produced by the IRMPD of hexafluoroethane confirms that the primary dissociation pathway involves C-C scission. Evidence of a second

dissociation pathway, producing C_2F_5 and a F atom is also presented.

In summary, we propose the following reaction mechanism for the IRMPD of "neat" hexafluoroethane:

$$C_2F_6 + h\nu \rightarrow 2\ CF_3 \qquad (5.2)$$

$$C_2F_6 + h\nu \rightarrow C_2F_5 + F \qquad (5.3)$$

$$CF_3 + CF_3 \rightarrow C_2F_6 \qquad (-5.2)$$

$$C_2F_5 + F \rightarrow C_2F_6 \qquad (-5.3)$$

$$CF_3 + F \rightarrow CF_4 \qquad (5.7)$$

$$CF_3^{\dagger} + C_2F_6 \rightarrow CF_4 + C_2F_5 \qquad (5.8)$$

$$CF_3 + C_2F_5 \rightarrow C_3F_8 \qquad (5.9)$$

$$C_2F_5 + C_2F_5 \rightarrow C_4F_{10} \qquad (5.10)$$

and at higher fluence, in addition to the above:

$$CF_3 + h\nu \rightarrow CF_2 + F \qquad (5.5)$$

$$CF_2 + CF_2 \rightarrow C_2F_4 \qquad (5.6)$$

$$C_2F_5 + h\nu \rightarrow CF_2 + CF_3 \qquad (5.11)$$

In the presence of hydrogen the following reactions will replace reactions (5.7) and (5.8):

$$CF_3 + H_2 \rightarrow CHF_3 + H \qquad (5.12)$$

$$CF_3 + H \rightarrow CHF_3^{\dagger} \rightarrow CF_2 + HF \qquad (5.13a)$$

$$\xrightarrow{+[M]} CHF_3 \qquad (5.13b)$$

$$H + C_2F_6 \rightarrow C_2F_5 + HF \qquad (5.14)$$

$$H_2 + F \rightarrow HF + H \qquad (5.15)$$

$$C_2F_6^{\dagger} + CHF_3 \rightarrow C_2F_6 + CHF_3^{\dagger} \qquad (5.16)$$

$$CHF_3^{\dagger} + h\nu \rightarrow CF_2 + HF \qquad (5.17)$$

$$C_2F_6^{\dagger} + H_2 \rightarrow C_2F_5H^{\dagger} + HF \qquad (5.18)$$

$$C_2F_5H^{\dagger} \rightarrow C_2F_4 + HF \qquad (5.19)$$

Acknowledgements are due to P.H. Beckwith for his collaboration in obtaining the data shown in Figs. 5.13 and 5.14 and to J.J. Orlando for his collaboration in collecting

the data shown in Figs. 5.13 and 5.16.

CHAPTER 6

CONCLUSIONS

6.1 Introduction

This chapter summarizes the important results obtained in this thesis and the conclusions drawn from them. Included are discussions of the following areas:

6.2) IRMPD of "neat" Hexafluoroethane

6.3) Effect of added H_2

6.4) The use of TDL's to monitor the stable products of IRMPD

6.5) TDL detection of transient species

6.6) Application of transient detection to reaction kinetics.

Sections 6.2, 6.3, and 6.4 are exclusive work of this thesis, while parts of sections 6.5 and 6.6 were in collaboration with P.H. Beckwith and J.J. Orlando.

6.2 IRMPD of "Neat" Hexafluoroethane

In this thesis the IRMPD of "neat" C_2F_6 has been investigated using tunable diode lasers to measure the stable and transient species involved. Some stable products were also measured by gas chromatography. The major photolysis products were CF_4, C_2F_4, C_3F_8, and C_4F_{10}.

The stable products CF_4, C_3F_8, and C_4F_{10} were not reported in the previous investigations of the IRMPD of hexafluoroethane in the presence of radical scavengers.[96,97] The time-resolved detection of trifluoromethyl radicals confirms that C-C bond scission is the primary dissociation pathway involved in the IRMPD of hexafluoroethane. The understanding of the overall chemical mechanism of IRMPD of C_2F_6, and reaction of the intermediates formed, has been considerably extended. In addition, evidence for the abstraction of F from C_2F_6 by CF_3^+ to form CF_4 and C_2F_5 is presented.

6.3 Effect of Added H_2

Again, the understanding of the overall chemical mechanism has been advanced by the addition of H_2 to C_2F_6 prior to IRMPD. This eliminates CF_4 as a reaction product, while the other products observed in the IRMPD of "neat" hexafluoroethane; C_2F_4, C_3F_8 and C_4F_{10}, are still observed, although the latter two are in reduced yields. The absence of CF_4 when H_2 is added to hexafluoroethane confirms that CF_4 is not a primary dissociation product. The small amount of CHF_3 that is detected when C_2F_6 is irradiated in the presence of H_2 is the result of hydrogen abstraction by the primary dissociation product CF_3. Another dissociation channel forming C_2F_5 and F is deduced from the observation of C_3F_8 and C_4F_{10}.

6.4 The Use of TDL's to Monitor the Stable Products of IRMPD

Tunable diode lasers have been successfully employed in this work to measure CF_4, C_2F_4 and CHF_3 yields produced by the IRMPD of C_2F_6. The yields of these fluorocarbon species were determined from prepared calibration plots of the line center absorption coefficient (of an individual ro-vibrational line) versus partial pressure of the fluorocarbon species. The narrow linewidth of the TDL allows for the distinction between different molecules in a mixture. In addition to selectivity, the TDL method was found to be sensitive, with 4-5 mTorr amounts being routinely measured. The diode laser employed in this case was tunable over a range of ~ 150 cm^{-1}, and could be easily tuned to single-mode emission regions for analysis of each of the three fluorocarbon products analyzed in this manner. A further point that should be emphasized is the non-destructive nature of measurement by TDL's which allows for the subsequent analysis of the sample by other methods which may be inherently destructive.

6.5 TDL Detection of Transient Species

In the course of this work a high frequency modulation technique was developed to monitor transient infrared absorptions with a tunable diode laser. The technique has been employed in this work to monitor CF_3 and CF_2 produced via CO_2 laser IRMPD of various fluorocarbon

species.

Presently the technique allows for a time resolution of 2 μs, however electrical noise associated with the TEA CO_2 laser precludes any accurate absorption measurements for about the first 25 μs. The sensitivity has been shown to be limited solely by detector noise, with minimum detectable absorbances of ~ 3×10^{-5}. The use of a more powerful TDL or better detector would improve the sensitivity attainable. Problems such as optical fringing that can occur in cw experiments are eliminated. Further work is underway at McMaster to improve the time-resolution and sensitivity of the technique.

The high frequency modulation technique, when employed with the capillary waveguide cell possesses two advantages over other attempts at monitoring transient IR absorption produced by IRMPD. The first advantage is that the waveguide cell confines the CO_2 laser pump beam and the TDL probe. The CO_2 pump beam therefore possesses a rather uniform fluence over the entire length of the waveguide. The confined TDL probe beam is not subject to the deflections that can occur in a conventional photolysis cell due to thermal lensing effects. Therefore true absorption can be separated from probe beam deflection. Secondly, the technique takes advantage of the tunability of the TDL. By tuning the TDL, actual absorption features can be scanned providing unambiguous identification of the

transient species.

It was observed that in the case of CF_2 molecules a factor of ~ 50 times more absorption could be produced in a single CO_2 laser pulse using the IRMPD technique than could be produced using the fast flow, steady state microwave discharge set up. The high frequency modulation technique, in conjunction with IRMPD, may therefore be useful in spectroscopic studies where it is sometimes difficult to produce enough transient species for study.

In addition the observation of CF_3 radicals immediately following the IRMPD of hexafluoroethane confirms that the primary dissociation pathway involves C-C bond cleavage.

6.6 Application of Transient Detection to Reaction Kinetics

The TDL modulation technique developed in the course of this work can be applied to study fast reaction kinetics of unstable free radicals. When the linestrength of a particular ro-vibrational line of a transient species is known (or can be measured using the TDL modulation technique), the time-resolved detection of this particular absorption line can be used to study reaction kinetics. In this work the recombination rate of CF_3 radicals was measured following the IRMPD of hexafluoroacetone. The recombination rate constant for CF_3 radicals was measured to be $(2.2\pm0.5) \times 10^{-12}$ cm^3 molecule^{-1} s^{-1} which is in good

agreement with the latest literature value of (3.0±0.4) x 10^{-12} cm^3 $molecule^{-1}$ s^{-1}.

The TDL modulation technique has been employed successfully by Orlando and Smith[122,124] to monitor the dimerization of CF_2 and the reaction of CF_3 radicals with O_2 and NO. The technique therefore appears to be an effective way to study reaction kinetics of transient species. The technique could be extended to the study of other transient species provided a suitable precursor is available which undergoes efficient IRMPD.

REFERENCES

1. Isenor, N.R., and Richardson, M.C., Appl. Phys. Lett. 18 224 (1971).

2. Ambartzumian, R.V., and Letokhov, V.S., "Multiple Photon Infrared Laser Photochemistry," in "Chemical and Biochemical Applications of Lasers," Vol. 3 Moore, C.B., ed., Acad. Press. New York, 167 (1977).

3. Ambartzumian, R.V., and Letokhov, V.S., Acc. Chem. Res. 10 61 (1977).

4. Lupo, D.W, and Quack, M., Chem. Rev. 87 181 (1987).

5. King, D.S., "Infrared Multiphoton Excitation and Dissociation", in "Dynamics of the Excited State," Lawley, K.P., ed., John Wiley & Sons Ltd., New York, 105 (1982).

6. Schulz, P.A., Sudbo, A.S., Krajnovich, D.J., Kwok, H.S., Shen, Y.R., and Lee, Y.T., Ann. Rev. Phys. Chem. 30 379 (1979).

7. Lyman, J.L., Quigley, G.D., and Judd, O.P., in "Multiphoton Excitation and Dissociation of Polyatomic Molecules," Cantrell, C.D., ed., Springer-Verlag, Berlin (1980).

8. Fuss, W., and Kompa, K.L., Prog. Quant. Electr. 7 117 (1981).

9. Bagratashvili, V.N., Letokhov, V.S., Makarov, A.A., and Ryabov, E.A., Laser Chem. 1 211, 4 1, 4 171 (1983), 4 311 (1984), 5 53 (1984).

10. Ambartzumian, R.V., Chekalin, N.V., Doljikov, N.S., Letokhov, V.S., and Ryabov, E.A., Chem. Phys. Lett. 25 515 (1974).

11. McAlpine, R.D., and Evans, D.K., "Laser Isotope Separation by Selective Multiphoton Decomposition Process," in "Photodissociation and Photoionization", Lawley, K.P., ed., John Wiley & Sons Ltd., New York, 31 (1985).

12. Eng, R.S., Butler, J.F., and Linden, K.J., Opt. Eng. 19 945 (1980).

13. Hudgens, J., and McDonald, J.D., J. Chem. Phys. 76 173

(1982).

14. Steinfeld, J.I., and Houston, P., in "Laser and Coherence Spectroscopy," Plenum Press, New York, 1 (1980).

15. Ambartzumian, R.V., Letokhov, V.S., Makarov, G.N., and Puretzky, A.H., Sov. Phys. JETP 41 871 (1975).

16. Bagratashvili, V.N., Vainer, Yu.G., Doljikov, V.S., Letokhov, V.S., Makarov, A.A., Malyavkin, L.P., Ryabov, E.A., and Silkis, E.E., Opt. Lett. 6 148 (1981).

17. Ambartzumian, R.V., Knyazev, I.N., Lobko, V.V., Makarov, G.N., and Puretzky, A.A., Appl. Phys. 19 75 (1979).

18. Bagratashvili, V.N., Knyazev, I.N., Letokhov, V.S., and Lobko, V.V., Optics Comm., 18 525 (1976).

19. Alimpiev, S.S., Karlov, N.V., Sartakov, B.G., and Khokhlov, E.M., Optics Comm. 26 45 (1978).

20. Bloembergen, N., and Yablonovitch, E., in "Laser Spectroscopy III," Hall, J.L., and Carlsten, J.L., eds., Springer Series in Optical Sciences,

Springer-Verlag, Berlin, Vol. 7 86 (1977)

21. Herman, I.P., and Marling, J.B., Chem. Phys. Lett. 64 75 (1979).

22. Alimpiev, S.S., Bagratashvili, V.N., Karlov, N.V., Letokhov, V.S., Lobko, V.V., Makarov, A.A., Sartakov, B.G., and Khokhlov, E.M., JETP Lett. 25 547 (1977).

23. Bagratashvili, V.N., Doljikov, V.S., and Letokhov, V.S., Sov. Phys. JETP 49 8 (1979).

24. Alimpiev, S.S., Karlov, N.V., Mesyats, G.A., Nikiforov, S.M., Oraevskii, V.M., Prokhorov, A.M., Sartakov, B.G., Khokhlov, E.M., and Shtarkov, A.L., JETP Lett. 30 259 (1979).

25. Alimpiev, S.S., Karlov, N.V., Nikiforov, S.M., Prokhorov, A.M., Sartakov, B.G., Khokhlov, E.M., and Shtarkov, A.L., Optics Comm. 31 309 (1979).

26. Platonenko, V.T., JETP Lett. 25 46 (1977).

27. Platonenko, V.T., Sov. J. Quant. Elect. 8 1010 (1978).

28. Fuss, W. and Hartman, J., J. Chem. Phys. 70 5468

(1979).

29. Akulin, V.M., Alimpiev, S.S., and Karlov, N.V., Sov. Phys. JETP 47 257 (1978).

30. Knyazev, I.N., Letokhov, V.S., and Lobko, V.V., Opt. Comm. 25 337 (1978).

31. Kolomiiskii, Ju.R., and Ryabov, E.A., Sov. J. Quant. Elect. 8 375 (1978).

32. Fuss, W., Kompa', K.L., and Tablas, F.M.G., Farad. Disc. 67 180 (1979).

33. Dai, H.L., Kung, A.H., and Moore, C.B., Phys. Rev. Lett. 43 761 (1979).

34. Fukumi, T., Opt. Commun. 30 351 (1979).

35. Bloembergen, N., Optics Comm. 15 416 (1975).

36. Ambartzumian, R.V., Gorokhov, Yu.A., Letokhov, V.S., Makarov, G.N., Puretzky, A.A., and Furzikov, N.P., JETP Lett. 23 194 (1976).

37. Ivanco, M., Evans, D.K., and McAlpine, R.D., "Two-color

Multiphoton Excitation of Methanol Induced by a CO_2 and an HF Laser," in "Laser Applications in Chemistry", Evans, D.K., ed., Proc. SPIE 669, 46-51 (1986).

38. Bagratashvili, V.N., Doljikov, V.S., Letokhov, V.S., Makarov, A.A., Ryabov, E.A., and Tyakht, V.V., Sov. Phys. JETP 50 1075 (1979).

39. Mukerjee, P., and Kwok, H.S., J. Chem. Phys. 84 1285 (1985).

40. Bagratashvili, V.N., Vanier, Yu.G., Doljikov, V.S., Letokhov, V.S., Makarov, A.A., Maliavkin, L.P., Ryabov, E.A., and Silkis, A.G., Opt. Lett. 6 148 (1981).

41. Bagratashvili, V.N., Vanier, Yu.G., Doljikov, V.S., Koliakov, S.F., Makarov, A.A., Malyavkin, L.P., Ryabov, E.A., Silkis, E.G., and Titov, V.D., JETP Lett. 30 471 (1979).

42. Bagratashvili, V.N., Vanier, Yu.G., Doljikov, V.S., Koliakov, S.F., Letokhov, V.S., Makarov, A.A., Malyavkin, L.P., Ryabov, E.A., Silkis, E.G., and Titov, V.D., Sov. Phys. JETP 53 512 (1981).

43. Ambartzumian, R.V., Gorokhov, Yu.A., Letokhov, V.S.,

Makarov, G.N., and Puretzky, A.A., Sov. Phys. JETP 44 231 (1976).

44. Kolodner, P., Winterfeld, C., and Yablonovitch, E., Opt. Comm. 20 119 (1977).

45. Ambartzumian, R.V., Gorokhov, Yu.A., Letokhov, V.S., and Puretzky, A.A., JETP Lett. 22 177 (1975).

46. Grant, E.R., Coggiola, M.J., Lee, Y.T., Schulz, P.A., Sudbo, Aa.S., and Shen, Y.R., Chem. Phys. Lett. 52 595 (1977).

47. King, D.S., and Stephenson, J.C., Chem. Phys. Lett. 51 48 (1977).

48. Bagratashvili, V.N., Ionov, S.I., Kuzmin, M.V., and Letokhov, V.S., Sov. Phys. JETP 64 453 (1987).

49. Articles listed in "Infrared Laser Spectroscopy Applications and Techniques," Reprint List, (Spectra Physics, Laser Analytics Division, 25 Wiggins Avenue, Bedford, MA, 01730, July 1986).

50. Beckwith, P.H., Orlando, J.J., Reid, J., and Smith, D.R., J. Photochem. 34 267 (1986).

51. Rao, K.N., "Molecular Spectroscopy: Modern Research," Vol. II, Academic Press, New York, 165 (1976).

52. Penner, S.S., in "Quantitative Molecular Spectroscopy and Gas Emissivities," Addison-Wesley Inc., Reading, 31 (1959).

53. Young, C., and Chapman, R.E., J. Quant. Spectrosc. Radiat. Transfer 14 679 (1974).

54. Reid, J., and Labrie, D., Appl. Phys. B26 203 (1981).

55. Streit, G.E., Wells, J.S., Fehsenfeld, F.C., and Howard, C.J., J. Chem. Phys. 70 3439 (1979).

56. Eng, R.S., Petagna, G., and Nill, K.W., Appl. Opt. 17 1723 (1978).

57. Thrush, B.A., and Tyndall, G.S., J. Chem. Soc., Faraday Trans:II, 78 1469 (1982).

58. Buchanan, J.W., Thrush, B.A., and Tyndall, G.S., Chem. Phys. Lett. 103 167 (1983).

59. Davies, P.B., Kho, C.J., Leong, W.K., and Lewis-Bevan, W., J. Chem. Soc., Chem. Commun. 690 (1982).

60. Hirota, E., "High Resolution Spectroscopy of Transient Molecules," Springer-Verlag, Berlin, (1985).

61. Gudeman, C.S., and Saykally, R.J., Ann. Rev. Phys. Chem. 35 387 (1984).

62. Laguna, G.A., and Baughcum, S.L., Chem. Phys. Lett. 88 568 (1982).

63. Kanamori, H., Butler, J.E., Kawaguchi, K., Yamada, C., and Hirota, E., J. Mol. Spectrosc. 113 262 (1985).

64. Yamada, C., Kanamori, H., Horiguchi, H., Tsuchiya, S., and Hirota, E., J. Chem. Phys. 84 2573 (1986).

65. Balla, R.J., and Pasternack, L., J. Phys. Chem. 91 73 (1987).

66. Knapp, K., and Hanson, R.K., Appl. Opt. 22 1980 (1983).

67. Dang, C., Reid, J., and Garside, B.K., IEEE J. Quantum Electron QE-19 755 (1983).

68. Harradine, D., Foy, B., Laux, L., Dubs, M., and Steinfeld, J.I., J. Chem. Phys. 81 4267 (1984).

69. O'Neill, J.A., Ye Cai, J., and Flynn, G.W., J. Chem. Phys. 84 50 (1986).

70. Sugawara, K., Nakanaga, T., Takeo, H., and Matsumura, C., Chem. Phys. Lett. 130 560 (1986).

71. Sugawara, K., Nakanaga, T., Takeo, H., and Matsumura, C., Chem. Phys. Lett. 134 347 (1987).

72. Levy, M.R., Reisler, H., Mangir, M.S., and Wittig, C., Opt. Eng. 19 29 (1980).

73. Jang, J.C., and Setser, D.W., J. Phys. Chem. 83 2809 (1979).

74. Ishikawa, Y., and Arai, S., Chem. Phys. Lett. 103 68 (1983).

75. Kato, S., Makide, Y., Tominaga, T., and Takeuchi, K., J. Phys. Chem. 91 4278 (1987).

76. Yogev, A., and Benmair, R.M.J., Chem. Phys. Lett. 46 290 (1977).

77. Chowdhury, P.K., Mittal, J.P., and Rama Rao, K.V.S., J. Photochem. 24 373 (1984).

78. Dvornikova, K.V., Platonov, V.E., Urasimova, V.P., and Yakobson, G.G., Bull. Acad. Sci. USSR Chem. Sci. 20 2253 (1971).

79. Camaggi, G., and Gozzo, F., J. Chem. Soc., Chem. Commun. 236 (1967).

80. Marling, J.B., and Herman, I.P., Appl. Phys. Lett. 34 439 (1979).

81. Herman, I.P., and Marling, J.B., Chem. Phys. Lett. 64 75 (1979).

82. Tuccio, S.A., and Hartford Jr., A., Chem. Phys. Lett. 65 234 (1979).

83. Herman, I.P., and Marling, J.B., J. Chem. Phys. 72 516 (1980).

84. Makide, Y., Hagiwara, S., Kurihara, O., Takeuchi, K., Ishikawa, Y., Arai, S., Tominaga, T., Inoue, I., and Nakane, R., J. Nucl. Sci. Technol. 17 645 (1980).

85. Makide, Y., Hagiwara, S., Tominaga, T., Takeuchi, K., and Nakane, R., Chem. Phys. Lett. 82 18 (1981).

86. Takeuchi, K., Inoue, I., Nakane, R., Makide, Y., Kato, S., and Tominaga, T., J. Chem. Phys. 76 398 (1982).

87. Neve de Mevergnies, M., Verhoeven, F., del Marmol, P., and Koch, G., J. Chem. Phys. 77 4786 (1982).

88. Makide, Y., Kato, S., Tominaga, T., and Takeuchi, K., Appl. Phys. B. 28 341 (1982).

89. Neve de Mevergnies, M., Appl. Phys. B. 29 125 (1982).

90. Neve de Mevergnies, M., Appl. Phys. B. 41 61 (1986).

91. Bagratashvili, V.N., Doljikov, V.S., Letokhov, V.S., and Ryabov, E.A., Appl. Phys. 20 231 (1979).

92. Neve de Mevergnies, M., Appl. Phys. Lett. 34 853 (1979).

93. Hackett, P.A., Gauthier, M., Willis, C., and Pilon, R., J. Chem. Phys. 71 546 (1979).

94. Hackett, P.A., Willis, C., and Gauthier, M., J. Chem. Phys. 71 2682 (1979).

95. Hackett, P.A., Gauthier, M., Nip, W.S., and Willis, C.,

J. Phys. Chem. 85 1147 (1981).

96. Arai, S., Watanabe, T., Ishikawa, Y., and Oyama, T., Chem. Phys. Lett. 112 224 (1984).

97. Fisk, G.A., Chem. Phys. Lett. 60 11 (1978).

98. Mercer, P.D., and Pritchard, H.O., J. Chem. Soc. 2843 (1957).

99. Tschuikow-Roux, E., J. Chem. Phys. 43 2251 (1965).

100. Politanskii, S.F., and Shevchuk, V.U., Kinetics and Catalysis 9 411 (1968).

101. Tschuikow-Roux, E., and Marte, J.E., J. Chem. Phys. 42 2049 (1965).

102. Tschuikow-Roux, E., J. Chem. Phys. 42 3639 (1965).

103. Modica, A.P., and Sillers, S.J., J. Chem. Phys. 48 3283 (1968).

104. Davies, P.B., Lewis-Bevan, W., and Russell, D.K., J. Chem. Phys. 75 5602 (1981).

105. Rothman, L.S., Appl. Opt. 20 791 (1980).

106. Beckwith, P.H., Brown, C.E., Danagher, D.J., Smith, D.R., and Reid, J., Appl. Opt. 26 2643 (1987).

107. Yamada, C. and Hirota, E., J. Chem. Phys. 78 1703 (1983).

108. Kato, S., Makide, Y., Takeuchi, K., and Tominaga, T., J. Phys. Chem. 88 3977 (1984).

109. Rossi, M., and Golden, D.M., Int. J. Chem. Kinet. 11 775 (1979).

110. Hsieh, T., and Hanrahan, R.J., Radiat. Phys. Chem. 12 51 (1978).

111. McAlpine, I., and Sutcliffe, H., J. Phys. Chem. 73 3215 (1969).

112. Hackett, P.A., Weinberg, E., Gauthier, M., and Willis, C., Chem. Phys. Lett. 82 89 (1981).

113. Owen Jr., G.E., Pearson, J.M., and Swarc, M., Trans. Farad. Soc. 61 1722 (1965).

114. Atkinson, B., and McKeagan, D., Chem. Commun. 189 (1966).

115. Plumb, I.C., and Ryan, K.R., Plasma Chem. Plasma Process. 6 11 (1986).

116. Goldberg, I.B., and Schneider, G.M., J. Chem. Phys. 65 147 (1976).

117. Nip, W.S., Drouin, M., Hackett, P.A., and Willis, C., J. Phys. Chem. 84 932 (1980).

118. Stone, J., Thiele, E., Goodman, M.F., Stephenson, J.C., and King, D.S., J. Chem. Phys. 73 2259 (1980).

119. Brown, C.E., Orlando, J.J., Reid, J., and Smith, D.R., accepted for publication in Chem. Phys. Lett. (1987).

120. Bittenson, S., and Houston, P.L., J. Chem. Phys. 67 4819 (1977).

121. Jalenak, W.A., and Nogar, N.S., Chem. Phys. 41 407 (1979).

122. Orlando, J.J., and Smith, D.R., submitted to J. Phys. Chem. (1987).

123. Selamoglu, N., Rossi, M.J., and Golden, D.M., Chem. Phys. Lett. 124 68 (1986).

124. Orlando, J.J., Reid, J., and Smith, D.R., accepted for publication in Chem. Phys. Lett. (1987).